Durham E-Theses

Characterisation of the oxidoreductase Erol-Lß and the misfolding of the secretory pathway substrate HLA-B27

Lemin, Andrew James

How to cite:

Use policy

Characterisation of the oxidoreductase Ero1-Lβ

and the misfolding of the secretory pathway

substrate HLA-B27

Andrew James Lemin

A thesis submitted for the degree of Master of Science

School of Biological and Biomedical Sciences

University of Durham

February 2007

i
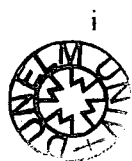
1 9 APR 2007

Declaration

I declare that the composition of this thesis, and all data presented herein, is the result of my own work. No part of the material offered has previously been submitted for a higher degree. This body of work has been achieved under the supervision of Dr. Adam M. Benham.

This copy has been supplied for the purpose of research or private study on the understanding that it is copyright material and that no quotation from this thesis may be published without proper acknowledgement.

Andrew James Lemin

February 2007

Acknowledgements

Abstract

The endoplasmic reticulum (ER) is the site of oxidative folding for proteins entering the secretory pathway. Here, nascent polypeptides acquire disulfide bonds, which confer both stability and functionality on secretory and ER-resident proteins. In eukaryotes, this process is catalysed by the disulfide oxidoreductase protein disulfide isomerase (PDI). Many mammalian homologs of PDI have been described including the pancreas-specific homolog PDIp. PDI is 'recharged' by the disulfide oxidoreductase Ero. Accepted electrons are then passed to molecular oxygen via an Ero-bound flavin adenine dinucleotide (FAD) molecule.

We provide data showing that human Ero1-Lβ protein is able to form disulfide-dependent homodimers *in vivo*. We also provide evidence that the yeast G252S and H254Y FAD-binding mutants exhibit reduced affinity for PDI. Since the Ero1-Lα C391A mutant can rescue the *ero1-1* temperature-sensitive mutant, Ero-PDI association and Ero-Ero dimerisation may be significant in maintaining the oxidative protein folding pathway in the ER. Homodimerisation was not affected by FAD-binding mutants, suggesting that the *ero1-1* and *ero1-2* phenotypes cannot be accredited to the failure of Ero1p to homodimerise. We also make the first steps towards characterising the interactions of PDIp with the human Ero1-Lα and Ero1-Lβ proteins. In order to observe protein-protein interactions, we characterise a polyclonal anti-Ero1-Lβ antibody for intended use in immunoprecipitations and immunoblotting.

Quality control measures are in place to ensure that only natively folded proteins are permitted to exit the secretory pathway. Chaperone molecules such as immunoglobulin-binding protein (BiP) retain unfolded or misfolded proteins in the ER, which are eventually retrotranslocated out of the ER and degraded. When misfolded proteins accumulate in the ER, however, the folding capacity of the ER may be exceeded. This triggers a cellular response pathway called the unfolded protein response, aimed at restoring homeostasis in the ER via transcription regulation and translational attenuation.

We provide evidence that misfolding/misoxidation of the major histocompatability complex (MHC) class I heavy chain HLA-B27 in HeLa cells causes the UPR to be triggered. Possession of the HLA-B27 allele in lymphoblastoid cell lines results in some UPR signalling. Interestingly, analysis of IRE1-mediated XBP1 splicing shows a distinct difference in sensitivity of the UPR to induction by the pharmacological agents dithiothreitol (DTT) and tunicamycin. Since possession of HLA-B27 is highly associated with development of the chronic inflammatory disease ankylosing spondylitis, induction of the UPR as a consequence of HLA-B27 misfolding may have implications in disease pathogenesis.

Table of Contents

List of Figures

3.1.2 Results

3.1.2.1 Ero1-Lβ forms homodimers in vivo

3.1.2.2 Mutations in the FAD-binding site of Ero1-Lβ diminish,

but do not prevent interaction with PDI

3.1.2.3 The G252S and H254Y mutants are able to form homodimers

3.1.2.4 Assessment of Ero1-Lβ in an insulin reduction assay

3.1.2.5 Purified Ero1-Lβ does not contain FAD

3.1.3 Discussion

3.1.3.1 Homodimerisation of wild-type Ero-1Lβ

3.1.3.2 Reduction of the ability of FAD-binding mutants to interact with PDI

and the formation of FAD-binding mutant homodimers

3.1.3.3 The use of purified Ero1-Lβ in the insulin reduction assay

3.2 Characterisation of an anti-Ero1-Lβ polyclonal antibody

3.2.1 Introduction

3.2.2 Results

3.2.2.1 Polyclonal antiserum from rabbit B2 is able to recognise

transfected but not endogenous Ero1-Lβ

3.2.2.2 Polyclonal antiserum from rabbit B2 is able to immunoprecipitate

transfected Ero1-Lβ

3.2.2.3 Antisera from rabbit B2 do not cross-react with Ero1-Lα

3.2.3 Discussion

3.3 Towards the characterisation of the interactions between the

PDI homolog, PDIp and Ero1-Lα and Ero1-Lβ

3.3.1 Introduction

3.3.2 Results

3.4 ER stress response signalling in HLA-B27-expressing cells

3.4.1 Introduction

3.4.2 Results

3.4.3 Discussion

4. Final Discussion

4.1 The importance of FAD and Ero-Ero dimerisation in oxidative

    protein folding

4.2 Interactions of pancreatic PDIp with the Eros

4.3 Characterisation of a polyclonal anti-Ero1-Lβ antibody

Abbreviations

AS	Ankylosing spondylitis
ATF6	Activating transcription factor 6
B27-Tg	HLA-B27/β_2m transgenic
BiP	Immunoglobulin binding protein
BPTI	Bovine pancreatic trypsin inhibitor
BSA	Bovine serum albumin
cDNA	Complimentary deoxyribose nucleic acid
CP4H	Collagen prolyl-4 hydroxylase
DNA	Deoxyribose nucleic acid
DTT	Dithiolthreitol
ER	Endoplasmic reticulum
ERAD	Endoplasmic reticulum-associated degradation
Ero	Endoplasmic reticulum oxidoreductin
FAD	Flavin adenine dinucelotide
FMN	Flavin mononucleotide
GOx	Glucose oxidase
GSH	Reduced glutathione
GSSG	Oxidised glutathione
HC	Heavy chain

hCMV	Human cytomegalovirus
hERO	Human endoplasmic reticulum oxidoreductin
HLA	Human leukocyte antigen
IBD	Inflammatory bowel disease
IFN	Interferon
Ig	Immunoglobulin
ILT	Immunoglobulin-like transcripts
IP	Immunoprecipitation
IRE1	Inositol-requiring kinase 1
KIR	Killer immunoglobulin receptor
LIR	Leukocyte immunoglobulin receptor
LPS	Lipopolysaccharide
mAb	Monoclonal antibody
MHC	Major histocompatibility complex
mRNA	Messenger ribose nucleic acid
MTP	Microsomal triglyceride-transfer protein
NEM	N-Ethylmaleimide
NF- B	Nuclear factor B
NK	Natural killer
NMR	Nuclear magnetic resonance
NR	Non-reducing
OD	Optical density

ORF	Open reading frame
pAb	Polyclonal antibody
PBS	Phosphate buffered saline
pBS	pBluescript II
PDI	Protein disulfide isomerase
PDIp	Pancreas-specific protein disulfide isomerase
PERK	RNA-activated protein kinase (PKR)-like endoplasmic reticulum kinase
pK_a	The negative logarithm of the acid dissociation constant
Pro-CPY	Pro-carboxypeptidase Y
R	Reducing
ReA	Reactive arthritis
RNA	Ribose nucleic acid
RNase A	Bovine pancreatic ribonuclease A
ROS	Reactive oxygen species
RT-PCR	Reverse transcriptase polymerase chain reaction
SDS	Sodium dodecyl sulphate
SDS-PAGE	Sodium dodecyl sulphate polyacrylamide electrophoresis
SpA	Spondyloarthropathy

Tm   Tunicamycin

TSF   Thioredoxin super-family

UPR   Unfolded protein response

UPRE   Unfolded protein response element

WB   Western blot

WT   Wild-type

XBP1   X-box binding protein 1

$\beta_2 m$ β_2 microglobulin

Chapter 1

Introduction

1. Introduction

1.1 *General Introduction*

In order for proteins to carry out their specific biological function they must assume their correct conformation, folding into the precise three-dimensional structure required for functional activity. This correct conformation is based upon the primary amino acid structure. Establishment of the secondary structure of proteins is characterised by the spontaneous formation of alpha-helices and beta-sheets.

For proteins entering the eukaryotic secretory pathway, formation of a tertiary or quaternary protein structure takes place in the endoplasmic reticulum (ER) (Gething and Sambrook, 1990; Jessop *et al.*, 2004; Kemmink *et al.*, 1996). The secretory pathway describes the route taken by proteins destined for the extra-cellular environment, be it cell-surface expression or secretion. ER resident proteins are also folded in the ER. Progression through the secretory pathway involves entry of nascent poly-peptides into the ER, post-translational modifications, the adoption of their secondary, tertiary and possibly quaternary structures and their trafficking to the cell surface in secretory vesicles via translocation to the Golgi (Jessop *et al.*, 2004)(Fig. 1).

Oxidative folding and the addition of disulfide bonds characterises the tertiary structure of secretory proteins. Disulfide bonds are formed in the ER via adjacent free cysteine residues, forming an S-S bridge upon oxidation of two thiol groups (Anfinsen *et al.*, 1961) (Fig. 2). Disulfide bonds are slow to form spontaneously and it was discovered by
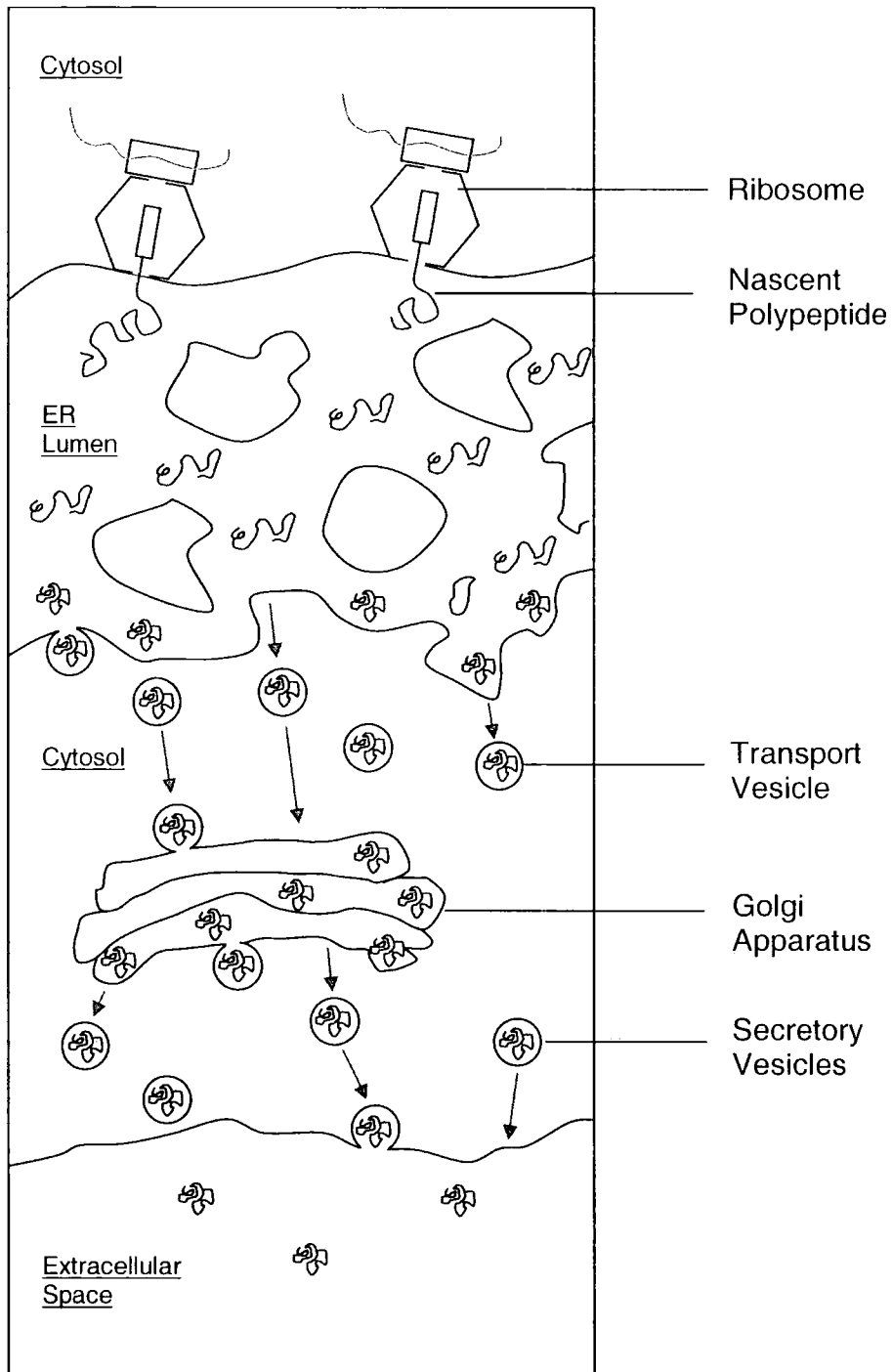
Figure 1. **A model of the secretory pathway.** Nascent polypeptides are co-translated into the ER where they undergo folding events, eventually adopting their native conformation. Fully folded proteins are then transported to the Golgi where they are packaged into secretory vesicles and fuse with the plasma membrane and are released into the extracellular space.

Goldberger and colleagues in 1963 that this reaction is in fact catalysed *in vivo* (Goldberger *et al.*, 1963).
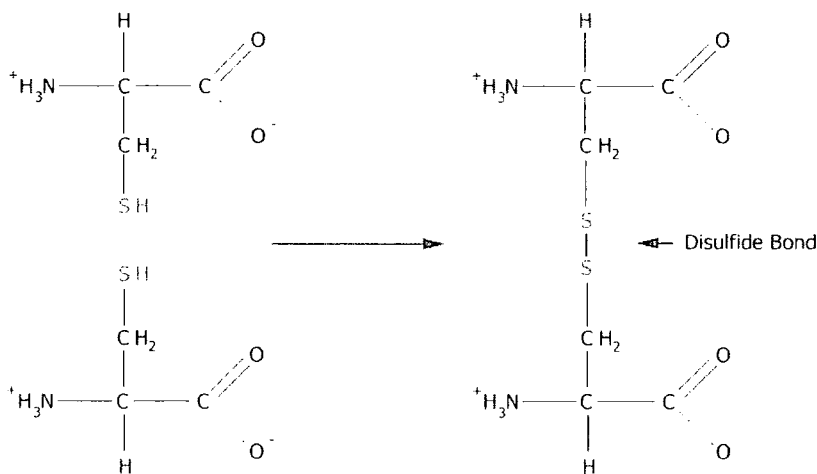
Figure 2. Disulfide bond formation. Disulfide bonds form between two cysteine residues. The thiol group (-SH) on the side chain of the amino acid takes part in a thiol-disulfide exchange with a oxidoreductase catalyst resulting in a covalent S-S disulfide bond between two cysteine side chains.

The formation of inter-chain disulfide bonds plays a vital role. As well as increasing protein stability in the extra-cellular environment, disulfide bridges confer functionality on secretory proteins (Shiroishi *et al.*, 1984). Establishment of disulfide bonds is regarded as one of the final steps in the maturation of secretory proteins.

Being the site of oxidative folding, the protein composition (Benham and Braakman, 2000; Trombetta and Parodi, 2003; Tu and Weissman, 2004) and redox environment (Hwang *et al.*, 1992) within the ER is distinct from that of the cytosol. The method by which the cell controls the ER redox environment is partially understood. It is believed, however, that glutathione is the major redox buffer in eukaryotic cells (Hwang *et al.*, 1992). The ratio of reduced glutathione (GSH) to oxidised glutathione (GSSG) is ~100:1 in the cytosol compared with ~3:1 in the ER. Thus, the oxidising environment in the ER favours disulfide bond formation.

1.2 *Protein folding in the prokaryotes*

1.2.1 *The Bacterial Dsb family*

It was studies with the bacterium *Escherichia coli* that lead to the identification and characterisation of the first bacterial redox protein, DsbA (Bardwell *et al.*, 1991; Kamitani *et al.*, 1992; Raina and Missiakas, 1997). Bardwell and colleagues studied the DsbA null mutant *dsbA⁻* which exhibited compromised disulfide bond formation. This initiated an effort to identify other redox proteins using genetic screens based on the ability or inability of *E. coli* cells to cope with changes in the redox environment (Missiakas *et al.*, 1993; Missiakas *et al.*, 1994; Missiakas *et al.*, 1995; Shevchik *et al.*, 1994). The result of this effort was the identification of other *E. coli* Dsb proteins and their relationship with the cytoplasmic redox protein thioredoxin and the glutaredoxins (See Table 1).

Table 1 - The various redox proteins of *E. coli*

Gene name	Protein name	Mw of monomer (kDa)	Cellular location	Function (pH7, 30°C)
dsbA	DsbA	21	Periplasm	Oxidant
dsbB	DsbB	20	inner membrane	Oxidant
dsbC	DsbC	2 x 23	Periplasm	Disulfide isomerase
dsbD	DsbD	50	inner membrane	Reductant
dsbE	DsbE	20	Periplasm	Reductant
trxA	Thioredoxin	12	Cytoplasm	Reductant
trx B	Thioredoxin reductase	2 x 70	Cytoplasm	Reductant
grx A	Glutaredoxin 1	10	Cytoplasm	Reductant
grx B	Glutaredoxin 2	27	Cytoplasm	Reductant
grx C	Glutaredoxin 3	10	Cytoplasm	Reductant
gor	Glutaredoxin reductase	48	Cytoplasm	Reductant
gshA	Glutathione synthetase	-	Cytoplasm	synthesises the tripeptide glutathione

Reproduced from (Raina and Missiakas, 1997)

The structure, biochemistry and function of thioredoxin, the four Dsb proteins and the three glutaredoxins (Table 1) have since been extensively studied (Akiyama *et al.*, 1992; Andersen *et al.*, 1997; Chen *et al.*, 1999; Holmgren, 1985; Holmgren, 1988; Holmgren and Aslund, 1995; Kamitani *et al.*, 1992; Xiao *et al.*, 2005; Zapun *et al.*, 1995). These proteins are not identical, however they all exhibit redox activity. Both thioredoxin and the glutaredoxins act as reductants, as do DsbD and DsbE. DsbA and DsbB function as oxidants while DsbC acts as a disulfide isomerase (Table 1). All these proteins carry an active-site containing two cysteine residues in a C-X-X-C formation which is typically referred to as a thioredoxin domain. Consequently, these proteins are collectively referred to as the thioredoxin super-family. The actives site cysteines may exist as two species; in their reduced form, Dsb-$(SH)_2$, or in their oxidised form, Dsb-S_2 with an intramolecular disulfide bond between the two cysteines. In the C-X-X-C motif of the Dsb proteins the *N*-terminal cysteine is solvent exposed and has a very low pK_a value – around 3.5 in DsbA (Nelson and Creighton, 1994). Thus, the terminal cysteine of the Dsb proteins is fully deprotonated and found as a thiolate ion with a negative charge. The difference in stability of the reduced and oxidised forms of Dsb is a consequence of the stabilisation of this negative charge (Nelson and Creighton, 1994). This stabilisation effect drives the reaction between oxidised DsbA and reduced substrate proteins, since the reduction of DsbA is more favourable. Residues in the vicinity of the active site cysteines play an important role. Histidine 32, which lies within the C-X-X-C motif is significant in determining the redox properties of DsbA (Grauschopf *et al.*, 1995). Point mutation of this residue leads to a dramatic decrease in redox potential, diminishing the ability of DsbA to donate disulfide bonds. It has been proposed that electrostatic interactions,

absent in the histidine mutant, are responsible for stabilising the thiolate anion of the N-terminal cysteine (Guddat *et al.*, 1997).

1.2.2 *Thioredoxin and Glutaredoxin*

Thioredoxin is one of the best characterised redox enzymes. It is a small ubiquitous protein that is evolutionarily conserved across both prokaryotes and eukaryotes and, as a consequence of its redox active cysteine residues, serves as a model for our understanding of *E. coli* Dsb proteins and the eukaryotic equivalents; the protein disulfide isomerase-like subfamily. The crystal structure of *E. coli* thioredoxin was solved by Katti and colleagues in 1990 at a high resolution of 1.68 Å (Katti *et al.*, 1990) (Fig. 4). The highly conserved, characteristic thioredoxin fold comprises a β-α-β-α-β-α-β-β-α structure encompassing the reactive C-X-X-C motif (Katti *et al.*, 1990).

1.2.3 *Thioredoxin super-family properties*

Members of the thioredoxin super-family have been shown to directly pass intramolecular disulfide bonds to protein substrates by cycling between dithiol and disulfide forms during catalysis (Darby and Creighton, 1995a; Darby and Creighton, 1995c; Holmgren, 1995). Cycling between redox states mediates the transfer of redox equivalents between enzyme and substrate. When the active site of the thioredoxin super-family exists in its reduced form (TSF-S$_2$), the N-terminal cysteine in the C-X-X-C motif becomes deprotonated at physiological pH, and is essentially exposed (Kemmink *et al.*, 1996). This nucleophillic cysteine is consequently able to react with the sulfhydryl (-SH) groups of protein substrates thus forming what is termed a 'mixed disulfide' (Walker *et*

al., 1996). The *C*-terminal cysteine, however, is buried within the thioredoxin fold and characteristically reacts with the *N*-terminal cysteine alone (Kemmink *et al.*, 1996). Of course, if the enzyme is a reductant, or isomerase, the thiolate attacks a disulfide bond of the substrate, again forming a mixed disulfide (Holmgren, 1995; Jeng *et al.*, 1998). The mixed disulfide is resolved by attack from the other active site cysteine.

Although members of the super-family share a degree of structural similarity, each member can exhibit different activities. The common thioredoxin motif which they share permits a degree of functional flexibility, allowing isomerisation, reducing and oxidising activities. The specificity of the family members is to a certain extent determined by their environment. DsbA is localised in the oxidising environment of the bacterial periplasm thus acts as an oxidase whilst Glutaredoxin1 is a good reductant as a consequence of its localisation in the reducing cytoplasm of *E. coli*. Different members also exhibit unique chemistry, each mixed disulfide occurring with a distinct stability and reactivity (Wunderlich *et al.*, 1993; Zapun *et al.*, 1993; Zapun *et al.*, 1995). This is mainly due to differences in the pK_a values of the nucleophillic cysteine and their redox potential (Carvalho *et al.*, 2006) (Table 2). This difference is due, in part, to the identity of the two X-X residues that are flanked by the active cysteines (Chivers *et al.*, 1996; Huber-Wunderlich and Glockshuber, 1998; Krause *et al.*, 1991) (Fig. 3).

Thioredoxin	Cys-Gly-Pro-Cys
DsbA	Cys-Pro-His-Cys
DsbB	Cys-Val-Leu-Cys
DsbC	Cys-Gly-Tyr-Cys
DsbD	Cys-Val-Ala-Cys
DsbE	Cys-Pro-Thr-Cys
PDI	Cys-Gly-His-Cys

Reproduced from Raina & Missiakas, 1997

Figure 3.Thiol/disulfide active site motifs from various members of the thioredoxin super-family.

Reproduced from Söling *et al.*, 1999

Figure 4. **Ribbon model of the crystal structure of *E. coli* thioredoxin**. As determined by Katti and colleagues (Katti *et al.*, 1990). The cysteine residues of the active site (green), Asp26 are shown as ball and stick representations. α-Helical elements are shown in red and β-elements in yellow.

The functional roles of the much-studied thioredoxin super-family are wide and varied. DsbA is a potent catalyst of peptide oxidation (Wunderlich *et al.*, 1993; Zapun and Creighton, 1994), however, because of its rapid activity, errors often occur in processing, resulting in incorrect, non-native disulfides forming. The isomerisation of these disulfides is carried out by dimeric DsbC (Rybin *et al.*, 1996; Sone *et al.*, 1997; Zapun *et al.*, 1993). As a consequence of this, the effect of the *dsbC* null mutation on the growth of *E. coli* is not as strong as either the *dsbA* or *dsbB* null mutations (Rietsch *et al.*, 1996). DsbC exerts isomerase activity on incorrectly formed disulfide bonds. Evidence of this comes from studying proteins targeted to the periplasm. Urokinase, a protein that contains 12 disulfide bonds is undetectable in the DsbC null mutant. However, the yield of alkaline phosphatase, which only contains two disulfide bonds, is only lowered by 15% (Rietsch *et al.*, 1996). DsbA is recycled by DsbB located in the inner membrane of *E. coli*, delivering electrons to the electron transport chain (Kobayashi *et al.*, 1997). DsbD maintains DsbC and DsbG in their reduced forms by receiving electrons from cytoplasmic thioredoxin (Chung *et al.*, 2000; Joly and Swartz, 1997). The role of the glutaredoxins is as reductants, however the mechanisms are slightly more complex involving the participation of glutathione and glutathione reductase which together regenerate the reduced enzyme (Fernandes and Holmgren, 2004; Yang and Wells, 1991). Thioredoxin reduction is achieved by thioredoxin reductase by a similar mechanism (Holmgren, 1988; Holmgren, 1989).

Table 2 – Redox potential and pK_a values of members of the thioredoxin super-family

Member name	Function	Redox potential (mV)	Reference	pK_a value	Reference
Thioredoxin	Reductant	-270	(Miranda-Vizuete et al., 1997)	6.3-10	(Aslund et al., 1994; Chivers et al., 1997; Dillet et al., 1998; Dyson et al., 1991; Forman-Kay et al., 1992; Klappa et al., 1998a; Langsetmo et al., 1991; Puig et al., 1994; Tagaya et al., 1989; Wetterau et al., 1990)
DsbA	Oxidant	From -90 to -125	(Hoog et al., 1983; Huber-Wunderlich and Glockshuber, 1998; Wilson et al., 1995; Wunderlich and Glockshuber, 1993)	3.5	(Grauschopf et al., 1995; Jeng et al., 1995; Mossner et al., 1998; Vlamis-Gardikas and Holmgren, 2002)
				<4	(Darby and Creighton, 1995a)
Glutaredoxin1	Reductant	-233	(Aslund et al., 1994)	3.8	(Gan and Wells, 1988; Yang and Wells, 1991)
Glutaredoxin2	Reductant	-198	(Aslund et al., 1994)		
PDI	Oxidant, Isomerase	-180	(Lundstrom et al., 1992)	4.5	(Kortemme and Creighton, 1995)
				6.7	(Freedman et al., 1988)
				<5	(Darby and Creighton, 1995b)

The functional roles of the much-studied thioredoxin super-family are wide and varied. DsbA is a potent catalyst of peptide oxidation (Wunderlich *et al.*, 1993; Zapun and Creighton, 1994), however, because of its rapid activity, errors often occur in processing, resulting in incorrect, non-native disulfides forming. The isomerisation of these disulfides is carried out by dimeric DsbC (Rybin *et al.*, 1996; Sone *et al.*, 1997; Zapun *et al.*, 1993). As a consequence of this, the effect of the *dsbC* null mutation on the growth of *E. coli* is not as strong as either the *dsbA* or *dsbB* null mutations (Rietsch *et al.*, 1996). DsbC exerts isomerase activity on incorrectly formed disulfide bonds. Evidence of this comes from studying proteins targeted to the periplasm. Urokinase, a protein that contains 12 disulfide bonds is undetectable in the DsbC null mutant. However, the yield of alkaline phosphatase, which only contains two disulfide bonds, is only lowered by 15% (Rietsch *et al.*, 1996). DsbA is recycled by DsbB located in the inner membrane of *E. coli*, delivering electrons to the electron transport chain (Kobayashi *et al.*, 1997). DsbD maintains DsbC and DsbG in their reduced forms by receiving electrons from cytoplasmic thioredoxin (Chung *et al.*, 2000; Joly and Swartz, 1997). The role of the glutaredoxins is as reductants, however the mechanisms are slightly more complex involving the participation of glutathione and glutathione reductase which together regenerate the reduced enzyme (Fernandes and Holmgren, 2004; Yang and Wells, 1991). Thioredoxin reduction is achieved by thioredoxin reductase by a similar mechanism (Holmgren, 1988; Holmgren, 1989).

Table 2 – Redox potential and pK_a values of members of the thioredoxin super-family

Member name	Function	Redox potential (mV)	Reference	pK_a value	Reference
Thioredoxin	Reductant	-270	(Miranda-Vizuete et al., 1997)	6.3-10	(Aslund et al., 1994; Chivers et al., 1997; Dillet et al., 1998; Dyson et al., 1991; Forman-Kay et al., 1992; Klappa et al., 1998a; Langsetmo et al., 1991; Puig et al., 1994; Tagaya et al., 1989; Wetterau et al., 1990)
DsbA	Oxidant	From -90 to -125	(Hoog et al., 1983; Huber-Wunderlich and Glockshuber, 1998; Wilson et al., 1995; Wunderlich and Glockshuber, 1993)	3.5	(Grauschopf et al., 1995; Jeng et al., 1995; Mossner et al., 1998; Vlamis-Gardikas and Holmgren, 2002)
				<4	(Darby and Creighton, 1995a)
Glutaredoxin1	Reductant	-233	(Aslund et al., 1994)	3.8	(Gan and Wells, 1988; Yang and Wells, 1991)
Glutaredoxin2	Reductant	-198	(Aslund et al., 1994)		
PDI	Oxidant, Isomerase	-180	(Lundstrom et al., 1992)	4.5	(Kortemme and Creighton, 1995)
				6.7	(Freedman et al., 1988)
				<5	(Darby and Creighton, 1995b)

1.3 *Protein folding in the eukaryotes*

1.3.1 *PDI structure and function*

Long before the characterisation of DsbA however, a protein able to rearrange incorrect disulfide bonds and catalyse the oxidation and reduction of disulfide bonds in eukaryotes was identified (Goldberger *et al.*, 1963). By studying the reactivation of ribonuclease as a model for the formation of natively folded secretory proteins, Goldberger and colleagues were able to isolate a key redox enzyme which was subsequently named protein disulfide isomerase or PDI. Since its initial discovery, PDI has been the subject of intense examination and has become the archetypal eukaryotic disulfide oxidoreductase. PDI is thought to be the primary catalyst of protein folding involving disulfide bond formation in the eukaryotic endoplasmic reticulum. Interestingly, it has been shown to complement DsbA deficient *E. coli*, increasing the yield of heterologously expressed disulfide-containing proteins in both *E. coli* and cultured insect cells (Hsu *et al.*, 1996; Ostermeier *et al.*, 1996).

In 1985, over 20 years after the initial discovery of PDI, Edman and colleagues managed to sequence PDI and publish data on the domain architecture of the oxidoreductase (Edman *et al.*, 1985). They provided structural evidence showing that mammalian PDI is composed of four thioredoxin-like domains termed **a**, **b**, **b'** and **a'** and an anionic tail named **c**. PDI also contains an *N*-terminal signal sequence and a –KDEL ER retrieval sequence at the *C*-terminus (Edman *et al.*, 1985). The catalytic domains **a** and **a'** possess the characteristic thioredoxin fold and are located towards the two ends of the molecule (Fig. 5). These domains not only possess the thioredoxin fold but in fact show high

sequence homology to thioredoxin (Ferrari *et al.*, 1998). Each active site possesses the two catalytic cysteines, between which lie a glycine and histidine residue (Fig. 3). Thus, it is the **a** and **a'** domains that contribute to the thiol disulfide exchange activity of PDI. Flanked by the two active domains are the non-catalytic **b** and **b'** domains. Despite not participating directly in oxidoreductase function, these domains are thought to be important for the disulfide rearrangement activities of PDI (Kemmink *et al.*, 1997) and possibly substrate binding activity (Klappa *et al.*, 1998a). This multi domain structure differs from the single thioredoxin fold of DsbA and thioredoxin itself.
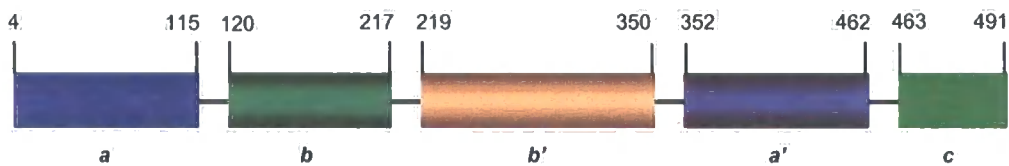
Figure 5. **PDI domain structure**. PDI consists of 2 active site thioredoxin-like domains *a* and *a'* and two non-reactive thioredoxin-like domains *b* and *b'*. The boundaries for the domains *a* and *b* are those defined by NMR (Kemmink *et al.*, 1999). Reproduced from (Kemmink *et al.*, 1997)

PDI is a highly abundant ER resident protein, making up approximately 0.8% of total cellular protein (Freedman *et al.*, 1994). Much like thioredoxin, PDI is highly conserved between species. PDI is essential for eukaryotic oxidative protein folding; as illustrated by its requirement for *S. cerevisiae* viability (Farquhar *et al.*, 1991).

1.3.2 *Catalytic activity of PDI*

The redox activity of PDI is due to the reactivity of the N-terminal cysteine residue in the

two thioredoxin-like C-X-X-C motifs. Like other members of the super-family, the

function of PDI is defined by the biochemistry of the sequence both immediately

surrounding and within the active site, as well as the residues and features of the three-

dimensional environment surrounding the reactive cysteines. It has been shown that the

pK_a value of the N-terminal cysteine of the active site is 4.5 (Table 2) and that this

reactive cysteine is stabilised by the histidine residue within the thioredoxin fold (Fig. 3)

and by the partial positive charges at the N-terminus of an α-helix occurring soon after

the catalytic cysteine (Kortemme and Creighton, 1995). Together, these features generate

a less stable disulfide bonded protein which is responsible for the oxidative function of

PDI. This has been contrasted with the relatively more stable oxidised version of

thioredoxin, which permits its reductant capabilities (Freedman *et al.*, 1995).

As previously discussed, the redox function of an oxidoreductase is in part determined by

its immediate redox environment. The redox environment of the ER favours the oxidation

of disulfide bonds reflected by the relatively high lumenal concentration of GSSG. The

redox activity of PDI is accounted for by the presence of the two-thioredoxin-like motifs

CGHC. Oxidation of the substrate requires conversion of an active site disulfide to a

dithiol, while reduction requires the conversion of a dithiol active site to a disulfide.

There is, however, plenty of evidence showing that the major function of PDI is not as an

oxidase or reductase but as an isomerase (Gilbert, 1998; Schwaller *et al.*, 2003; Walker

and Gilbert, 1997). Isomerisation results in no net redox state change but requires the

breaking of a substrate disulfide for rearrangement. Isomerisation therefore requires the active site cysteines of PDI in their reduced form so they may attack non-natively formed substrate disulfides, catalysing their rearrangement. Both the active sites have been shown to contribute to PDI activity. In 1994, however, a study suggested that the two domains are not equivalent in their catalytic properties, with the amino-terminal domain providing the majority of catalytic activity and the carboxyl-terminal domain being involved in steady-state binding of the substrate (Lyles and Gilbert, 1994). However, a more recent study shows that it is the **b'** domain that provides the principle peptide-binding site of PDI (Klappa *et al.*, 1998a). Recent work by Kulp and colleagues also endeavoured to study the domain architecture of PDI and also reported an asymmetry in function, albeit dissimilar from Lyles & Gilbert's report (Kulp *et al.*, 2006). They provided evidence showing an asymmetry of rate of oxidation of PDI by its natural oxidant endoplasmic oxidoreductase 1 protein (Ero1p), which will be discussed later. This has a dual effect; allowing an enhanced rate of oxidation of the second catalytic domain (**a'**) and the substrate-mediated inhibition of oxidation of the first catalytic domain (**a**). This asymmetry permits the two active thioredoxin-like folds to exhibit two distinct functional roles. The C-terminal active site (**a'**) is efficient at oxidising RNase A but defective at catalysing the formation of native disulfides. Conversely, the N-terminal active site (**a**) is a poor oxidase but corrects non-native disulfide bonds, rearranging them to produce a functional RNase A protein.

Using the substrate bovine pancreatic ribonuclease A (RNase A), Walker and colleagues aimed to study PDI active site mutants in order to gain an insight into the oxidase and

isomerase activity *in vivo*. Four mutants were produced, each one possessing a single active site cysteine. Kinetic analysis of these mutants showed that the N-terminal cysteines of each active site are essential for oxidation and rearrangement during the refolding of reduced RNase A (Walker *et al.*, 1996). The C-terminal active site cysteines were not essential for isomerisation activity but were essential for RNase A oxidation. It was suggested therefore that the C-terminal cysteines provide PDI with an escape from covalent disulfide bond intermediates of RNase A during isomerisation. A more recent study using shuffled domain mutants in the Δpdi1 null strain of yeast, suggests that most of PDI's multidomain structure is dispensable for its essential function in yeast and that only low level (<5%) isomerase activity is required for yeast viability (Xiao *et al.*, 2001). Contrastingly, it has been shown that high redox and isomerase activity of PDI on bovine pancreatic trypsin inhibitor (BPTI) requires both the redox-inactive (**b** and **b'**) and redox active (**a** and **a'**) domains (Darby *et al.*, 1998). However, the only shuffled domain mutant used by Xiao and colleagues that exhibited levels of isomerase activity comparable to wild-type possessed the **b' a' c** domains, suggesting that one or more of the **b** domains may be important in isomerase activity. Since the **b'** domain has been implicated in substrate-binding (Klappa *et al.*, 1998a), it may be feasible that this domain could potentially recognise misfolded proteins, an essential part of the isomerase pathway.

1.3.3 *Other functions of PDI*

1.3.3.1 *Chaperone activity*

PDI exhibits chaperone activity, a non-redox related function of PDI. The responsibility of ER-resident molecular chaperones (Ellis and Hemmingsen, 1989) is to bind to misfolded proteins in order to a) inhibit aggregation and to b) prevent misfolded proteins from exiting the ER and traversing through the secretory pathway. Molecular chaperones do not directly accelerate folding itself but seek to increase the quality of proteins exiting the ER, ensuring proteins that do so are natively folded and thus functional. ER-resident chaperones will therefore bind with nascent polypeptides entering the ER.

Disulfide oxidoreductases should only require catalytic concentrations in order to facilitate disulfide bond formation or rearrangement. It is interesting that PDI exists at millimolar concentrations in the ER. With studies showing PDI being essential for cell viability and $\Delta pdi1$ null mutations of yeast being rescued by mammalian PDI with little foldase capability, it seems that some other function of PDI is essential for yeast viability. In order for PDI to exhibit its isomerase activity, direct recognition of misfolded proteins would allow the oxidoreductase to perform rearrangement of non-native disulfide-bonded substrates. LaMantia & Lennarz were able to demonstrate the binding of unfolded proteins by PDI, suggesting that the oxidoreductase may demonstrate chaperone activity (LaMantia and Lennarz, 1993). This was investigated by Puig & Gilbert in 1994 by studying the folding of the enzyme lysozyme (Puig and Gilbert, 1994). They were able to demonstrate chaperone-like activity of PDI increasing the recovery of lysozyme by preventing aggregation. Interestingly they discovered a novel anti-chaperone activity,

where the yield of native lysozyme is substantially lower in the presence of PDI than in its absence. This facilitated the formation of inactive disulfide cross-linked aggregates and retained misfolded proteins in the ER when the level of unfolded protein exceeded the chaperone and foldase capacity of the ER (Puig and Gilbert, 1994; Puig *et al.*, 1994). Whether this proposed activity is functionally significant *in vivo* is unknown. However, it has been suggested that anti-chaperone activity is a consequence of multivalent binding of partially aggregated substrates to PDI (Primm *et al.*, 1996). Considering PDI exists at millimolar concentrations in the ER, folding substrates *in vivo* are unlikely to be subject to conditions in which PDI has significant anti-chaperone activity.

1.3.3.2 The β subunit of collagen prolyl 4-hydroxylase

Collagen prolyl 4-hydroxylase (CP4H) is an enzyme which catalyses the formation of 4-hydroxylprolines in the collagens. The formation of 4-hydroxylprolines is essential for the formation of the collagen triple helix at body temperature (Myllyharju, 2003). The enzyme exists as an $\alpha_2\beta_2$ tetramer in vertebrates with a molecular weight of 240 kD with the individual subunits being 63 kD and 55 kD respectively (Berg and Prockop, 1973; Pankalainen *et al.*, 1970; Tuderman *et al.*, 1975). The β subunit of CP4H was cloned in 1987 and was found to be identical to PDI (Koivu *et al.*, 1987; Pihlajaniemi *et al.*, 1987). When β subunits were removed from CP4H, they had no prolyl 4-hydroxylase activity but did have approximately 50% of the wild-type PDI activity in rearranging the disulfide bonds of scrambled RNase A and even when present as an $\alpha_2\beta_2$ tetramer. PDI redox activity is not required for tetramer assembly or for prolyl 4-hydroxylase activity. No

high resolution structure exists for CP4H, therefore the position of PDI in the tetramer and the orientation of the subunits within the enzyme are unknown.

Various studies have shown that the absence of the β subunit causes the α subunit to aggregate resulting in a loss of activity (Helaakoski *et al.*, 1995; Kivirikko and Myllyla, 1982; Veijola *et al.*, 1994; Vuori *et al.*, 1992). The primary function of PDI in CP4H appears to be to keep the α subunit in a soluble state. Since the α subunit does not possess an ER retention signal, PDI may also be responsible for retaining the enzyme in the lumen of the ER (Vuori *et al.*, 1992).

1.3.3.3 *The β subunit of microsomal triglyceride-transfer protein*

The microsomal triglyceride-transfer protein (MTP) is a 155 kD protein which catalyses the transport of triglyceride, cholesteryl ester and phosphatadylcholine through membranes. In addition, MTP is required for the assembly of apoB-containing lipoproteins in the liver and intestinal cells. MTP exists as an $\alpha\beta$ heterodimer with subunits weighing 97 kD and 55 kD respectively. The smaller 55 kD subunit has been identified as PDI (Wetterau *et al.*, 1990). The larger α subunit is active only in the complex; however, the isolated PDI subunit has no lipid-transfer activity. As with collagen prolyl 4-hydroxylase, PDI may serve to retain MTP in the lumen of the ER, since the α subunit lacks an ER retrieval signal. In the absence of PDI, the α subunit aggregates, as in CP4H. The role of PDI might also be to maintain the α subunit in its soluble form (Wetterau *et al.*, 1991). The redox activity of PDI is not required for MTP activity or formation of the heterodimer (Lamberg *et al.*, 1996).

1.3.3.4 *Retrotranslocation*

Recent studies have highlighted a role for PDI in retrotranslocation and subsequent degradation of protein substrates (Forster *et al.*, 2006; Tsai and Rapoport, 2002; Tsai *et al.*, 2001). PDI is able to bind polypeptides in the reduced state and unfolded these substrates for retrotranslocation. Heterodimeric cholera toxin from *Vibrio cholerae* was used to study this. After secretion, the A subunit is cleaved into the A1 toxic domain and the A2 domain which are connected by a disulfide bond. In the ER, the A subunit hijacks the retrotranslocation machinery so that the A1 domain reaches the cytosol where it is resistant to proteasomal degradation (Rodighiero *et al.*, 2002). *In vitro* studies revealed that, acting as a redox-driven chaperone, PDI is responsible for unfolding the A and A1 domain preparing the toxin for retrotranslocation (Tsai *et al.*, 2001). PDI may change its affinity for substrates during cycles of oxidation and reduction of disulfide bonds, binding maturing unfolded proteins when oxidised and unfolding proteins for retrotranslocation when in a reduced state. Thus, PDI may function as a novel chaperone.

1.3.4 *The PDI family*

As in prokaryotes, there are numerous oxidoreductase homologous to PDI in both yeast and mammalian cells. The group of mammalian PDI homologs includes ERp57, ERp72, P5, PDIR, PDIp, ERp44, ERp29, ERp18, ERdj5, PDILT and EndoPDI. Like PDI, the majority of these are multidomain foldases that possess the characteristic thioredoxin fold. Many of these proteins also possess the C-X-X-C active site that provides thioredoxin with its redox activity. Few endogenous substrates have been identified for PDI homologs, hence it is not clear whether these PDI homologs serve a role in

reduction, oxidation or disulfide isomerisation in the ER. However, many homologs have been implicated in a wide range of processes including recruitment to large multi-protein complexes and recognition of misfolded proteins. The mammalian PDI homologs PDIp and ERp57 are especially interesting in that they share similar domain organisation to PDI as well as a strong overall sequence homology. They do however exhibit significant sequence variation in the **b'** domain, responsible for substrate binding, suggesting that these PDI isoforms may demonstrate specialised substrate binding properties (Klappa *et al.*, 1998a). A summary of the function and features of some of these homologs is provided in Table 3.

1.3.4.1 *ERp57*

One of the best characterised PDI homologs is ERp57 (ER-60/ERp60/GRP58Q2/HIP-70). Research on ERp57 has revealed that it has a similar domain organisation to that of PDI (Alanen *et al.*, 2003; Ferrari and Soling, 1999) and possesses two thioredoxin-like domains, **a** and **a'**, both containing C-H-G-C active sites in similar positions to those of PDI. ERp57 differs however in its ER retention sequence, possessing a QEDL variant. Overall sequence identity between PDI and ERp57 is 29% and similarity is 56% (Koivunen *et al.*, 1996). ERp57 has been shown to exhibit thiol-dependent reductase activity similar to that of PDI (Bourdi *et al.*, 1995; Hirano *et al.*, 1995; Srivastava *et al.*, 1993). Despite such similarity in structure and function, ERp57 is unable to substitute PDI as the β subunit in collagen prolyl 4-hydroxylase (Koivunen *et al.*, 1996).

Table 3 – Eukaryotic homologs of Protein Disulfide Isomerase

Protein name	Size (kDa)[1]	Number of Thioredoxin-like domains (CXXC)	Distinctive features	Domain architecture	References
S. cerevisiae homologs					
Pdi1p	58	2	Essential for viability	**a b b' a' c**	(LaMantia and Lennarz, 1993; Scherens et al., 1991)
Mpd1p	36	1		**a c**	(Tachikawa et al., 1995)
Mpd2p	32	1		**a c**	(Tachikawa et al., 1997)
Eug1p	58	2	CXXS active site	**a b b' a' c**	(Tachibana and Stevens, 1992)
Eps1p	81	1	ER- membrane protein	**a c**	(Wang and Chang, 1999)
Selected mammalian homologs					
PDI	55	2	General peptide-binding site mapped to **b'** domain	**a b b' a' c**	(Edman et al., 1985; Ferrari and Soling, 1999; Klappa et al., 1998a)
ERp72	71	2	Calcium binding	**a b b' a' c**	(Ferrari and Soling, 1999; Lundstrom-Ljung et al., 1995; Mazzarella et al., 1990; Nigam et al., 1994)
ERp57	54	2	Interaction with nascent monoglycosylated glycoproteins	**a b b' a' c**	(Ferrari and Soling, 1999; Hirano et al., 1995; Molinari and Helenius, 1999; Oliver et al., 1997; Zapun et al., 1998)

P5	46	1		a c	(Ferrari and Soling, 1999; Fullekrug et al., 1994; Lundstrom-Ljung et al., 1995)
PDIR	57	1		b a a a	(Ferrari and Soling, 1999; Hayano and Kikuchi, 1995)
PDIp	55	2	Pancreas-specific expression	a b b' a' c	(Desilva et al., 1997; Ferrari and Soling, 1999)

[1] Size of yeast proteins are obtained by predicting the molecular weights based on full DNA sequence and do not reflect signal-sequence cleavage or glycosylation of the proteins in vivo.
Reproduced from (Frand et al., 2000) supplemented with data from (Freedman et al., 2002)

ERp57 is distinct in its function to bind glycoproteins. Evidence for this has come from cross-linking experiments revealing interactions between ERp57 and glycoproteins and either the lectin-like proteins calnexin and calreticulin (Oliver et al., 1997). Calnexin and calreticulin are both ER-resident chaperones that interact specifically with glycoproteins, aiding folding and providing quality control. They are able to recognise monoglucosylated proteins via either the P-domain of calreticulin and the luminal domain of calnexin (Ellgaard et al., 2001; Schrag et al., 2001). Both calreticulin and calnexin can bind processed N-glycans moieties of the form $GlcNAc_2Man_9Glc_1$ (Rodan et al., 1996).

One well characterised function of ERp57 is as an important component of the major histocompatability complex (MHC) class I peptide loading complex. ERp57 is found in association with the heavy chain-β_2m dimers together with calreticulin (Dick et al., 2002; Hughes and Cresswell, 1998). Details of the modes of association of the peptide loading

complex have been extensively studied and have given rise to a proposed scheme in which class I heavy chains bind calnexin immediately upon translocation and glycosylation, and calreticulin replaces calnexin when β_2m associates. ERp57 is believed to promote appropriate disulfide bond formation in the class I heavy chain.

1.3.4 *Protein misfolding and ER-associated degradation*

Since it is possible for any two cysteines, present in the primary structure of a polypeptide, to form a disulfide, it is of the utmost importance that proteins that are misfolded, be identified and folded into their native conformations. As discussed, PDI exhibits isomerase function to correct the formation of these non-native structures. Many chaperone molecules, including PDI, have been shown to be extremely important in retaining misfolded proteins in the ER (Ellgaard *et al.*, 1999; Hurtley *et al.*, 1989). Terminally misfolded proteins, that is, proteins that will never adopt their native formation cannot very well be bound to ER chaperones indefinitely. The fate of these aberrant proteins therefore is to be retro-translocated out of the ER via either the Sec61 channel or p97/Derlin-1 and degraded by the proteasome in a process known as ER-associated degradation (ERAD) (Bonifacino and Weissman, 1998; Brodsky and McCracken, 1999; Carlson *et al.*, 2006; Plemper and Wolf, 1999; Sun *et al.*, 2006; Tsai *et al.*, 2002).

When protein misfolding exceeds the capacity of the ER to retrotranslocate and degrade proteins, cellular responses endeavour to restore homeostasis. The transmembrane ER sensors IRE1, ATF6 and PERK all associate with BiP in the ER lumen. When BiP is

sequestered away from these ER sensors to bind misfolded proteins, the cytosolic portion of these proteins is activated, triggering the unfolded protein response (UPR). IRE1, AFT6 and PERK work directly or indirectly to upregulate transcription of genes involved in ER regulation such as chaperones and ER-associated degradation (ERAD) machinery or to attenuate translation in order to increase the folding capacity of the ER. The UPR will be discussed further in Chapter 3.4.

1.4 *The ER-resident Ero protein*

1.4.1 *Yeast Ero1p*

The relative abundance of GSSG in the ER led to the theory, proposed in the key paper by Hwang and colleagues in 1992, that oxidised glutathione might serve as the source of oxidising equivalents utilised during disulfide bond formation *in vivo* (Hwang *et al.*, 1992). Papers by Frand and Kaiser (1998), Cuozzo & Kaiser (1999) and Pollard and colleagues (1998), however, provided evidence to suggest that glutathione is in fact not essential for oxidative protein folding in the ER and disulfide bond formation relies upon a different electron acceptor (Cuozzo and Kaiser, 1999; Frand and Kaiser, 1998). Using the yeast *S. cerevisiae*, Frand & Kaiser began a genetic dissection of oxidative protein folding, managing to isolate *ERO1* (endoplasmic reticulum oxidoreductin 1) which encodes a novel but conserved ER membrane protein essential for the net formation of protein disulfide bonds. Secretory proteins that normally contained disulfide bonds remain in the ER in a reduced state in the *ero1-1* mutant. Introduction of the thiol oxidant diamide restored viability in *ero1* mutants, providing evidence that Ero1p activity introduces oxidising equivalents into the ER via its two pairs of conserved cysteines

(Frand and Kaiser, 2000). This was further corroborated by the observation that overexpression of *ERO1* confers resistance to otherwise toxic levels of the reductant dithiothreitol (DTT), a phenotype distinct from that of *PDI1* overexpression.

Further investigation by Frand and Kaiser in 1999 led to the suggestion that Ero1p is responsible for the reoxidation of PDI (Frand and Kaiser, 1999). Direct interaction between the two ER-resident proteins was indicated by the isolation of mixed disulfides between Ero1p and Pdi1p, representing intermediates in the transfer of disulfide bonds from Ero1p to Pdi1p. This data suggested that oxidising equivalents are directly transferred from Ero1p to Pdi1p, sustaining Pdi1p predominantly in its disulfide form. This of course parallels the prokaryotic pathway of oxidative folding, where DsbB serves to reoxidise DsbA, the primary oxidant of substrate proteins in *E. coli* (Missiakas *et al.*, 1993). In the absence of PDI, Ero1p-mediated oxidative folding still takes place, only at a slower pace, possibly via interactions of Ero1p with other electron acceptors such as GSSG, Mpd1p or Mpd2p. Frand & Kaiser's model or Ero1p-mediated oxidative protein folding can be seen in figure 6.

This central paper however, failed to answer an important and obvious question; how is Ero1p reoxidised? Studies with *E. coli* have shown that the reoxidation of DsbB occurs primarily via the transfer of electrons to molecular oxygen at the later stages of the respiratory electron transport chain via cytochrome *bd* or *bo* oxidase (Kobayashi and Ito, 1999; Kobayashi *et al.*, 1997).
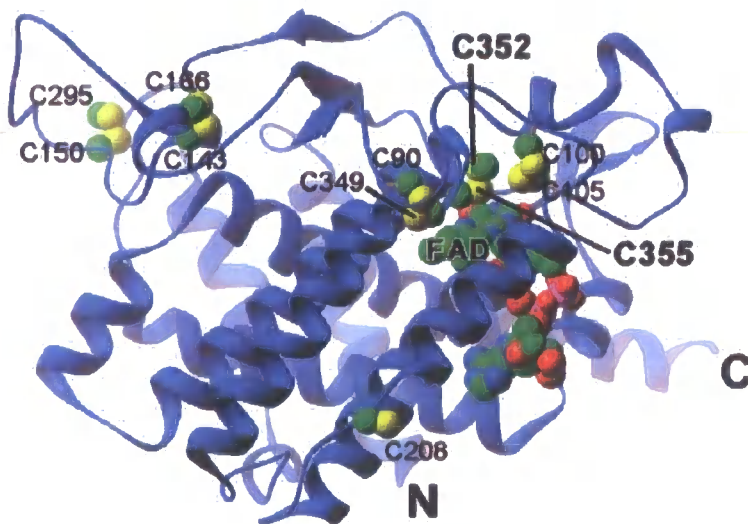
Figure 6. **Crystal structure of Ero1p**. Ero1p crystal structure with α-helices represented as cylinders (grey) and b-sheets as arrows (red). Secondary structural elements are numbered. Cysteine residues are labelled with the active site cysteines nearest FAD in bold.
Ero1p crystal structure data taken from (Gross *et al.*, 2004).

This is not the case for Ero1p; in 2002, Tu & Weissman provided evidence that Ero1p uses a flavin-dependent reaction to pass electrons directly to molecular oxygen, possibly generating reactive oxygen species (ROS) that may contribute to oxidative stress (Tu and Weissman, 2002). Depletion of riboflavin from the yeast *S. cerevisiae* results in defective oxidative folding and overexpression of *FAD1*, which converts flavin mononucleotide (FMN) into flavin adenine dinucleotide (FAD), suppresses the temperature sensitivity of the *ero1-1* mutant (Tu *et al.*, 2000). Together these data suggest that oxidative folding in yeast is dependent on levels of cellular FAD. Ero1p itself is a novel FAD-binding protein,

providing further evidence that FAD is important in oxidative protein folding. The crystal structure of Ero1p was recently solved, allowing identification of the FAD binding site (Fig. 6). FAD is thought not to be the terminal electron acceptor, since an excess of free FAD cannot drive Ero1p-catalysed disulfide formation under anaerobic conditions (Tu and Weissman, 2002). Further *in vitro* work showed that Ero1p directly consumes molecular oxygen, and taken together with the anaerobic data, suggests that molecular oxygen rather than FAD is the terminal electron acceptor.

1.4.2 Human Ero1-Lα and Ero1-Lβ

Recently, the human homologs of Ero1p have been described, termed Ero1-Lα and Ero1-Lβ. It has been shown that both of these proteins complement the *ero1-1* yeast mutant demonstrating that both human EROs are functional homologs of the *S. cerevisiae* Ero1 protein. Both proteins contain the conserved C-X-X-C-X-X-C motif involved in transferring oxidative equivalents and both are capable of forming mixed disulfide intermediates with PDI (Benham *et al.*, 2000; Cabibbo *et al.*, 2000; Dias-Gunasekara *et al.*, 2005; Mezghrani *et al.*, 2001; Pagani *et al.*, 2000). In Ero1p, the N-terminal and C-terminal active sites differ in their function. Mutation of either C352 or C355 completely inactivated Ero1p, preventing oxidation of the Ero1p protein itself and implying that this pair is required for generation of disulfide bonds. However, mutation of either C100 or C105 largely but not completely inactivated Ero1p and impaired the formation of Ero1p-PDI mixed disulfides, implying that the C100/C105 pair is involved in disulfide transfer to PDI. Figure 7 is a cartoon representing the thiol-disulfide exchange pathway of electrons from substrate to terminal electron acceptor.

Ero1-Lα and Ero1-Lβ accelerate the generation of disulfide bonds, however, the absence of any human ERO (hERO)-substrate mixed disulfides suggests that, as postulated for yeast Ero1p, their activity is to oxidise PDI. The reasons why humans and mice both possess two ERO proteins while the yeast *S. cerevisiae* possesses just the one is not yet fully understood. Ero1-Lβ transcript expression can be induced by inducing ER stress, possibly suggesting separate regulation pathways (Pagani *et al.*, 2000). Interestingly, both hEROs exhibit differential tissue expression, with Ero1-Lα highly expressed in the oesophagus, whilst Ero1-Lβ being more abundant in the pancreas, stomach, testis and pituitary gland, suggesting that human EROs might participate in tissue specific oxidation pathways (Dias-Gunasekara *et al.*, 2005; Pagani *et al.*, 2000).
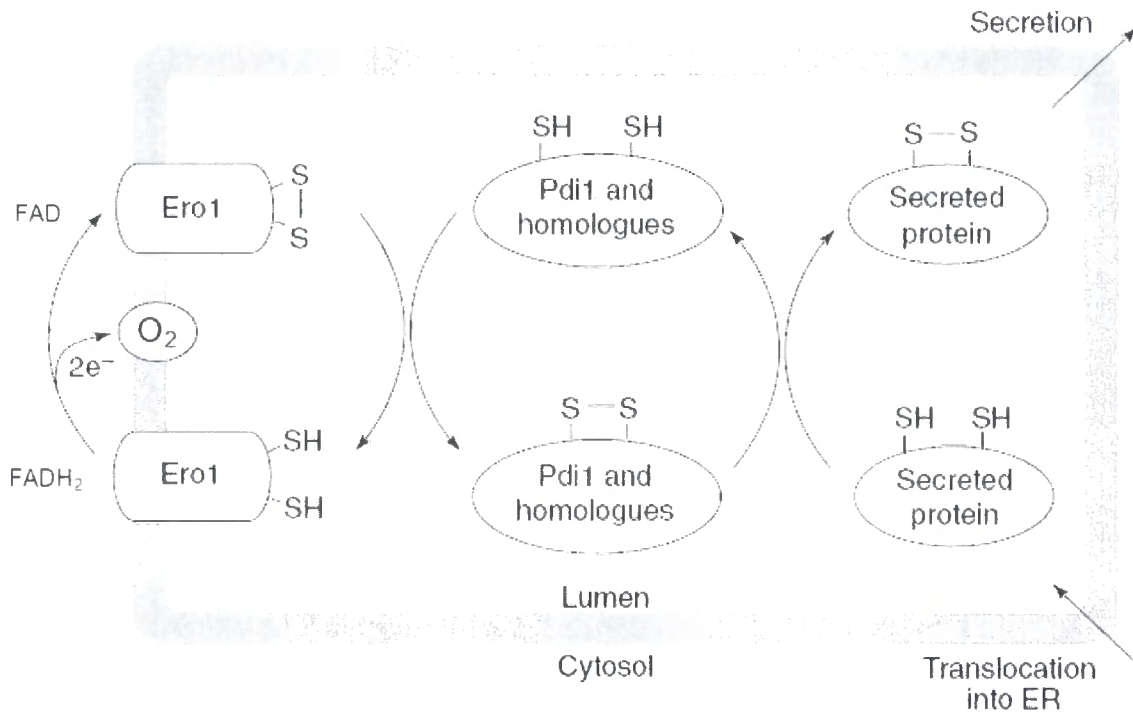
Figure 7. **Ero1p-mediated disulfide bond formation.** Nascent polypeptides enter the ER in their reduced form where there are oxidised by PDI by thiol-disulfide exchange and, if correctly folded, are secreted out of the cell. Reduced PDI is then reoxidised by Ero1 by thiol-disulfide exchange. Ero1 is then reoxidised by FAD (not shown) and two electrons are passed to a terminal electron acceptor, now identified as O_2 (O_2).Taken from Frand & Kaiser, 2000

1.5 *Thesis Aims*

This thesis endeavours to enhance our understanding of oxidative protein folding in the mammalian endoplasmic reticulum. With the identification of numerous disulfide oxidoreductases and their homologs, a concerted effort is now required to characterise these proteins and answer the question: why is there a need for so many different oxidoreductases? The recent identification of the EROs has led to a more complete understanding of the disulfide bond formation/rearrangement pathway, but still leaves many questions unanswered, including the role of FAD in providing oxidising equivalents (Tu and Weissman, 2002) and the unusual tissue distribution of the human EROs (Cabibbo *et al.*, 2000; Pagani *et al.*, 2000).

Although no co-crystallisation data exists for Ero1p and Pdi1p, biochemical evidence of disulfide-dependent PDI-Ero1-Lα binding has been obtained (Chakravarthi and Bulleid, 2004; Molteni *et al.*, 2004) and also very recently interactions between both PDI and the PDI homolog ERp44 with Ero1-Lβ have been characterised (Dias-Gunasekara *et al.*, 2005; Mezghrani *et al.*, 2001; Otsu *et al.*, 2006). The recent discovery of the formation of hERO homodimers (Dias-Gunasekara *et al.*, 2005) raises important questions about the role of hEROs in disulfide bond formation and shows us that the mammalian ER oxidation machinery is more complex than anticipated. This work aims to develop an understanding of hERO-hERO and hERO-PDI interactions, focusing particularly on the G252S and H254Y mutations in the hERO FAD-binding site.

The use of specific antibodies to study protein interactions is well documented. It is essential that antibodies recognise only the target protein the antibody was raised against. When using antibodies to study protein interactions, it is imperative that the antibodies are fully characterised, identifying any cross-reactivity and background signals as well as confirming recognition of the target protein. Our current anti-peptide polyclonal anti-Ero1-Lβ antibody is unable to immunoprecipitate Ero1-Lβ. Since co-immunoprecipitation is a powerful tool in elucidating protein interactions, an antibody that will immunoprecipitate Ero1-Lβ will prove helpful in these studies. This work helps characterise a polyclonal antibody raised against a recombinant, truncated human Ero1-Lβ.

In 1997, work by Desilva and colleagues led to the isolation of the pancreatic oxidoreductase pancreatic protein disulfide isomerase PDIp (Desilva *et al.*, 1997). PDIp shares around 46% identity with PDI as well as identical domain organisation (Desilva *et al.*, 1996). Since its initial characterisation, it has been speculated that PDIp is required for the folding of pancreas-specific proteins like zymogen, although this has not yet been substantiated by experimentation. PDIp has, however, been shown to bind misfolded RNase A and zymogen-derived peptides (Klappa *et al.*, 1998b). The interactions of PDIp with the endoplasmic reticulum oxidoreductins alpha and beta have yet to be characterised. This work investigates the interactions of hEROs with PDI and its homologue PDIp.

Finally, this work also aims to study the relationship between the UPR and the ER folding machinery, using the overexpression of the major histocompatability complex (MHC) class I molecule, HLA-B27, as a model.

Chapter 2

Materials & Methods

2. Materials and Methods

2.1 *Cell Lines, Tissues and Antibodies*

Rat pancreatic AR42J cells and human pancreatic Panc1 cells were maintained in Dulbecco's modified Eagle's medium (D-MEM) (Invitrogen), human cervical carcinoma HeLa cells were maintained in minimum essential medium (MEM) (Invitrogen), human lymphoblastoid, WEWAK1, JESTHOM, HOM-2 (all from ECACC) and the human monocyte THP1 (a gift from J. Robinson, Newcastle University, UK) cells were maintained in RPMI 1640 (Invitrogen). All cell lines were supplemented with 8 % foetal calf serum (FCS) (Sigma) (except AR42J which received 10% FCS), 2 mM Glutamax, 100 units ml^{-1} penicillin and 100 µl ml^{-1} streptomycin (Invitrogen) and propagated at 37 °C under 5 % CO_2. Sterile cell culture passage took place every 2-4 days. Pancreatic tissue was obtained from CD1 mice.

The polyclonal rabbit antisera against PDI (Benham *et al.*, 2000), Ero1-Lα (D5) (Mezghrani *et al.*, 2001) and Ero1-Lβ (Dias-Gunasekara *et al.*, 2005) have been described. The mouse monoclonal antibody HA-7 (Sigma) and the anti-myc monoclonal antibody 9B11 (Cell Signalling) were both commercially available. The HC10 monoclonal antibody was a gift from J. Neefjes, Netherlands Cancer Institute, The Netherlands. The rabbit polyclonal anti-PDIp antibody was a gift from M. S. Lan, Children's Hospital New Orleans, USA.

2.2 *Constructs*

The cDNA encoding HLA-B27*05 (verified by DNA sequencing) was a gift from J. Neefjes (Netherlands Cancer Institute, The Netherlands). The cDNA encoding PDIp (verified by DNA sequencing) was a gift from M. S. Lan, Children's Hospital New Orleans, USA. The wild-type pcDNA3Ero1-Lβ-HA and pcDNA3Ero1-Lβ-myc constructs were a gift from R. Sitia, San Raffaele Del Monte Tabor Foundation, Milan, Italy. The Ero1-LβG252S and Ero1-LβH254Y mutant constructs have been described (Dias-Gunasekara *et al.*, 2006). The pcDNA3PDILT-myc construct has been described (van Lith *et al.*, 2005).

2.3 *Digestion and Ligation*

Constructs and vectors were restriction digested for 2 h at 37 °C and subsequently analysed by on a 1 % agarose gel. DNA was cut from the gel and purified using the gel extraction kit (Qiagen). Purified DNA was run on a 1 % agarose gel with standard concentration of DNA. Concentration of purified DNA was estimated using the pixel definition programme TINA 2.0. Ligation was performed at room temperature for either 2 h or overnight with T4 DNA ligase (Promega) using various vector:insert ratios. DH5α was subsequently transformed with post-incubation ligation reactions and plated.

2.4 *Cell Transfection*

Sub-confluent HeLa cells in 6-cm dishes were washed with HBSS (Invitrogen) and optiMEM (Invitrogen) serum-free medium. Cell transfection was performed with

lipofectAMINE 2000 (Invitrogen) according to manufacturer's instructions. Cells were transfected with 1 μg DNA for 6 h in the presence of optiMEM. Post-incubation, cells were washed with optiMEM and HBSS and replaced with complete medium. Cells were then lysed for analysis 24 h post-transfection.

2.5 *Cell Lysis*

Post-transfection cells or mouse tissue were lysed for protein analysis at 4 °C in 200 μl MNT lysis buffer (1 % Triton X-100, 30 mM Tris-HCl, 100 mM NaCl, 20 mM MES, pH 7.4) supplemented with 20 mM *N*-ethylmaleimide (NEM) and 10 μg ml^{-1} protease inhibitors chymostatin, leupeptin, antipain and pepstatin A (Sigma). Alternatively, cells were lysed in 1 ml/10 cm^2 TRI-reagent (Sigma) for RNA isolation and subsequent RT-PCR.

2.6 *Cell treatments*

Cells were grown to a density of ~2-10 x 10^5 cells/ml (calculated using a haemocytometer). THP1, HOM-2, and JESTHOM cells were then plated at a 1:2 dilution with fresh RPMI 1640 (Invitrogen). 10 mM DTT or 10 ng ml^{-1} tunicamycin (Sigma) was added to induce ER stress. Treatments were staggered in order to achieve the desired course of treatment and then subjected to MNT lysis or lysis in tri reagent for RNA analysis. 250 μl tri reagent was added to cells and vortexed. Lysed cells were stored at - 20 °C for RNA extraction according to the manufacturer's protocol. HeLa cells were washed with PBS and replaced with fresh MEM (Invitrogen) supplemented with 10 mM

DTT (Sigma) for 6 h. Cells were then washed with PBS and lysed in 389 μl tri reagent for RNA extraction according to the manufacturer's protocol. THP1 cells were grown up and plated at 1:2 with fresh RPMI 1640. Cells were treated with 20 μg ml^{-1} lipopolysaccharide to induce differentiation to macrophages. Treatments were staggered in order to achieve the desired time course. Cells were then lysed in 250 μl tri reagent for subsequent RNA extraction according to manufacturer's protocol.

2.7 RNA Isolation and RT-PCR

Total RNA from cell lines was extracted using Tri reagent (Sigma) according to the manufacturer's protocol. The concentration of extracted RNA was determined by spectrophotometry and diluted to 50 ng μl^{-1}. 50 ng total cell RNA was subjected to reverse transcriptase polymerase chain reaction (RT-PCR) using the AccessQuick RT-PCR kit (Promega). Primers for XBP1 and β-actin were used to detect the relative expression of these mRNAs. The RT-PCR cycle used was: 1h 45 °C, 2' 94 °C, (30'' 94 °C, 1' 60 °C, 1' 72 °C) 30x, 5' 72 °C, 4 °C ∞. XBP1 cDNA was then subjected to PstI digest. All cDNA was either run on 1 % or 2 % agarose gel, as indicated, at 100 mV for ~50 min before exposure to UV light.

2.8 PstI Digestion

Amplified XBP1 cDNA was subjected to PstI digest to detect the presence of spliced mRNA. If not loaded on a gel to check for signal, total RT-PCR product (or total PCR product minus 5 μl if XBP1 RT-PCR product was loaded beforehand) was digested using

1 μl enzyme in a total volume of 15 μl. Digests were for 2 h at 37 °C and then DNA was extracted from the restriction digest using the PCR purification kit (Qiagen) according to the manufacturer's protocol. Extracted digested DNA was then run on 2% agarose gel to visualise the digested and undigested DNA.

2.9 *Immunoprecipitation*

Immunoprecipitations were carried out with post-nuclear total cell lysates using 0.5 μl of anti-HA or anti-myc, 8 μl of anti-PDI or rabbit bleed antiserum immobilised on 50 μl of a 20 % suspension of Protein A sepharose beads. Immunoprecipitations were performed on a rotator for 2 h at 4 °C. Beads were then washed twice with lysis buffer before antibody was liberated by boiling. Immunoprecipitating proteins were analysed by SDS-PAGE and Western blotting.

2.10 *In vitro transcription and translation*

In vitro transcription of pcDNA3Ero1-Lα-myc and pcDNA3Ero1-Lβ-myc constructs were performed using 5 μg of DNA linearised with *EagI*, pBluescriptIIPDIp was linearised with *XbaI*, pcDNA3PDILT-myc was linearised with *MluI* and pBluescriptIIPDI was linearised with *XbaI*. T7 RNA polymerase-driven transcription reactions were performed using the Promega riboprobe system according to the manufacturer's protocol. 2 μg RNA was translated using the Flexi rabbit reticulocyte lysate (Promega) according to the manufacturer's protocol. Proteins we either translated

on their own or co-translated. Translations were subsequently analysed by SDS-PAGE and Western blotting.

2.11 *SDS-PAGE*

Samples were prepared for SDS-PAGE separation by the addition of 2x loading buffer in the presence or absence of 50 mM dithiothreitol (DTT) (Sigma), boiled for 5 min at 95 °C and spun down at 4 °C. All Blue Precision Plus protein standard (250-10 kD) (BioRad) was used as a protein marker. Samples were run on 8 % SDS-PAGE gels for ~50 min at 15 mV in 1x Tris-Glycine SDS buffer (Sigma) in order to resolve all proteins. PVDF transfer membranes (Millipore) were prepared for transfer in methanol and washed in 1x transfer buffer. Gels were then wet transferred in 1x transfer buffer for 2 h at 30 mV. Membranes were then block in 8 % milk in PBST (100 ml dm^{-3} PBS, with 0.1% Tween 20 (Sigma)) for 60 min.

2.12 *Western Blotting*

Membranes were incubated with either HC10 (1:200), anti-PDI (1:1000), anti-Ero1-Lα (D5) (1:500), anti-Ero1-Lβ (1:50), anti-HA (1:2000), anti-myc (1:4000) or anti-PDIp (1:800) antibodies for 60 min before being washed five times with PBST. Membranes were then incubated with the corresponding secondary antibody (DAKO) (anti-mouse for HC10, anti-myc and anti-HA and anti-rabbit for anti-PDI, anti-Ero1-Lα, anti-Ero1-Lβ and anti-PDIp) at 1:3000 for 60 min then subsequently washed five times with PBST.

Proteins were then visualised with 200 µl enhanced chemiluminescence fluid (Amersham) and exposed to film (Kodak).

2.13 *Insulin Reduction Assay*

The incubation mixture contained 0.18 mM insulin (Sigma) and various concentrations of dithiothreitol (DTT) (Sigma) purified PDI, purified Ero1-Lβ, Flavin adenine dinucleotide (FAD) (Sigma) or bovine serum albumin (BSA) (Sigma). Reactions were made up to 75 µl using phonate buffered saline (PBS) (Sigma). Samples were placed in a UVette (Eppendorf) at room temperature or at 37 °C for the indicated time. Turbidity was analysed at 600 nm using a spectrophotometer (Eppendorf).

Chapter 3

Results

3.1 The role of FAD in the interactions and function of Ero1-Lβ

3.1.1 Introduction

Recent genetic and biochemical studies have led to the identification of essential components of the eukaryotic oxidative protein folding machinery. The conserved ER-resident protein Ero1p is required for oxidative protein folding since compromised Ero1p function results in sensitivity to the reductant DTT and the accumulation of the reduced forms of PDI and substrate proteins (Frand and Kaiser, 1998; Pollard *et al.*, 1998). This phenotype mimics that resulting from the loss of the bacterial redox enzyme DsbB (Bardwell *et al.*, 1993). Ero1p is a membrane-associated flavoprotein able to generate disulfide bonds and transfer them to PDI which then directly catalyses disulfide formation in substrate proteins (Frand and Kaiser, 1999; Tu *et al.*, 2000). Thus, Ero1p acts as the source of oxidising equivalents for PDI-mediated oxidative substrate folding.

Overexpression of *FAD1*, which converts flavin mononucleotide (FMN) to flavin adenine dinucleotide (FAD) was able to suppress the temperature sensitivity of the *ero1-1* mutant indicating that oxidative folding in yeast is dependent on levels of free FAD (Tu *et al.*, 2000). An *in vitro* model was constructed with purified components to test this theory and it was subsequently found that reactivation of denatured and reduced RNase A depends on the presence of PDI, ERO1 and oxidised flavin adenine dinucleotide (FAD) (Tu and Weissman, 2002). Under anaerobic conditions, free FAD alone is insufficient to drive

Ero1p-mediated disulfide formation and thus is not an efficient terminal oxidant for Ero1p (Tu and Weissman, 2002). Using an oxygen consumption assay, Tu and Weissman were able to show that in the presence of free FAD, Ero1p can couple its reoxidation directly to the reduction of O_2 (Tu and Weissman, 2002). Thus, Ero1p is able to harness the oxidising potential of molecular oxygen for the formation of disulfide bonds.

The high sensitivity of Ero1p to levels of free FAD is unusual since most flavoproteins contain tightly bound flavin cofactors. It has since been suggested that a cofactor relay system may exist where tightly bound FAD could pass electrons onto unbound FAD, which could then deliver them to a terminal electron acceptor. Sensitivity to free FAD could provide an important mechanism by which to regulate oxidative folding by coupling protein oxidation to folding load and/or the metabolic status of the cell, since FAD transport into the ER is a prerequisite for its oxidative effect (Papp *et al.*, 2005; Tu and Weissman, 2002). Given that a standard two-electron reduction of molecular oxygen produces hydrogen peroxide (H_2O_2), uncontrolled levels of Ero1p oxidase activity could lead to the production of reactive oxygen species (ROS), an over-oxidised ER and/or protein misfolding (Tu and Weissman, 2004). Regulation at the level of production of oxidising equivalents would potentially allow for efficient management of total oxidative folding in the ER. Interestingly, *RIB1*, the enzyme responsible for the first steps of riboflavin biosynthesis, is itself a target of the unfolded protein response (UPR) (Travers *et al.*, 2000).

Despite genetic and biochemical approaches confirming the essential components of Ero1p-mediated oxidative folding, it was not until 2004 that the mechanism by which FAD passes oxidising equivalents to Ero1p began to be elucidated. Gross and colleagues published the crystal structure of FAD-bound Ero1p in 2004 revealing the molecular details of the catalytic centre and the relationship between the functionally significant cysteines and the bound cofactor (Gross et al., 2004). Ero1p is predominantly α-helical with five short β-sheets and two extended loops (Fig. 1A). The position of the catalytically active C-X-X-C domain at Cys^{325}-Cys^{355} and Cys^{100}-Cys^{105} corroborates data from Frand & Kaiser in which PDI interacts with, and passes electrons to, Ero1p via its Cys^{100}-Cys^{105} active site which in turn transfers them internally to Cys^{352}-Cys^{355} (Frand and Kaiser, 2000). Further crystallographic evidence confirms the presence of a disulfide relay where Cys^{100} and Cys^{105} are located on a flexible loop capable of changing conformation by 17Å bringing Cys^{105} within disulfide-bonding distance of Cys^{352}.

Interestingly, the Cys^{352}-Cys^{355} disulfide is positioned adjacent to the FAD cofactor allowing this disulfide to be readily oxidised via FAD interaction (Fig 1B). Thus, electrons are transferred from a folding substrate to the catalytic active site of PDI to the Cys^{100}-Cys^{105} disulfide of Ero1p, intramolecularly to the Cys^{353}-Cys^{355} disulfide and then onto the bound FAD cofactor which may then transfer electrons to the pool of unbound FAD.
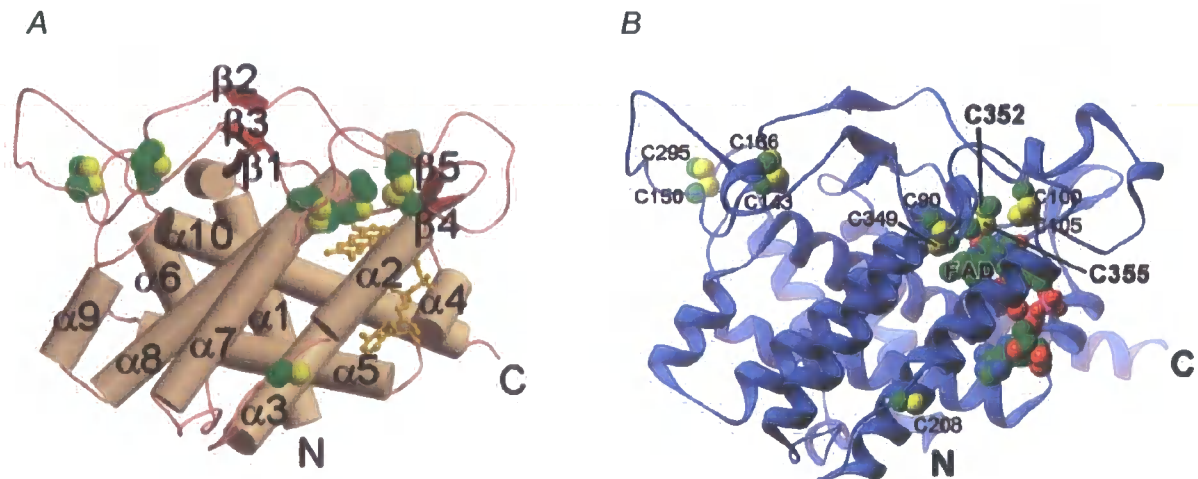
Figure 1. **Crystal structure of Ero1p.** A, Ero1p crystal structure with α-helices represented as cylinders (grey) and β-sheets as arrows (red). Secondary structural elements are numbered. B, The same view as in A is shown. Cysteine residues are labelled with the active site cysteines nearest FAD in bold. Ero1p crystal structure data taken from (Gross et al., 2004).

Ero1p shows structural similarity to the yeast sulfhydryl oxidase Erv2p despite sharing little or no sequence homology. Both molecules contain active site cysteine pairs in a C-X-X-C motif adjacent to the isoalloxazine ring of a bound FAD molecule. Four of the eight α-helices of Ero1p can be superimposed onto the helical bundle of Erv2p. However, the order of the helices in the primary structure is different (Gross et al., 2004). These two molecules differ in the way that electrons might exit FAD. Erv1p possesses a short clear channel leading directly to the N5 nitrogen lined with hydrophobic residues. Ero1p however, possesses no such channel and FAD is in fact buried within the Ero1p molecule

unavailable for molecular oxygen, or any other terminal electron acceptor, to gain access to the isoalloxazine ring of the bound FAD. This difference is reflected in their behaviour, with Erv2p restricted to using molecular oxygen as a terminal electron acceptor whilst Ero1p has been shown to be use other terminal electron acceptors under anaerobic conditions (Cuozzo and Kaiser, 1999).

The lethal temperature-dependent *ero1-1* mutant and the *ero1-2* mutant, which shows hypersensitivity to the reducing agent DTT, are both the result of a two separate single substitutions within the Ero flavin fold (Frand and Kaiser, 1998; Pollard *et al.*, 1998). The *ero1-1* mutation is a G229S substitution in Ero1p which is equivalent to Gly^{252} in the human ERO (hERO) Ero1-Lβ. The *ero1-2* mutation is H231Y which is equivalent to His^{254} in Ero1-Lβ. The remaining six points of contact between Ero1p and FAD are conserved in Ero1-Lα and Ero1-Lβ. The phenotypes of these mutants are most likely due to an interruption in the binding of FAD to Ero1p leading to a loss of function. Mutated FAD-binding motifs could potentially result in an unstably bound FAD or result in bound FAD being at a position when it is unable to react with the catalytic Cys^{352}-Cys^{355} disulfide. Thus, *ero1* mutants may prevent electron transfer. The aim of this work is to biochemically characterise *ero1* mutant interactions to further understand the role of FAD in oxidative protein folding.

The work in this chapter was carried out in parallel to the publication of Dias-Gunasekara and colleagues' work of 2005 and 2006 and accordingly contains data that relates to this

published work (Dias-Gunasekara *et al.*, 2005; Dias-Gunasekara *et al.*, 2006). Any conclusions derived from data leading directly to those publications during the course of my work are not referenced and are instead referred to as observations by the group. Some observations referred to as 'data not shown' are now published in the aforementioned articles.

3.1.2 Results

3.1.2.1 *Ero1-Lβ forms homodimers in vivo*

Both Ero1-Lα and Ero1-Lβ have been shown to form mixed disulfides with PDI, corroborating their role in providing oxidizing equivalents for disulfide bond formation *in vivo* (Cabibbo *et al.*, 2000; Mezghrani *et al.*, 2001). The presence of disulfide-dependent complexes in Ero1-Lβ C-X-X-C-X-X-C mutants that scarcely interacted with PDI (Data not shown) led to the speculation that Ero1-Lβ might form homodimers, especially as other members of the thioredoxin-like family can exist as homodimers (Liepinsh *et al.*, 2001). The formation of human Ero homodimers has also been postulated by others (Mezghrani *et al.*, 2001).

To investigate the homodimerisation of Ero1-Lβ and the formation of disulfide-dependent high-molecular weight complexes, two differentially tagged Ero1-Lβ proteins were constructed. A triple-tagged Ero1-Lβ-myc protein and a single-tagged Ero1-Lβ-HA (haemagglutinin) protein enable monomeric forms of the protein to be visible as two distinct bands on SDS-PAGE separation due to the different tag size (Fig. 2A). Other groups have shown that myc- and HA-tagged human Eros reside within the ER and are functionally comparable to their non-tagged equivalents (Anelli *et al.*, 2002; van Lith *et al.*, 2005) (S. Dias-Gunasekara and A.M. Benham, unpublished data).

Under non-reducing conditions, disulfide-dependent high molecular weight complexes are visible as a distinct band or a number or bands migrating higher up in the gel. Hence, transfected lysates were examined by SDS-PAGE in the absence of DTT, Western blotting for the Ero1-Lβ-myc using the α-myc mAb (Fig. 2B). The original lysates were generated by lysing in the presence of the alkylating agent N-Ethylmaleimide (NEM) which traps free cysteines. The use of an alkylating agent when studying disulfide-linked complexes in vivo also prevents the formation of post-lysis complexes. Monomeric Ero1-Lβ-myc was detected lower down in the gel (Fig. 2B, lanes 1 and 3). As expected, no HA-tagged Ero1-Lβ was detected. High-molecular weight complexes were detected in the WT-myc and WT-myc/WT-HA transfected lanes (Fig. 2B, lanes 1 and 3) and represented disulfide-dependent complexes.

In order to further investigate the components of the disulfide-dependent complexes seen in Figure 2B, lysates were prepared as before, transfecting HeLa cells with wild-type Ero1-Lβ either myc-tagged, HA-tagged or transfecting with both. Again, lysates were resolved on SDS-PAGE but this time membranes were immunoblotted with monoclonal antibodies to both tagged proteins (α-HA and α-myc) (Fig. 3A). Extensive high-molecular weight complexes were detected, as well as the monomeric form of Ero1-Lβ (Fig. 3A, lanes 1-3). The anti-myc and the anti-HA antibodies differed in their success at recognizing tagged Ero1-Lβ in non-reducing gels, as seen with the levels of monomeric Ero1-Lβ detected (Fig. 3A, compare lanes 1 and 3 with lane 2). This has also been observed by other investigations in our group (data not shown).
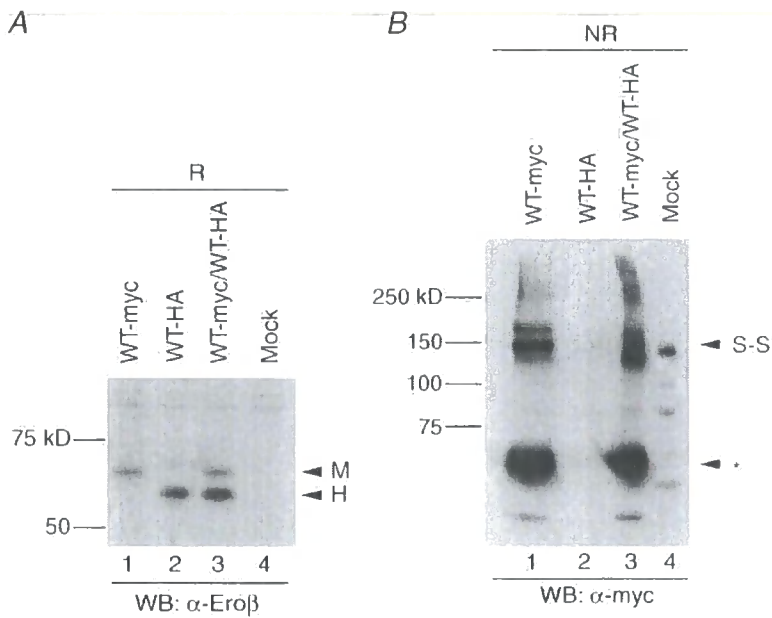
Figure 2. **Ero1-Lβ forms disulfide-dependent complexes in vivo.** *A,* Reducing gel (R) showing distinct migration of differentially tagged wild-type (WT) Ero1-Lβ. HeLa cells were subjected to liposome-mediated transfection of either a myc-tagged Ero1-Lβ (lane 1), HA-tagged Ero1-Lβ (lane 2), or myc- and HA-tagged double transfected Ero1-Lβ (lane 3) or mock transfected (lane 4) which were separated by SDS-PAGE and immunoblotted for using the α-Eroβ pAb. Myc-tagged (M) and HA-tagged (H) Ero1-Lβ are indicated. *B,* The same HeLa transfectants, lysed in the presence of NEM, were analysed under non-reducing conditions in order to preserve any disulfide-dependent complexes. Monomeric Ero1-Lβ (*) was detected using α-myc (lanes 1 and 3) and high-molecular weight complexes are visible ~150 kD in these lanes (S-S).

Complexes were more abundant in the double transfected sample (Fig. 3A, lane 3) where three distinct bands were detected. The uppermost and lowermost bands seen in the double transfected lysate correspond to high-molecular weight bands seen in the WT-myc transfected and WT-HA transfected samples respectively. These distinct bands are the result of myc-tagged homodimers (Fig. 3A, lane 1) and HA-tagged homodimers (Fig. 3A, lane 2). The middlemost band seen in the double transfected lysate is the result of homodimerisation of a myc- and an HA-tagged Ero1-Lβ.

To confirm an Ero-Ero interaction, HeLa cells were transfected as before and lysed in the presence of NEM. Lysates were subjected to immunoprecipitation with Protein A Sepharose beads. Immunoprecipitation involves the interaction of a protein of interest with an antibody conjugated to a Protein A bead (Fig. 3B). We took advantage of the differently tagged Ero1-Lβ molecules by conjugating the anti-myc antibody to Protein A sepharose beads to isolate the myc-tagged Ero1-Lβ in the transfected lysates. Once isolated, immunoprecipitates were taken up in loading buffer and separated by SDS-PAGE. To determine if Ero1-Lβ-HA indeed interacted (co-immunoprecipitated) with Ero1-Lβ-myc, the membrane was immunoblotted with anti-HA (Fig. 3C). Ero1-Lβ-HA was detected in the double transfected lysate, indicating that it had been pulled down with the anti-myc antibody via interaction with the myc-tagged Ero1-Lβ (Fig. 3C, lane 3). As expected, no signal, except antibody bands, was detected in the single transfected samples since Ero1-Lβ-HA was not pulled down by the protein A-conjugated anti-myc and the transfected Ero1-Lβ-myc was not recognized by immunoblotting with anti-HA. As a

control, non-IP samples were blotted for PDI showing comparable levels of protein in the lysates used (Fig. 3D). Taken together, (with the work of Dias-Gunasekara and colleagues) these data show that Ero1-Lβ is capable of forming extensive disulfide-dependent complexes. A major component of these complexes is disulfide-dependent Ero1-Lβ homodimers.
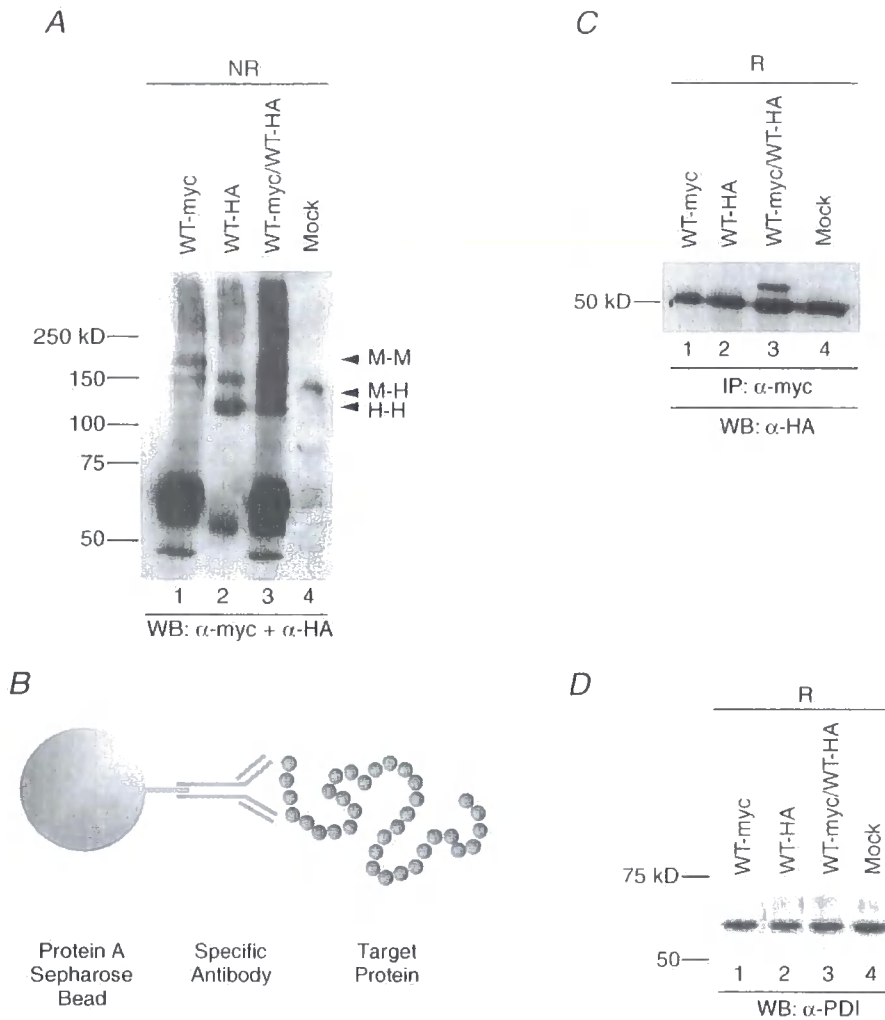
Figure 3. **Ero1-Lβ is capable of forming homodimers.** *A*, HeLa cells were transfected with either Ero1-Lβ-myc (WT-myc) (lane 1), Ero1-Lβ-HA (WT-HA) (lane 2), double transfected with both Ero1-Lβ-myc and Ero1-Lβ-HA (WT-myc/WT-HA) (lane 3) or mock transfected (lane 4). Proteins were lysed in the presence of NEM and resolved on a non-reducing (NR) SDS-PAGE gel before being subject to immunoblotting with using anti-myc and anti-HA. High-molecular weight complexes were resolved in all transfected lysates (compare lanes 1-3 with lane 4). A distinct band in lanes 1 and 3 was resolved corresponding to a WT-myc homodimer (M+M). Equally, a distinct band was seen in lanes 2 and 3 corresponding to a WT-HA homodimer (H+H). The WT-myc-WT-HA homodimer (M+H) was only observed in the double transfected sample (lane 3). *B*, Lysates of single and double tagged transfectants were obtained as in *A*. Immunoprecipitation was performed using the anti-myc antibody and immunoblotting with the anti-HA mAb. Anti-myc antibody heavy chain (HC) can be seen in all four IP samples migrating as a distinct band at ~50 kD (lanes 1-4). Ero1-Lβ-HA was detected (lane 3) after IP with the anti-myc mAb indicating an *in vivo* interaction between Ero1-Lβ -myc and Ero1-Lβ-HA.*C*, A protein A sepharose bead is conjugated to an antibody during incubation. Proteins in a cell lysate, for example, are isolated using an antibody specific for that protein. The mixture is then centrifuged and the supernatant removed isolating the target protein, and any associated molecules, for further analysis.   *D*, The same lysates used for the IP in B, were subjected to reducing (R) SDS-PAGE and immunoblotting with the pAb anti-PDI as a positive control for transfection.

3.1.2.2 *Mutations in the FAD-binding site of Ero1-Lβ diminish, but do not prevent interaction with PDI*

We next investigated the biochemical properties of the Ero1-Lβ equivalent of the temperature sensitive mutant *ero1-1* and the DTT-hypersensitive mutant *ero1-2*. Ero1p and Ero1-Lβ share conserved FAD binding residues (Fig. 4). We therefore engineered point mutations in Ero1-Lβ that corresponded to the *ero1* mutations. Site-directed mutagenesis was employed to produce myc-tagged Ero1-LβG252S and Ero1-LβH254Y mutants for functional analysis.

Firstly, expression of both mutant constructs was verified by transfection into HeLa cells. Tagged constructs were then immunoblotted with anti-Ero1-Lβ and anti-myc (Fig. 5A and B). Anti-Ero1-Lβ antibody recognised both wild-type Ero1-Lβ and the H254Y mutant (Fig. 5A, lanes 1 and 2). However, recognition of Ero1-Lβ G252S was relatively low (Fig. 5A, compare lanes 1 and 2 with lane 3). This is likely due to transfection efficiency or loading. Both mutants were constructed with C-terminal triple myc tags. Mutations in the FAD-binding domain of Ero1-Lβ should not affect their recognition by the anti-myc antibody since that epitope is located at the C-terminus of the protein.

Wild-type and mutant Ero1-Lβ transfected lysates were resolved by non-reducing SDS-PAGE, transferred to nitrocellulose and subjected to immunoblotting using the anti-myc antibody (Fig. 5B). Both wild-type and mutant monomeric Ero1-Lβ was resolved at equal

intensity (Fig. 5*B*, lanes 1-3) suggesting that stability of Ero1-Lβ was not compromised by G252S or H254Y mutations. By subjecting transfected lysates to non-reducing SDS-PAGE, we were also able to resolve a collection of trapped high-molecular weight species presumably composed of covalently interacting proteins (Fig. 5*B*, lanes 1-3).

PDI is a component of wild-type Ero1-Lβ complexes (Cabibbo *et al.*, 2000; Mezghrani *et al.*, 2001). We investigated the binding of Ero1-Lβ FAD-binding mutants with PDI in order to a) identify a component of the high molecular weight complexes formed under non-reducing conditions (Fig. 5*B*) and b) investigate the effect of point mutations in the FAD-binding site of Ero1-Lβ on association with its electron donor PDI.

Under non-reducing conditions both G252S and H254Y not only ran as a monomer but as a collection high-molecular weight complexes (Fig. 5*B*, lanes 2 and 3). Both mutant and wild-type lysates were then analysed for co-immunoprecipitation with the anti-PDI antisera (Fig. 5*C* and *D*). Both mutants specifically co-immunoprecipitated with PDI but to a lesser extent than wild-type Ero1-Lβ (Fig. 5*C*, compare lanes 2 and 3 with lane 1 and Fig. 5*D*, compare lanes 2 and 3 with lane 1). High-molecular weight co-immunoprecipitation complexes are visible in the non-reduced SDS-PAGE gel after anti-

A

B

C
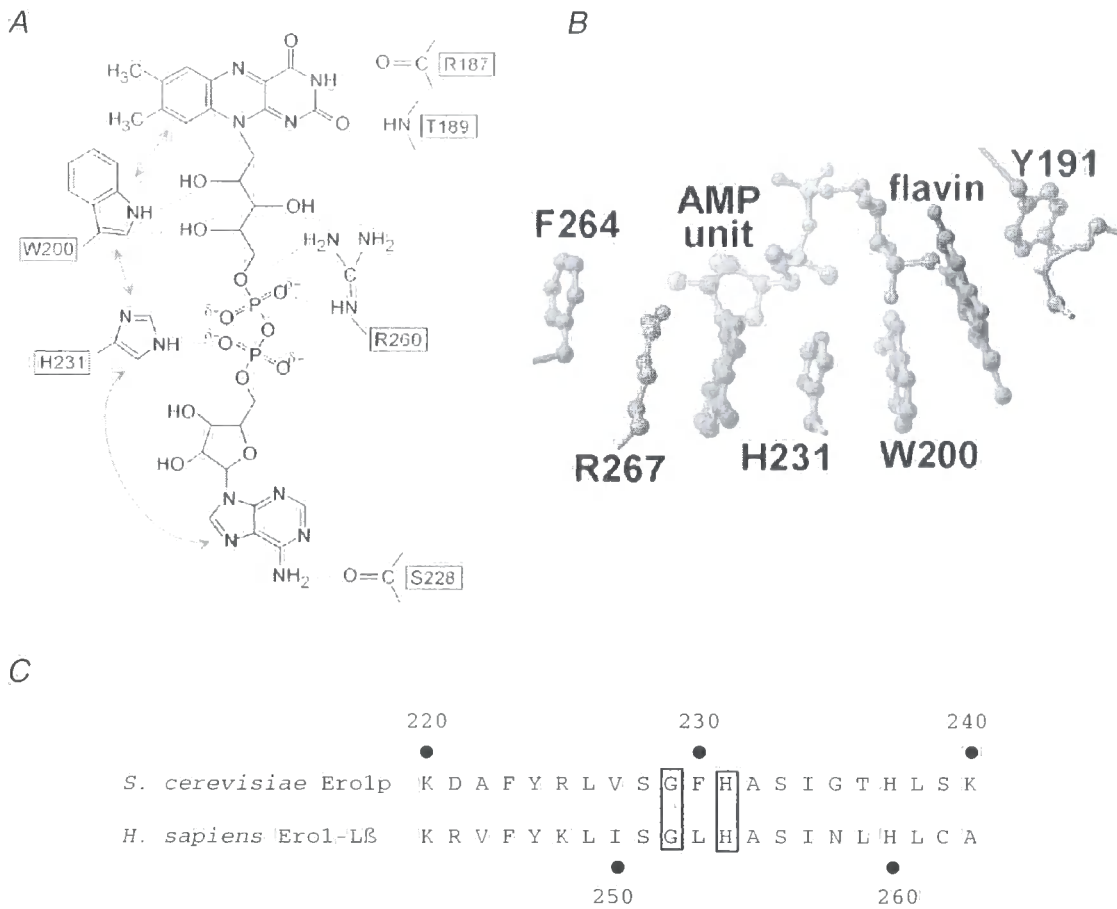
Figure 4. **Points of contact between flavin adenine dinucleotide (FAD) and yeast Ero1p.**
A, The FAD cofactor is held between helices $\alpha2$ and $\alpha3$ with the isoalloxazine and adenine rings buried in the protein. Ero1p makes a variety of contacts with FAD. Dashed lines indicate putative hydrogen bonds or salt bridges while double headed arrows represent stacking interactions between amino acid side chains and ring systems in the FAD. *B*, Residues involved in aromatic ring stacking are further illustrated in this ball and stick diagram. Residues are numbered based on the full length Ero1p sequence. *C*, Ero1p and human Ero1-Lβ protein sequence alignment showing the level of conserved residues. The *ero1-1* and *ero1-2* mutations Ero1p G229S and H231Y correspond to G252S and H254Y in Ero1-Lβ. Ero1p crystal structure data taken from (Gross *et al.*, 2004).

PDI immunoprecipitation (Fig. 5D, lanes 1-3). These complexes represent NEM-dependent, covalent, disulfide-dependent Ero1-Lβ-PDI dimers. The G252S mutant in particular, showed little association with PDI in the non-reducing gel compared to wild-type Ero1-Lβ and the mock sample suggesting that mutations in the FAD-binding site affected the ability of Ero-Lβ to disulfide bond with PDI. In the non-reduced gel, H254Y complexes resolve to a tight band, albeit less intense than wild-type (Fig. 5D, lane 2). Ero1-Lβ G252S and H254Y, both form non-disulfide-dependent complexes with PDI however, association is not as strong as wild-type Ero1-Lβ-PDI interactions. (Fig. 5C).

3.1.2.3 *The G252S and H254Y mutants are able to form homodimers*

Having shown that wild-type Ero1-Lβ is capable of forming homodimers we were interested in seeing if our FAD-binding mutants were able to dimerise. This would allow us to examine whether the *ero1-1* or *ero1-2* phenotypes could be explained by a failure of mutant Eros to self complex. The pattern of high-molecular weight complexes in the G252S and H254Y mutants was similar to that of the wild-type Ero1-Lβ (Fig. 5*B*, compare lanes 2 and 3 with lane 1), suggesting that, like wild-type Ero1-Lβ, homodimers may make up a portion of those complexes. The majority of Ero1-Lβ-PDI interactions are covalent (Fig. 5*B* and *D*) (Benham *et al.*, 2000; Mezghrani *et al.*, 2001; Pagani *et al.*, 2000) and occur via cysteine-cysteine interaction. Impaired Ero1-Lβ-PDI interaction might suggest that homodimer formation may also be impaired.

G252S and H254Y mutants with a single haemagglutinin tag were used to study interactions with their myc-tagged equivalents. The expression of the HA-tagged proteins was studied by single or co-transfection and subsequent anti-Ero1-Lβ immunoblotting after SDS-PAGE gel separation under non-reducing (Fig. 6*A*) or reducing (Fig. 6*B*) conditions. Differentially tagged proteins migrated into two distinct bands, as previously demonstrated (Fig. 2*A*). Expression of mutant-tagged proteins in this instance was slightly lower when compared with wild-type (Fig. 6*B*, compare lanes 1, 2 and 4 with lanes 3 and 5). Upon non-reducing analysis, HA-tagged single transfectants were not detected either in their monomeric or multimeric forms (Fig. 6*A*, lanes 2 and 3). This is consistent with other results showing that the Ero1-Lβ serum is inefficient at determining
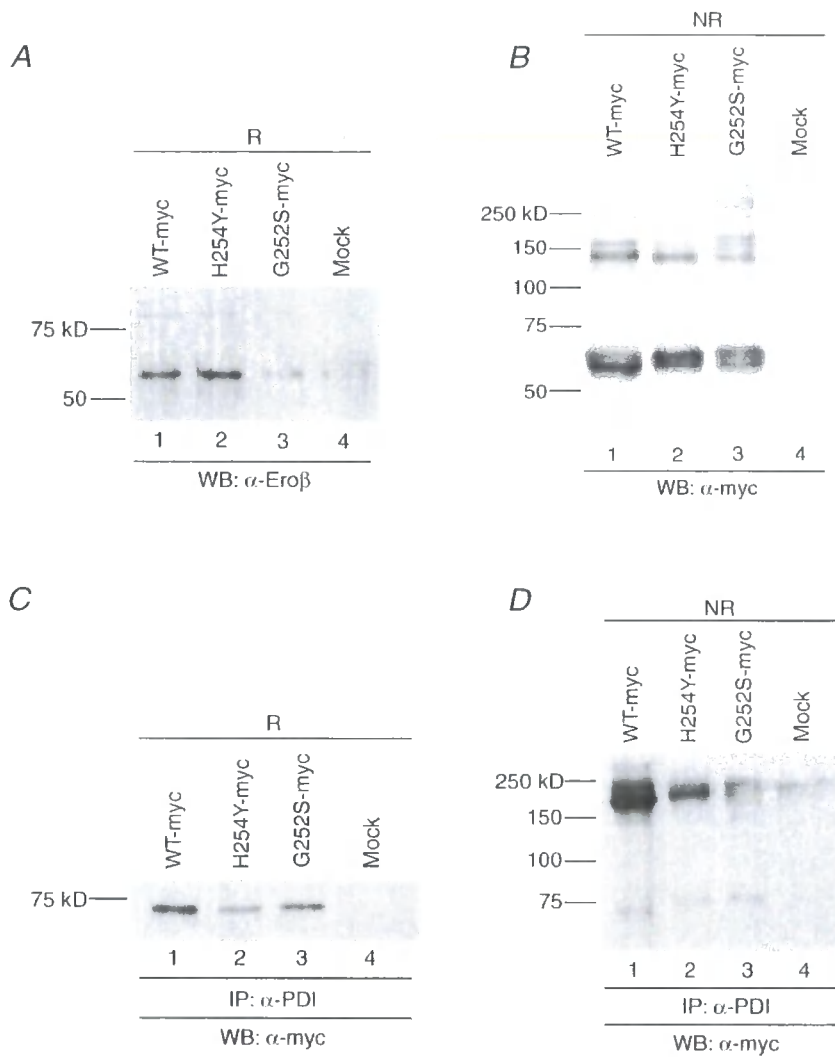
Figure 5. **Ero1-Lβ FAD mutants G252Y and H254Y form disulfide-dependent complexes despite poor association with wild-type PDI.** *A*, HeLa cells were transfected with myc-tagged wild-type Ero1-Lβ (WT) (lane 1), H254Y mutant (lane 2), G252S mutant (lane 3) or mock (lane 4). Post-nuclear lysates were analysed under reducing conditions (R) and immunoblotted for α-Eroβ. *B*, lysates were obtained as in *A* but were subjected to non-reducing (NR) SDS-PAGE and immunoblotted with α-myc to resolve both the monomeric form and the high-molecular weigh complexes. *C, D*, Lysates were prepared as in *A* and immunoprecipitated with α-PDI. Lysates were then immunoblotted with α-myc to detect any co-immunoprecipitating Ero1-Lβ under reducing (R) conditions (*C*) or non-reducing conditions (*D*).

non-reduced Ero1-Lβ (S. Dias-Gunasekara and A.M. Benham, unpublished data). The anti-HA antibody was then used in order to detect high-molecular weight complexes. Post-nuclear lysates were then subjected to immunoprecipitation using the anti-myc antibody, were analysed by SDS-PAGE under non-reducing conditions and immunoblotted using the anti-HA antibody (Fig. 6C). No complexes other than antibodies were resolved since disulfide bonded antibody bands migrate in the same area of interest as Ero complexes. In order to resolve this issue, the same co-immunoprecipitated samples were subjected to reducing SDS-PAGE and immunoblotted using the anti-Ero1-Lβ antibody (Fig. 6D). The anti-Ero1-Lβ antibody recognised both myc-tagged and HA-tagged Ero1-Lβ as expected (Fig 6D, lanes 1-3). Mock and single HA-tagged transfectants were not recognised by anti-myc immunoprecipitation and thus, were blank when blotted for Eroβ (Fig. 6D, lanes 4-6). H254Y-HA, G252S-HA and WT-HA tagged Ero1-Lβ clearly co-immunoprecipitated with H254Y-myc, G252S-myc and WT-myc respectively (Fig. 6D, lanes 1-3). The co-immunoprecipitation of differentially tagged Ero1-Lβ suggests that both wild-type and the FAD-binding mutants G252S and H254Y are capable of forming homodimers. Thus, point mutations in the FAD-binding domain do not prevent self-complexing or the formation of homodimers within the ER.
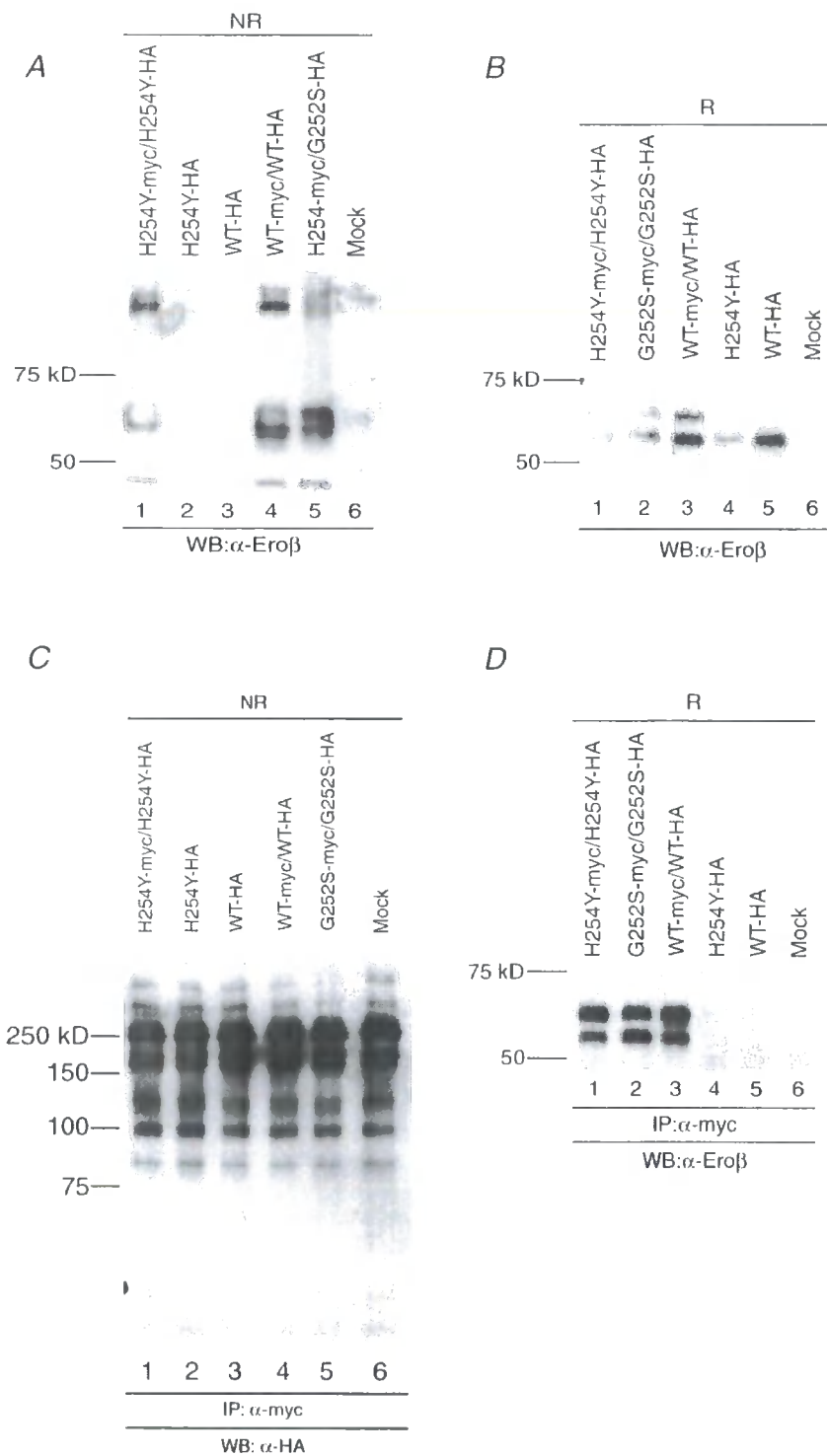
Figure 6. **The FAD-binding mutants of Ero1-Lβ are able to form homodimers.** *A*, HeLa cells were either single (lanes 2 and 3), double transfected (lanes 1 and 4-5) or mock transfected (lane 6) with wild-type (WT) (lanes 3 and 4) or mutant (lanes 1,2 and 5) Ero1-Lβ. Cells were lysed in the presence of NEM and subjected to non reducing (NR) SDS-PAGE in order to resolve monomeric and high-molecular weight complexes. Membranes were immunoblotted with the anti-Eroβ antibody. *B*, Lysates used in *A* were subjected to reducing (R) SDS-PAGE to disrupt and disulfide bonds and immunoblotted with the anti-Eroβ antibody. *C*, Lysates were subjected to immunoprecipitation (IP) with the anti-myc mAb using Protein A Sepharose beads. Co-immunoprecipitating molecules were then analysed by non-reducing SDS-PAGE and immunoblotted for anti-HA in order to visualise the formation of both covalent and non-covalent complexes. *D*, Lysates subjected to the IP in *C* were analysed under reducing conditions and imunoblotted for Ero1-Lβ using the anti-Eroβ antibody.

3.1.2.4 *Assessment of Ero1-Lβ in an insulin reduction assay*

Next we wished to study the functional activity of the purified protein using a closed *in vitro* system mimicking the components of the oxidative folding machinery present *in vivo*. The use of a spectrophotometric insulin assay was pioneered by Luthman in 1979 to study mammalian thioredoxin and thioredoxin reductase and was subsequently used by the group to study other members of the thioredoxin-like family (Holmgren, 1979; Lundstrom and Holmgren, 1990; Luthman and Holmgren, 1982). A simplified version of this assay was used to study the activity of purified Ero1-Lβ. The assay exploits the fact that, upon the reduction of insulin by the reductant DTT, intra-chain disulfide bonds in insulin are disrupted, leading to precipitation of the protein and an increase in turbidity. In a closed system mimicking that of oxidative folding *in vivo*, PDI will be able to recharge DTT by Ero1-mediated oxidation leading to the continual reduction of insulin. We were interested in seeing what effect Ero1-Lβ would have on PDI reductase activity and to confirm that Ero1-Lβ does not act directly on substrates as an oxidoreductase.

Firstly, reduction of insulin by DTT was optimised. It was important that levels of reduction were not too high prior to the introduction of oxidoreductases since catalysis of this reaction could send readings into an unreliable range. Insulin was used at 0.18 mM, a concentration within the range of published work (Lundstrom and Holmgren, 1990) and the effect of three concentrations of DTT were studied in a volume of 75 µl. Phosphate buffered saline (PBS) made up the remainder of the reaction volume and was therefore used to blank the OD readings. Readings were taken at 600 nm every 10 minutes for

approximately 2 hours at room temperature (Fig. 7A). As expected, PBS remained at baseline absorbance throughout the 180 minutes. A higher concentration of DTT caused quicker (OD_{600} reading of 0.5 after ~20 m with 10 mM DTT compared with ~35 m with 5 mM DTT) reduction of insulin and a higher end point (OD_{600} ~2.1 with 10mM DTT compared with ~1.75 with 5 mM DTT) due to the fact that more insulin was reduced. Since our spectrophotometer was accurate within a range of OD_{600} ~0.2-2.0, the absorbance levels were too high. Thus, a concentration of 3 mM DTT was used instead (Fig. 7B). During this assay, 0.87 μM of the purified enzyme PDI was introduced to see if it had an effect on insulin reduction. Upon the addition of PDI to the assay, levels of reduced insulin began to rise within ~20 minutes compared to that of the non-catalysed reactions which only showed levels of reduction above baseline after ~40 minutes. The use of 3 mM DTT produced levels of insulin reduction outside of the accuracy of the photospectrometer after 2 hours. However, when compared to the initial experiment, in which levels of insulin reduction were seen after ~20 minutes (10 mM DTT) and ~35 minutes (5mM DTT) (Fig. 7A), the use of 3 mM DTT does delay reduction somewhat.

A

The uncatalysed reduction of insulin by DTT

B

The reduction of insulin by DTT catalysed by PDI
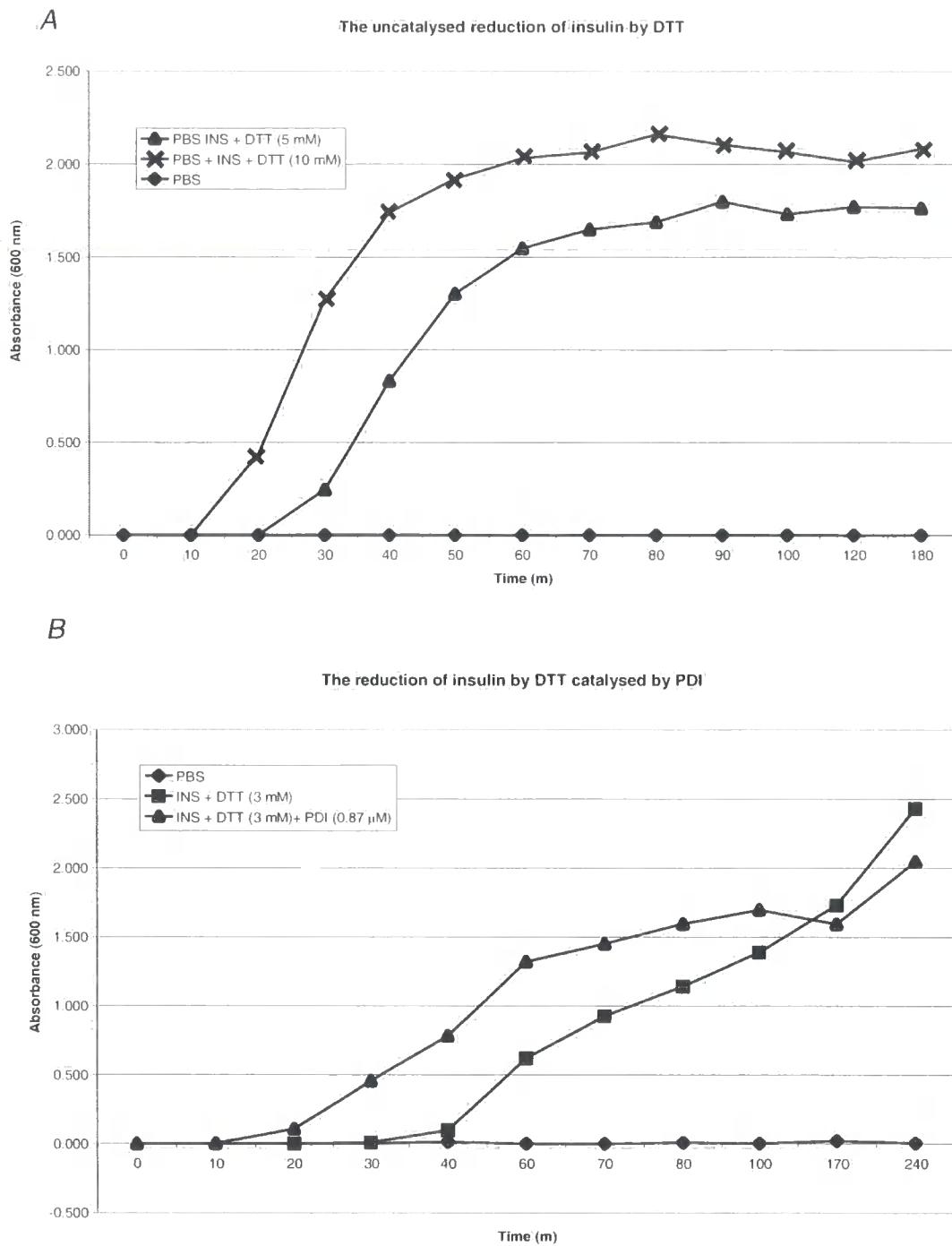
Figure 7. **The optimisation of the reduction of insulin by DTT.** *A*, 0.18 mM insulin was reduced by both 10 mM and 5 mM of DTT at room temperature in 75 µl PBS. OD_{600} readings were taken every 10 m for 2 h. *B*, Insulin was reduced as in *A* but using 3 mM DTT and 3 mM DTT with the addition of 0.87 µM purified PDI.

Next, a concentration range of DTT at 3 mM, 1 mM and 0.3 mM was used (Fig. 8A). Each concentration of DTT was either uncatalysed or supplemented with PDI at the concentration used in the previous assay. The reduction of insulin by DTT varied greatly depending on the concentration of DTT in this experiment. The uncatalysed reactions using 0.3 mM and 1 mM DTT barely left baseline level. Again, the 3 mM DTT reaction caused a high level of reduction with a maximum OD_{600} of ~1.2 which left the baseline level after ~30 minutes, slightly faster than the previous experiment. All catalysed reactions decreased the amount of time needed for the initiation of insulin reduction. Furthermore, the initiation of the reaction increased relative to the concentration of DTT used. That is to say, reduction increased upon treatment with higher concentrations of DTT which further increased upon the addition of a catalytic concentration of PDI. Since the aim of this experiment was to optimise the concentration of DTT, the reaction was only carried out for 100 minutes; therefore the experiment was terminated before maximum absorbance levels were obtained.

It was decided that, in the interests of assay sensitivity, a concentration of 1 mM DTT would be most appropriate. Next, the concentration of PDI was optimised in order to a) keep the assay within a sensitive range and b) to utilise the little purified protein efficiently (Fig. 8B). A reaction was set up where insulin reduction by PDI was monitored in the absence of DTT (Fig. 8B). PDI had no direct effect on insulin meaning any increase in turbidity of insulin upon the addition of PDI requires priming by DTT. By

A

The reduction of insulin by a concentration range of DTT -/+ PDI

B
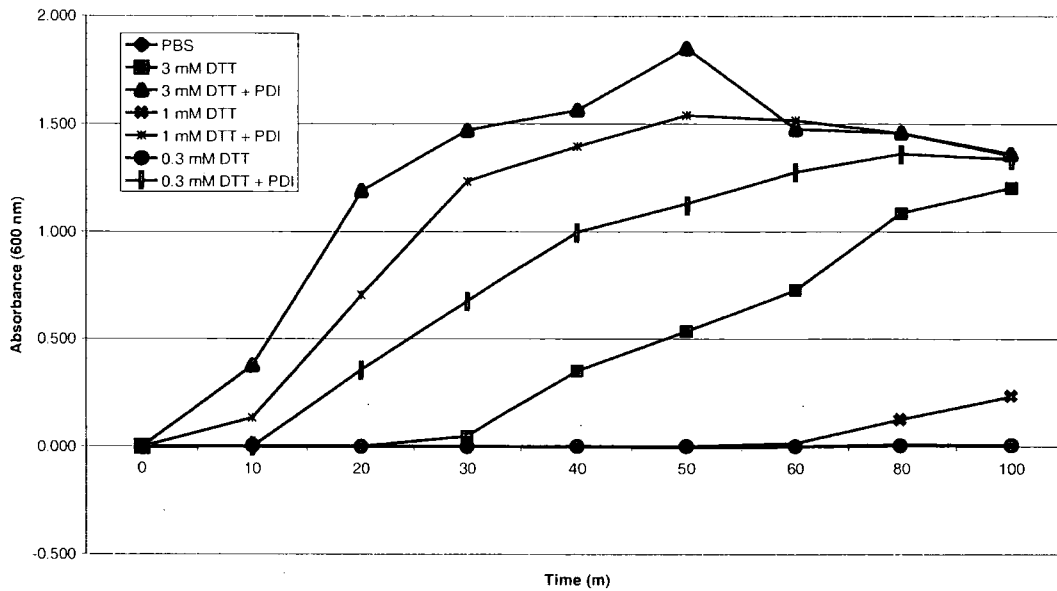
The reduction of insulin using a range of PDI concentration
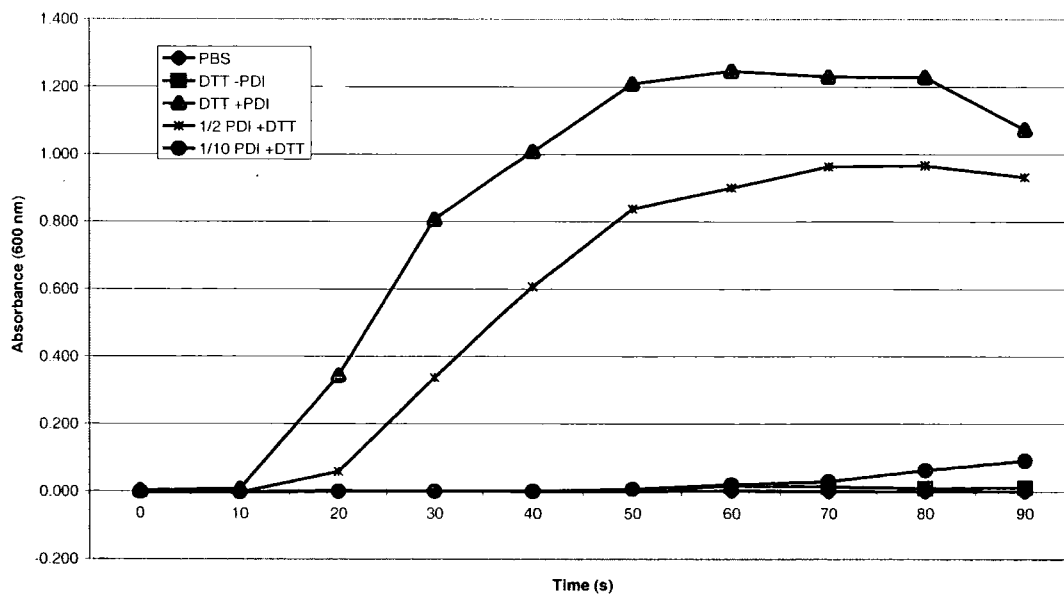
Figure 8. **Reduction of insulin by PDI.** *A*, 0.18 mM insulin was reduced by 3 mM, 1 mM and 0.3 mM of DTT at room temperature in 75 μl PBS in the presence or absence of 0.87 μM PDI. OD_{600} readings were taken every 10 m for 2 h. *B*, Insulin was reduced using 1 mM DTT in the presence of a range of PDI concentrations (0.87 μM, 0.435 μM (1/2) and 0.087 μM (1/10)).

lowering the concentration of PDI in the reaction by a factor of 2 or 10, the insulin reduction is much slower and becomes more similar to the uncatalysed reaction (Fig. 8B).

In order to obtain results within the appropriate range, optimisation of PDI in the assay was essential. By using 0.087 μM (1/10 the original concentration of PDI), OD readings were below the range required. Using 0.435 μM PDI (half the original concentration) left readings too high, therefore the next set of reactions utilised 0.218 μM, or a quarter of the original concentration of PDI. Besides using an optimised concentration of PDI, this set of reactions introduced purified Ero1-Lβ to the system at equimolar concentration to PDI. Any direct effect of Ero1-Lβ on insulin reduction i.e. in the absence of DTT would be observed (Fig. 9A). Despite only adding catalytic amounts of protein, we wanted to control for an increase in protein content. Non-catalytic bovine albumin serum was used in one reaction in place of Ero1-Lβ at equimolar concentration as a control. These reactions show that Ero1-Lβ has no direct effect on the reduction of insulin since no increase in turbidity was detected in the absence of DTT (Fig. 9A). Addition of PDI to the reaction increased the rate at which reduction is initiated, as expected. Upon addition of Ero1-Lβ to this reaction, the rate of insulin reduction is further increased with reduction significantly above PDI/DTT catalysed reaction. Interestingly, after 130 minutes both the PDI-catalysed and the Ero1-Lβ/PDI-catalysed reaction showed the same level of absorbance. The BSA control showed that Ero1-Lβ does not confer its effect merely by increasing protein or thiol/disulfide content.

Next, we studied the effect of a concentration range of Ero1-Lβ on insulin reduction to ask if a decrease in Ero1-Lβ concentration lead to a decrease in rate of insulin reduced. Ero1-Lβ was added at one fifth (0.453 µM) and one tenth (0.022 µM) the concentration used in the set of reactions presented in figure 9A (Fig. 9B). In this experiment, the effect of DTT on Ero1-Lβ/PDI insulin reduction was examined. Since Ero1-Lβ possesses oxidase activity, it is feasible that it may directly oxidise DTT, inhibiting further reduction of insulin in a PDI-independent manner. Thus, we investigated whether Ero1-Lβ mimics PDI activity in this assay (Fig. 9B). The reaction involving the components insulin, DTT and Ero1-Lβ showed levels of insulin reduction comparable to those using just insulin and DTT, suggesting that Ero1-Lβ exerts no direct oxidase activity. However, addition of Ero1-Lβ in the presence of PDI in these set of reactions did not increase the rate of insulin reduction (Fig. 9B). Conversely, the addition of Ero1-Lβ to these reactions seemed to partially inhibit the reduction of insulin since the highest rate of reduction was seen in the solely PDI-catalysed reaction suggesting that Ero1-Lβ may be competing for DTT with PDI. These data therefore, are contrary to those in Fig. 9A, which suggest that addition of Ero1-Lβ to PDI-catalysed reactions increased the rate of insulin reduction.

A

The direct and indirect effect on Ero1-Lβ on the reduction of insulin via PDI and DTT

B
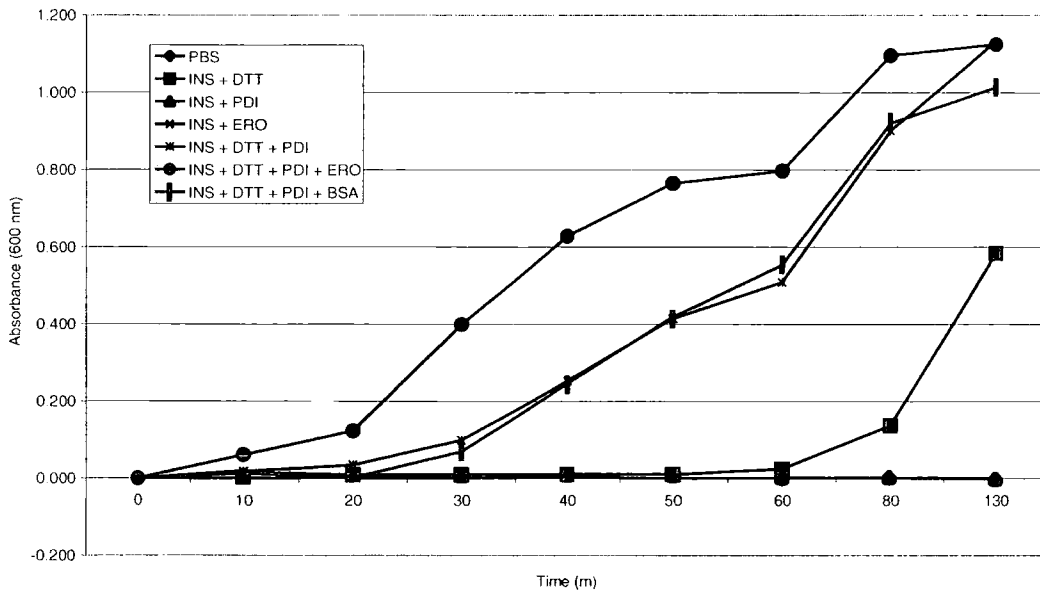
The reduction of insulin using a range of Ero1-Lβ concentrations
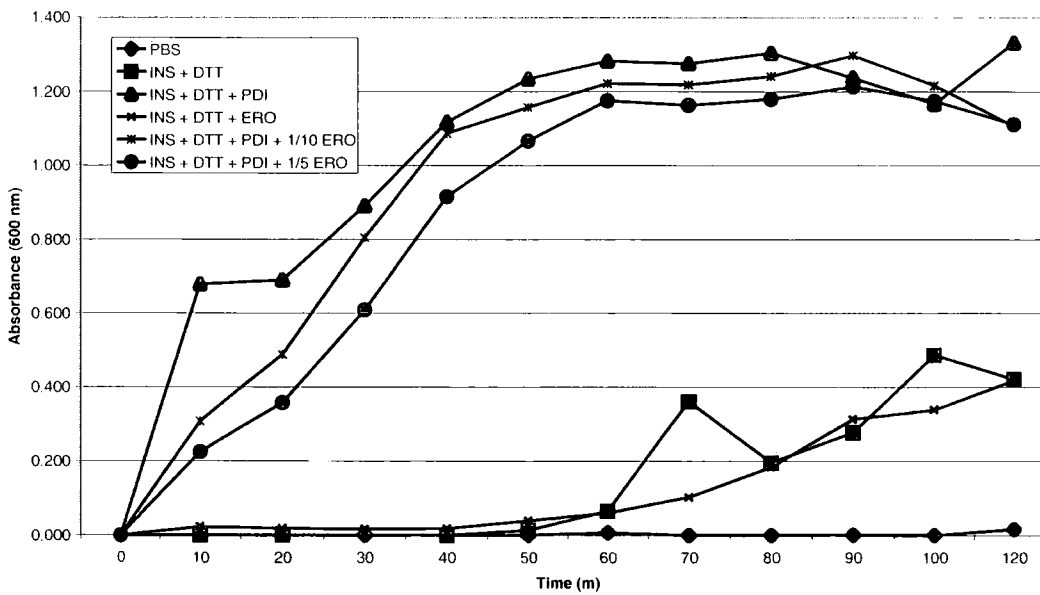
Figure 9. **The direct and indirect effect of Ero1-Lβ on insulin reduction.** *A*, Insulin was reduced as in previous assays but with the addition of both Ero and PDI where DTT was not added in order to examine their direct effect. Ero1-Lβ was added into reactions using a concentration range of 0.318 μM, 0.0635 μM (1/5) and 0.0318 μM (1/10) in order to study the effects of Ero1-Lβ activity.

A

The reduction of insulin using a range of Ero1-Lβ concentrations
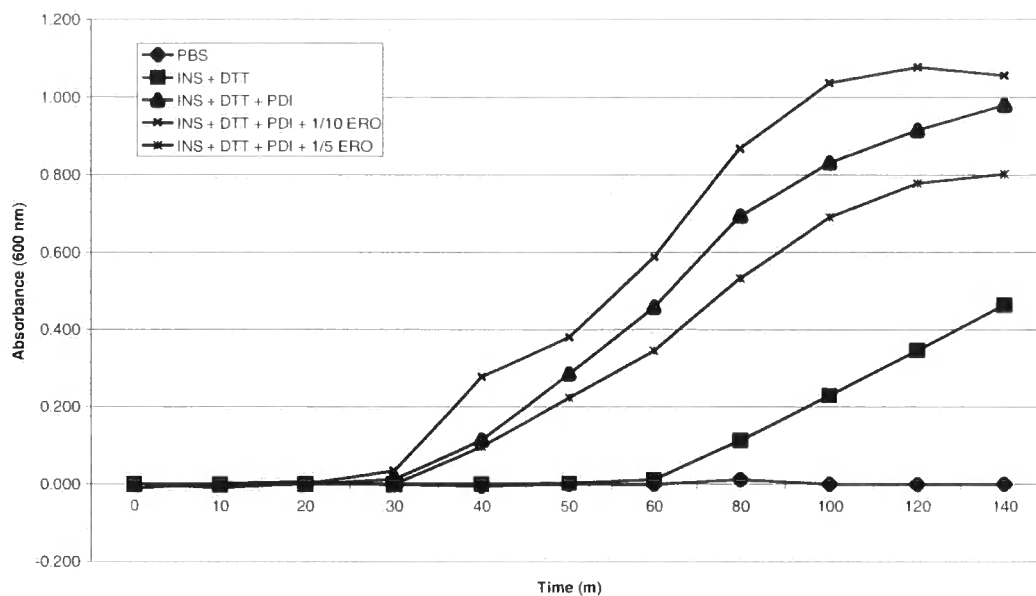
B

The effect of FAD on Ero1-Lβ-mediated insulin reduction
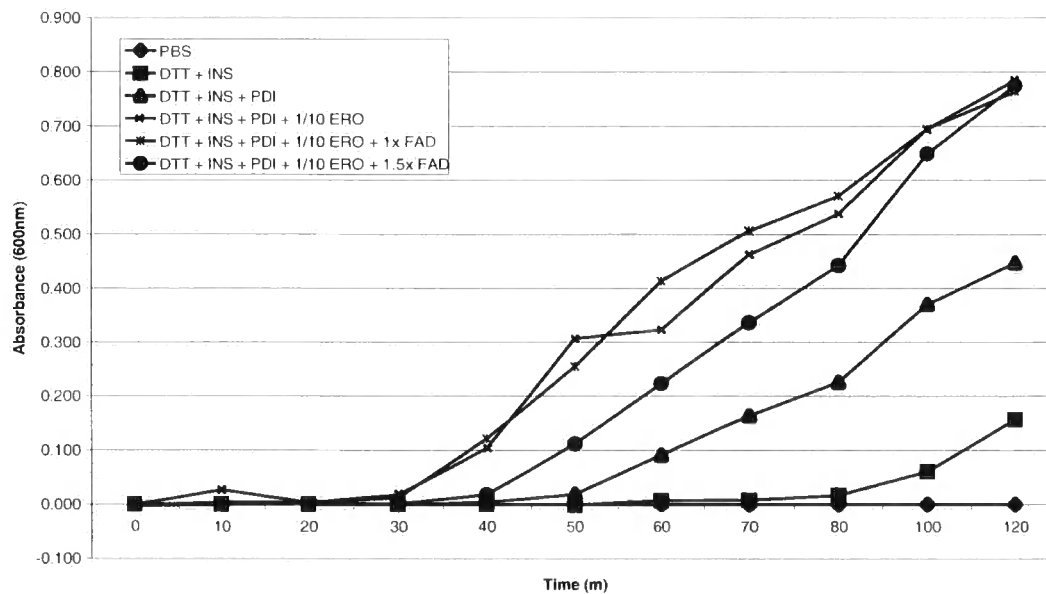
Figure 10. **The effect of a range of FAD concentrations on Ero1-Lβ-mediated insulin reduction.** *A*, A range of Ero1-Lβ concentrations was studied as in Fig. 9*B*. *B*, The addition of an equimolar concentration of FAD (1x) and in excess (1.5x) aimed to study the effects of FAD on Ero1-Lβ-mediated oxidative folding.

In order to obtain a definitive answer to whether or not our purified Ero1-Lβ influenced

the rate of insulin reduction, the set of reactions presented in figure 9B was repeated,

minus the control for the direct effect of Ero1-Lβ on DTT (Fig. 10A). Again, the solely

PDI-catalysed reaction and the addition of both concentrations of Ero1-Lβ to this reaction

mixture all exhibited insulin reduction. In this case however, the addition of Ero1-Lβ at

0.0218 μM (one tenth the concentration of PDI in the reaction), lead to a small increase in

rate of reduction. In opposition to this, the addition of a higher concentration on Ero1-Lβ

resulted in a level of insulin reduction slightly lower than that of the uncatalysed reaction.

Overall, we concluded that addition of Ero1-Lβ has limited or no effect on the rate of PDI

catalysed insulin reduction.

Since Ero1-Lβ is a flavoprotein, we supplemented our reaction with commercial flavin

adenine dinucleotide (FAD). The addition of FAD to the reaction mixture would

complete all the components deemed necessary for oxidative folding (Tu et al., 2000).

FAD was introduced at 0.022 μM (equimolar to Ero1-Lβ) (1x) and in excess of Ero1-Lβ

(0.0326 μM) (1.5x) into reactions containing 0.18 mM insulin, 1 mM DTT, 0.218 μM

PDI and 0.022 μM Ero1-Lβ (Fig. 10B). The addition of Ero1-Lβ to the PDI-catalysed

reaction increased the appearance of insulin reduction in this case with the level of insulin

reduction leaving baseline at ~40 minutes compared with ~60 minutes in the solely PDI-

catalysed reaction. However, the addition of FAD seemed to have no further effect on

insulin reduction. Moreover, addition of FAD in excess (1.5x) seemed to mildly inhibit

the reaction with reduction only leaving baseline after ~50 minutes. Together these data indicate that the addition of the flavin FAD does not influence Ero1-Lβ-mediated reduction of insulin via a PDI oxidation chain.

The data obtained for the insulin assay varied between experiments with Ero1-Lβ catalysing insulin reduction in only one experiment (Fig. 9A) and inhibiting insulin reduction in others (Fig. 9B and 10A). Since these reactions were carried out at room temperature, temperature fluctuations may be responsible for inconsistent data between rates in the experiments (Compare Fig. 9B with Fig. 10A and B). To investigate whether addition of Ero1-Lβ catalyses PDI-dependent reduction of insulin we kept temperature constant by performing the assay at 37 $^{\circ}$C (Fig. 11). Since the reaction would be much faster, OD_{600} readings were taken every minute. This technique allowed a much closer monitoring of insulin reduction but only small differences were observed upon the addition of Ero1-Lβ.

The initial effect of Ero1-Lβ on insulin reduction at 37 degrees celsius
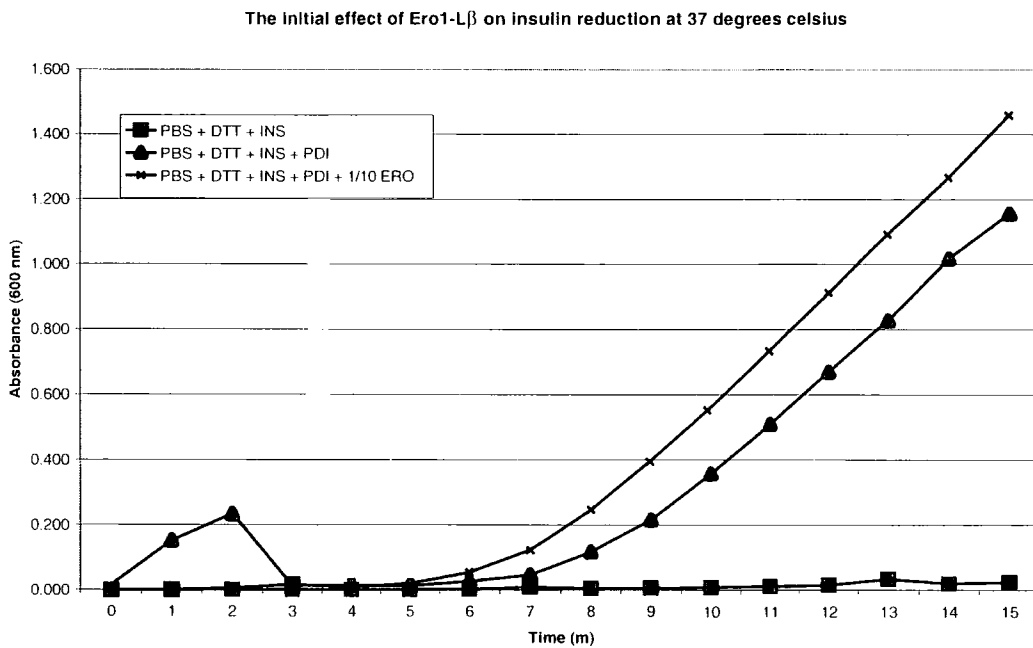
Figure 11. **The addition of Ero1-Lβ to the *in vitro* reduction system at 37 degrees Celsius.** A, This insulin reduction assay was completed at 37 °C, taking OD_{600} readings every minute. Insulin and DTT and PDI concentration are as optimised and Ero1-Lβ is added at 0.0318 µM.

3.1.2.5 *Purified Ero1-Lβ does not contain FAD*

Genetic approaches have confirmed that FAD is necessary for oxidative folding in the ER since depletion of riboflavin, a precursor of FAD, leads to defects in the oxidative folding of protein substrates (Tu *et al.*, 2000). Furthermore, more recent work has indicated that oxidative folding is sensitive to levels of free FAD, directly affecting the viability of yeast with a the *ero1-1* mutation (Tu and Weissman, 2002).

For our studies, an Ero1-Lβ expression construct was designed based on the truncated Ero1p that was successfully expressed and crystallised by Gross and colleagues (Gross *et al.*, 2004). Truncated Ero1-Lβ was expressed in Origami bacteria and purified using Ni Affinity chromatography. Ero1-Lβ was insoluble and had to be refolded using urea (D. Brown, J. A. Gatehouse and A. M. Benham, unpublished data). The amount of Ero1-Lβ obtained was very low, approximately 250 ng μl^{-1} corresponding to 0.375 μM concentration. In order to visualise this, 0.3125 μg was loaded on an SDS-PAGE gel with an equal amount of purified PDI and an equal volume of Ero1-Lβ-myc transfected lysate (Fig. 12*A*). Purified PDI resolved into a tight band approximately 60-65 kD, however the purified Ero1-Lβ was only detected at low levels, resolving as a faint band at ~50 kD (Fig. 12*A*, compare lane 2 with lane 1). Despite loading the same amount of protein, bands of equal intensity were not seen, suggesting that either the concentration of purified Ero1-Lβ was lower than anticipated or that the coomassie differentially stains the two proteins. A western blot was run to confirm the presence of purified Ero1-Lβ (Fig. 12*B*).
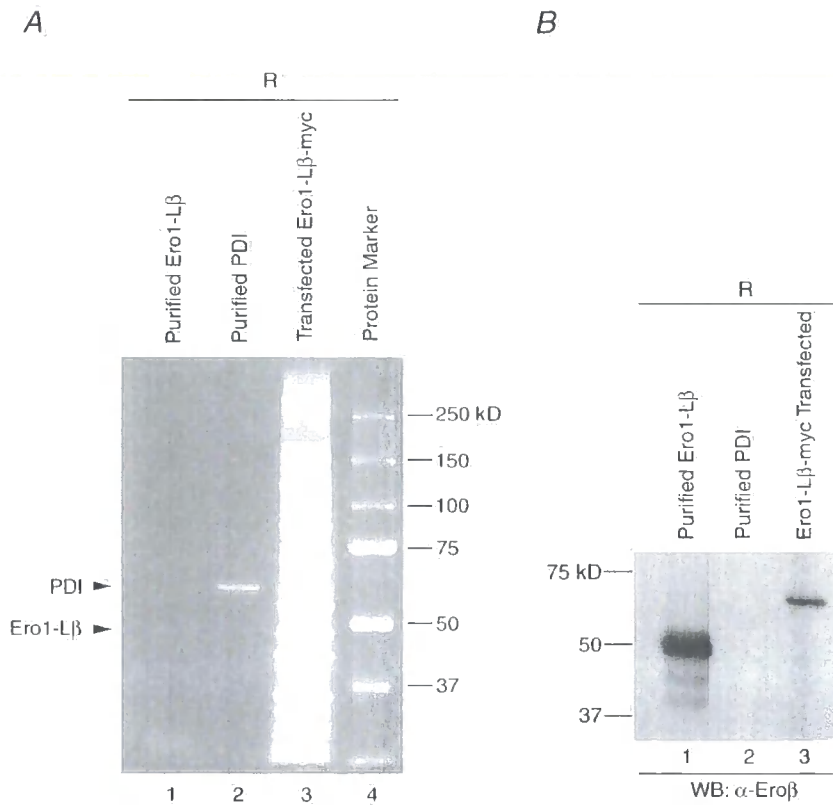
Figure 12. **Purification of Ero1-Lβ.** *A*, 0.3125 µg purified Ero1-Lβ and 0.3125 µg PDI were ran on reducing (R) SDS-PAGE. The resulting gel was coomassie stained in order to visualise all protein on the gel. *B*, The same reduced samples were loaded as in A, only this time were immunoblotted for the presence of Ero1-Lβ using the anti-Eroβ antibody. The immunoblotting confirms the presence of a faint Ero1-Lβ band in the coomiasse gel (compare *B*, lane 1 with *A*, lane 1).

In order to study Ero1-Lβ activity, it was important to establish whether or not the purified protein contained any FAD. We tested for the presence of FAD using spectrophotometry. Glucose oxidase was used as a positive control since each subunit of this homodimeric enzyme contains a co-enzyme molecule of FAD (Pazur and Kleppe, 1964). The characteristic fluorescence for flavin is 525nm as has been shown during studies with other FAD-bound enzymes (de Vet and van den Bosch, 2000; Rand *et al.*, 2006).

A range of glucose oxidase standards were analysed: one at equimolar concentration to the purified Ero1-Lβ purified stock (0.375 μM), one at 1 μM and one at the glucose oxidase stock concentration of 17.5 μM. An absorbance spectrum was taken in the range of 200-800 nm using all three standards (Fig. 13*A*, *B and C*). All standards gave an absorbance peak reading at 525 nm indicating the presence of flavin. Purified Ero1-Lβ however failed to show a similar peak, indicating the lack of FAD in the purified extract (Fig. 13*D*). Bovine serum albumin was used as a control for the presence of protein in the sample. A solution of BSA was made up to 0.1 μg/ml and its absorbance in the low wavelengths (200-350 nm) examined (Fig. 13*E*). A peak at ~200 nm indicated the presence of BSA. Purified Ero1-Lβ gave a peak at ~270 nm indicating that protein was indeed present in the purified Ero1-Lβ sample. Taken together with the very pale colour of the purified Ero1-Lβ protein solution, we concluded that the purified Ero1-Lβ does not contain FAD.
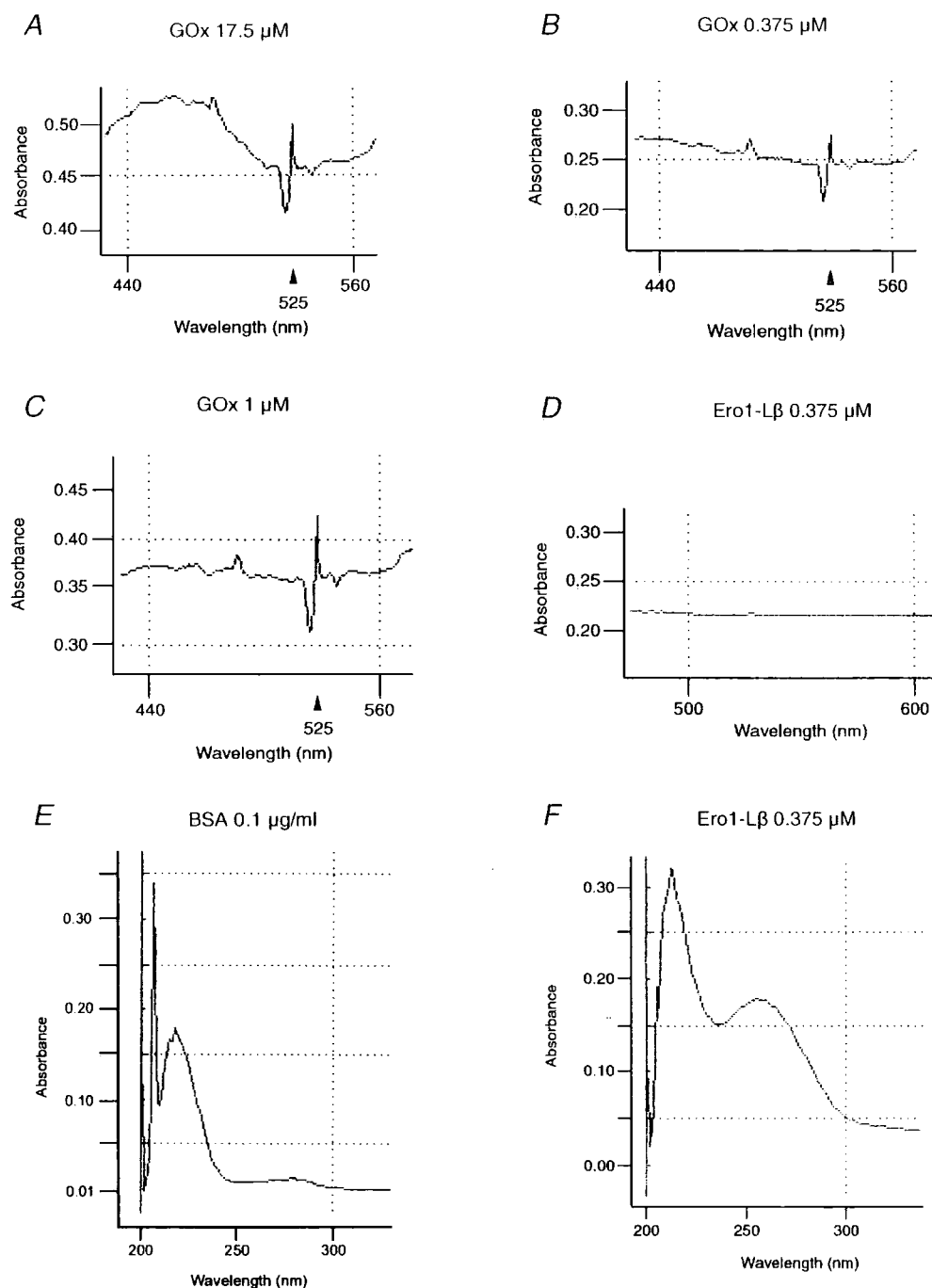
Figure 13. **Purified Ero1-Lβ does not contain FAD.** An absorbtion spectrum of the FAD-containing enzyme glucose oxidase (GOx) was undertaken using concentrations in excess (17.5 μM) (*A*), equimolar (0.375 μM) (*B*) and slightly in excess (1 μM) (*C*) to that of purified Ero1-Lβ. The absorbance of the purified Ero-Lβ was then taken but showed no sign of a characteristic flavin peak (*D*). A control for the presence of protein was undertaken using bovine serum albumin in excess of the concentration of purified Ero1-Lβ (*E*). Protein content of the purified Ero1-Lβ was then analysed (*F*).

3.1.3 Discussion

3.1.3.1 *Homodimerisation of wild-type Ero1-Lβ*

Here data is presented, showing that, taken together with the work of Dias-Gunasekara

and colleagues (Dias-Gunasekara *et al.*, 2005), Ero1-Lβ is able to form homodimers. The

functional significance of Ero homodimers remains unknown. However, previous work

has demonstrated that the Ero1-Lα mutant C391A shows a lower affinity for PDI yet it is

able to rescue the temperature sensitive yeast mutant *ero1-1* (Bertoli *et al.*, 2004; Cabibbo

et al., 2000; Pagani *et al.*, 2000). Thus, both hERO-PDI association and hERO

dimerisation may be important in maintaining the oxidative folding pathway in the ER.

Using co-immunoprecipitation techniques, we show that differentially tagged wild-type

Ero1-Lβ associates *in vivo* (Fig. 3). During lysis, the alkylating agent NEM was used to

trap any disulfide complexes by sequestering any thiols. Co-immunoprecipitated Ero1-Lβ

homodimerises as a mixture of covalent and non-covalent interactions. Homodimers were

also resolved under non-reducing conditions in the presence of SDS (Fig. 3).

Further work by our group led to the discovery that the C-X-X-C-X-X-C motif is

important in dimerisation. By studying the mutant C396A, they were able to show that

this residue is important for dimer establishment since the mutation did not give rise to

dimers. The Ero1p crystal data gathered by Gross and colleagues allowed a model for Ero

dimerisation to be developed (Gross *et al.*, 2004).

A

B
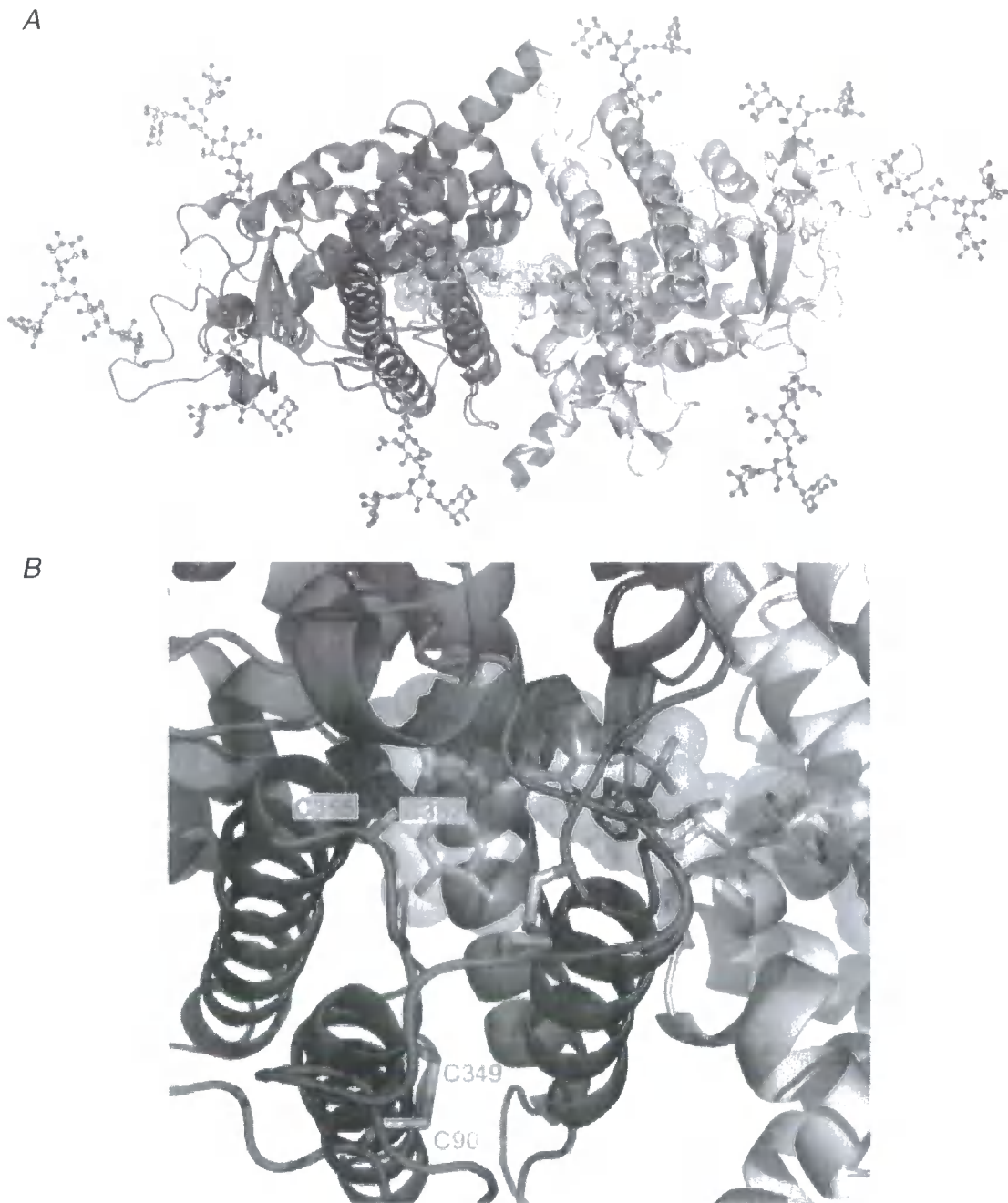
Figure 14. **A structural model of an Ero-Ero homodimer.** *A*, Here two Ero1p monomers form a homodimer through non-covalent hydrogen bonding of two symmetrical FAD molecules. The glycans are shown on the exterior of the dimer by ball and stick representation. *B*, A closer view of the dimer interface shows the location of the Ero1p active site cysteines (Cys^{352}-Cys^{355}) and the non-active cysteines (C^{90}-C^{349}). FAD is shown at the centre of the interface by the stick and space filling representation. This model is taken from (Dias-Gunasekara *et al.*, 2005)

This model illustrates the homodimerisation of two Ero1p molecules held together by hydrogen bonds at the interface (Fig. 14A). The dimer interface consists of the two bound FAD molecules adjacent to the active site cysteines (Cys^{352}-Cys^{355}) (Fig. 14B) which corresponds to Cys^{393}-Cys^{396} in Ero1-Lβ. Given that the C396A mutant abolishes the formation of dimers, it is likely that by mutating this residue the loss of dimers occurs indirectly via the loss of the FAD cofactor. The proximity of non-active site cysteines (upstream of the C-X-X-C-X-X-C motif) to the dimer interface, may account for the observation of disulfide-dependent complexes suggested by this chapter. The formation of disulfide bonds between free cysteines in Ero1-Lβ monomers could potentially strengthen the dimer. Mutations targeted towards these cysteines can now be used to test this hypothesis.

3.1.3.2 *Reduction in the ability of FAD-binding mutants to interact with PDI and the formation of FAD-binding mutant homodimers*

Observations that the C396A mutation disrupts the formation of dimers led to the hypothesis that mutations in the FAD-binding domain may also prevent dimerisation of Ero1-Lβ. Initially, the ability of these mutants to bind PDI was investigated. Previous work has shown that alkylation with NEM is required in mammalian cells to detect hEROs disulfide bound to PDI (Benham *et al.*, 2000; Mezghrani *et al.*, 2001). Since the mutations did not directly affect any active-site cysteines, it was assumed that PDI binding would not be affected by mutations in the FAD-binding domain. However, the yeast conditional *ero1-1* mutant strain is unable to oxidise yeast PDI and substrate

proteins remain in a reduced state (Frand and Kaiser, 1999). We provide data here showing that FAD-binding mutants have impaired covalent interaction with PDI (Fig. 6C and D). However, non-covalent interactions seem largely unaffected by the mutations, since monomeric Ero1-Lβ is detected after co-immunoprecipitation with PDI and analysis under non-reducing conditions (Fig. 6D). Hence, Ero1-Lβ can interact with PDI in a disulfide and flavin-fold independent manner. Both G252 and H254 therefore are required by Ero1-Lβ for covalent PDI association. This seems unusual considering these residues are not directly involved in PDI binding and the buried FAD cofactor is not likely to be adjacent to the Ero1-Lβ-PDI docking site. However, recent work has highlighted that Ero1-PDI specificity arises from both active site cysteines (Kulp *et al.*, 2006). This work contradicted previous studies which suggested that Ero1p cannot oxidise the *N*-terminal active site of PDI (Tsai *et al.*, 2002; Tu *et al.*, 2000)). Since the Ero1 proteins used in these studies was missing FAD, the presence of the cofactor may be essential for the complete recognition and hence interaction of the active site domains of PDI.

Despite the fact that FAD-binding mutants were able to associate with PDI, Ero-Ero interactions did not depend on the FAD-binding site. The phenotypes caused by the *ero1-1* and *ero1-2* mutants therefore can not be accredited to the failure of Ero1p to form homodimers.

3.1.3.3 *In vitro activity of Ero1-Lβ in the insulin reduction assay*

By using purified PDI and Ero1-Lβ we were able to construct an assay to study the activity of both proteins. An insulin reduction assay was designed and optimised based upon the one established by Luthman and colleagues in 1979 (Holmgren, 1979). PDI is able to oxidise DTT *in vitro* in a concentration-dependent manner (Fig. 8). In one experiment, the addition of catalytic concentrations of purified Ero1-Lβ increased the rate of insulin reduction (Fig. 9A). However, in the majority of experiments, no increased rate of reduction was observed, suggesting that the purified protein is inactive. Addition of FAD to the reaction did not increase the rate of oxidation further suggesting the purified Ero1-Lβ is inactive.

Inactivity of the Ero1-Lβ may be a consequence of the method by which it purified. Perhaps refolding of the protein during purification was not efficient and resulted in the formation of a non-native protein. Alternatively, inactivity may be a consequence of inefficient binding of FAD. Attempts can now be made to generate an active protein by optimising the refolding step of the purification method. Upon obtaining active, purified Ero1-Lβ, work will concentrate on studying its functional activity *in vitro*. As well as studying the effect of introducing active Ero1-Lβ to the insulin reduction assay, comparisons of functional activity can be made using other assays such as the RNase A assay. This assay has been successful in functional studies of redox isomerases (Fuchs *et al.*, 1967; Goldberger *et al.*, 1963; Lundstrom and Holmgren, 1990) and may help to further elucidate Ero1-Lβ and FAD function in disulfide bond formation.

3.2 Characterisation of an anti-Ero1-Lβ polyclonal antibody

3.2.1 Introduction

Antibodies are serum immunoglobulins (Igs) that are able to bind specific antigens. The ability of antibodies to bind antigen with a high degree of affinity and specificity make them a valuable tool in molecular and cellular biology. Some common uses of antibodies include being employed in the identification and separation of proteins in Western blots and immunoprecipitations, differentiation of cell types using flow cytometry and examination of protein expression in tissues by immunohistochemical staining.

When studying protein interactions, the identification of specific proteins is vital. Gel staining methods are common when using purified proteins, however, when total cell lysates are being analysed, this method is too unspecific. Custom polyclonal antibodies (pAb) and monoclonal antibodies (mAb) are available for protein analysis. In the case of pAbs, animals are given an injection of antigen or antigen/adjuvant mixtures to induce antibody production. This production is usually monitored by collecting blood from the animal during the course of immunisation. The serum will contain multiple antibodies against the same antigen. In the case of mAbs, animals are given injections of antigen or antigen/adjuvant mixtures to induce specific B cells, which can be fused with immortalised cells to produce hybridomas. These immortalised lymphocytes are products of a single B cell clone and thus, produce a single set of antibodies against the antigen the animal was raised against. Making the choice whether to use mAbs or pAbs is usually

influenced by the desired application and time or financial constraints. Polyclonal antisera can be obtained from rabbits within 1-2 months; however this depends on the primary and secondary response. The establishment of a hybridoma and the production of monoclonal antibodies however, can take up to 6 months (Leenaars and Hendriksen, 2005).

Since, mAbs target a specific, single antigenic epitope, any alteration in conformation by denaturation, reduction, post-translational modification or association with other proteins may influence binding affinity. The impact of conformational change on pAbs however is less likely to be a concern since pAbs recognise multiple epitopes. The use of pAbs for immunoprecipitation methods is advantageous since pAbs tends to recognise multiple epitopes better since polyclonal sera are a composite of antibodies with unique specificities. Another advantage of pAb use is their stability over a broad pH and salt concentration (Lipman et al., 2005).

Our aim was to produce an Ero1-Lβ polyclonal antibody for use in immunoprecipitation and immuno- or Western blotting. The antigen was a recombinant, truncated human Ero1-Lβ protein expressed in *E. coli*. The antibody was raised in New Zealand white rabbits by Sigma-Genosys. Although an anti-peptide Ero1-Lβ antibody has been previously made, it is unable to immunoprecipitate Ero1-Lβ (Dias-Gunasekara et al., 2006).

Animals were bled periodically in order to analyse the progression of the Ab response to immunisation. After the polyclonal sera were obtained from the animals, it was necessary to characterise the specificity and sensitivity to Ero1-Lβ. This chapter characterises polyclonal antibodies against recombinant Ero1-Lβ at various stages post-immunisation.

3.2.2 Results

3.2.2.1 *Polyclonal antiserum from rabbit B2 is able to recognise transfected but not endogenous Ero1-Lβ*

In total, three rabbits were immunised against Ero1-Lβ. When bleeds were received, they were left to clot overnight, and the serum was removed. This was centrifuged several times to remove any remaining blood cells and was subsequently treated with 0.01% sodium azide to prevent infection. Initially, antisera from each rabbit were tested for the ability to recognise transfected Ero1-Lβ-myc in a Western blot. Ero1-Lβ-myc was transfected into HeLa cells, cells were lysed and post-nuclear lysates were run on reducing SDS-PAGE. Proteins were then transferred to nitrocellulose and subsequently analysed by immunoblotting (Fig. 1). Antisera from rabbit B2 2nd and 3rd bleed (Fig.1A), rabbit B3 2nd and 3rd bleed (Fig. 1B) and rabbit B7 1st and 2nd bleed (Fig. 1C) were analysed. The ability of the antisera to detect endogenous Ero1-Lβ was also tested by using a mouse pancreas tissue lysate which expresses Ero1-Lβ. A non-transfected negative HeLa total cell lysate control was also used. As well as immunoblotting using the new antisera, lysates were also subjected to immunoblotting using the current anti-peptide Ero1-Lβ antibody and the anti-PDI antibody as a control. In the case of the B2 antisera tests, lysates were also subjected to immunoblotting with the anti-myc antibody in order to determine which band corresponded to Ero1-Lβ (Fig. 1A).
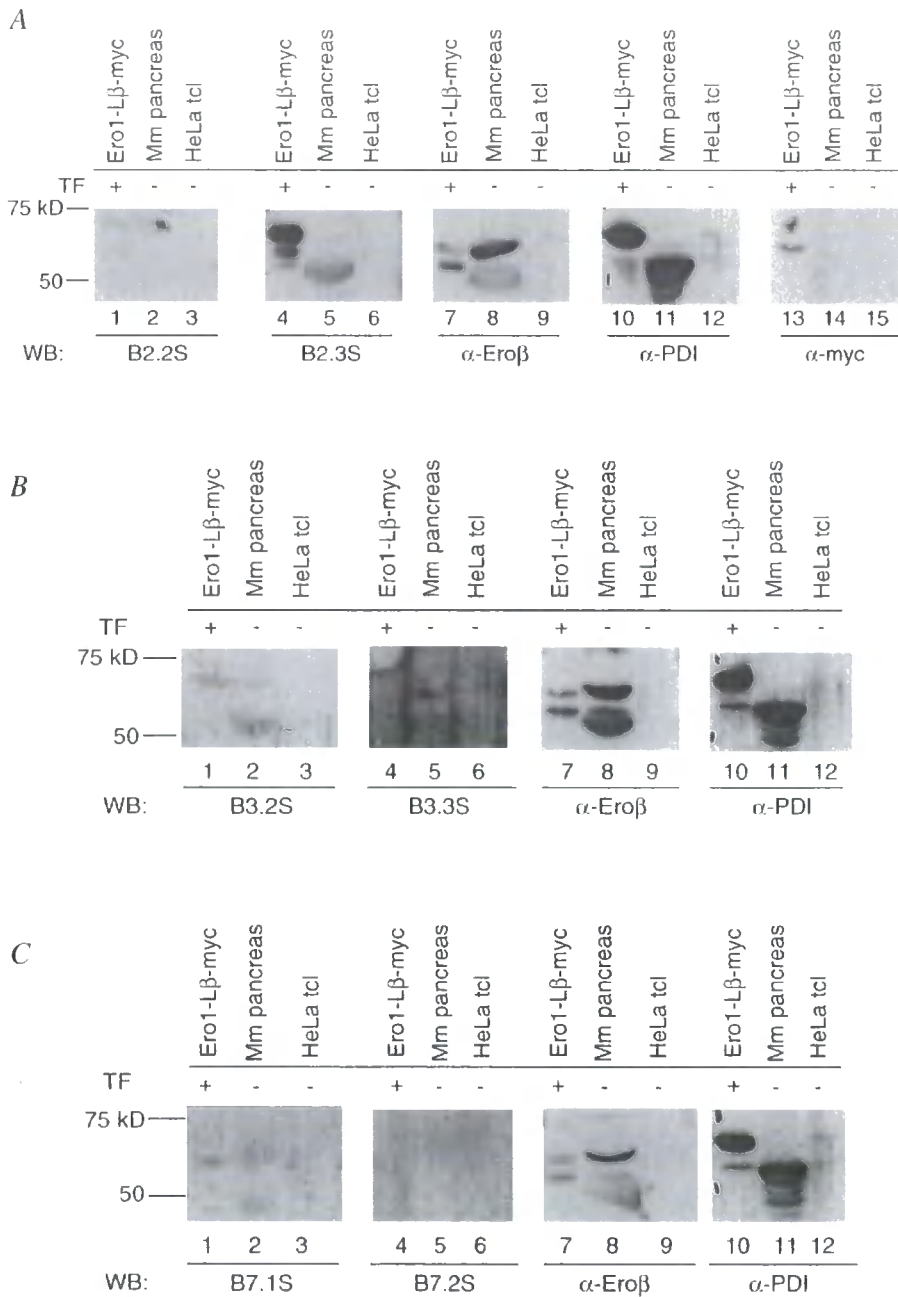
Figure 1. **B2 antiserum is able to recognise transfected Ero1-Lβ-myc**. Ero1-Lβ transfected cells (TF), mouse (Mm) pancreas and HeLa total cell lysates (tcl) were generated. Antisera from rabbit B2 2nd bleed (B2.2S) and 3rd bleed (B2.3S) (A), B3 2nd bleed (B3.2S) and 3rd bleed (B3.3S) (B) and B7 1st bleed (B7.1S) and 2nd bleed (B7.2S) (C) were analysed for recognition of Ero1-Lβ in Western blotting (WB) at 1:200. As controls, lysates were also immunoblotted for anti-Ero1-Lβ (α-Eroβ), anti-PDI and anti-myc (A only).

Immunoblotting using the B2 2nd bleed antiserum showed no detection of transfected or endogenous Ero1-Lβ (Fig. 1A, lanes 1 and 2). However, analysis of the 3rd bleed showed recognition of the Ero1-Lβ-myc transfected protein (Fig. 1A, lane 4). Immunoblotting with the anti-myc antibody (Fig. 1A, lanes 13-15) did not detect expression of Ero1-Lβ in the pancreas but Ero1-Lβ was detected in the transfected lysate as expected. The B2 3rd bleed, however, was unable to recognise endogenous Ero1-Lβ (Fig. 1A, lane 5). The current anti-Ero1-Lβ anti-peptide antibody, however, was able to recognise both endogenous and transfected Ero1-Lβ (Fig. 1A, lanes 7 and 8).

Analysis of rabbit B3 2nd bleed revealed a weak recognition of transfected Ero1-Lβ and endogenous Ero1-Lβ (Fig. 1B, lanes 1 and 2). After further immunisation, recognition of endogenous Ero1-Lβ and transfected Ero1-Lβ remained weak. (Fig. 1B). The image produced from B3 3rd bleed analysis is rather overexposed, meaning that it is likely that only low levels of endogenous Ero1-Lβ were detected. Regardless, rabbit B3 was more successful at recognizing endogenous Ero1-Lβ than rabbit B2.

Analysis of rabbit B7s 1st and 2nd bleed showed no recognition of endogenous or transfected Ero1-Lβ (Fig. 1C, lanes 1 and 2). Taken together, these data show that after 2 boosts, antiserum from rabbit B7 was unable to recognise endogenous or transfected Ero1-Lβ, B3 was not able to recognise transfected Ero1-Lβ but was able to weakly recognise endogenous Ero1-Lβ from mouse pancreas and rabbit B2 antisera was able to

recognise transfected Ero1-Lβ-myc, showing a moderate to strong signal. Despite this,

B2 failed to recognise endogenous Ero1-Lβ from mouse pancreas.

In order to confirm that the band seen in figure 1A lane 4 was the transfected Ero1-Lβ-

myc, the antiserum from the 3rd bleed of rabbit B2 was analysed after transfected lysates

had been subject to immunoprecipitation with the anti-myc antibody (Fig. 2A). Pre-

immune serum from the B2 rabbit was used as a negative control in this instance and the

current anti-peptide Ero1-Lβ antibody was used as a positive control. Lysates were

generated by transfection of cDNA from two Ero1-Lβ-myc maxipreps into HeLa cells.

Mouse pancreas provided an Ero1-Lβ-positive lysate while untransfected HeLa lysate

provided a negative control. Lysates were subjected to immunoprecipitation with the anti-

myc antibody for 2 h at 4 °C. The protein A sepharose beads were then washed twice

with lysis buffer before proteins were liberated. Any immunoprecipitating or co-

immunoprecipitating proteins were then loaded onto SDS-PAGE gel and subsequently

immunoblotted.

After IP, the current anti-Ero1-Lβ antibody recognised both old and new transfected

Ero1-Lβ (Fig. 2, compare lane 12 with lane 9). This antibody also recognised a non-

specific band from mouse pancreas lysate (Fig. 2, lane 10). Conversely, pre-immune

serum from the B2 rabbit was unable to recognise either transfected or endogenous Ero1-

Lb (Fig. 2, lanes 1-2 and 4). Antiserum from the 3rd bleed was able to recognise Ero1-Lβ-

myc translated from both old and new constructs (Fig. 2, lanes 5 and 8).
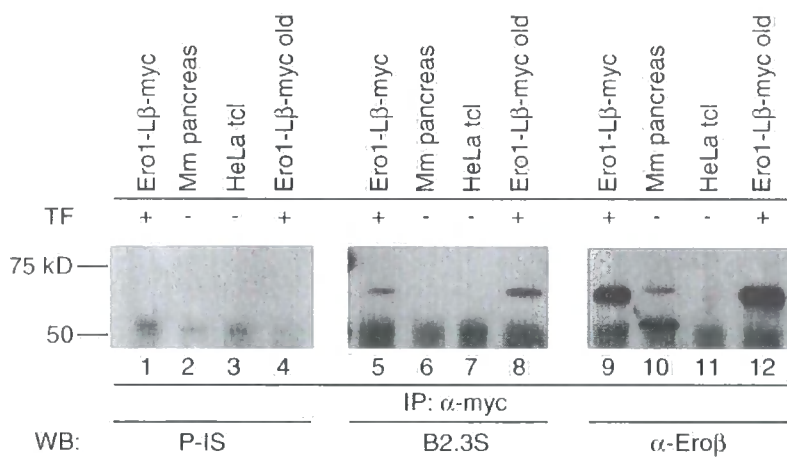
Figure 2. **B2 antiserum recognises transfected Ero1-Lβ-myc after immunoprecipitation.**
A, transfected (TF), tissue (Mm pancreas) and HeLa total cell lysates (tcl) were generated. Lysates were subjected to immunoprecipitation (IP) using the anti-myc antibody to isolate transfected myc-tagged proteins. Isolated proteins were detected using Western blotting (WB) using B2 pre-immune serum (P-IS) (lanes 1-4), 3rd bleed antiserum (B2.3S) (lanes 5-8) (both at 1:200) and the current polyclonal antibody against Ero1-Lβ (α-Eroβ) (lanes 9-12).

Contrastingly, this polyclonal serum was unable to recognise endogenous Ero1-Lβ (Fig.

2, lane 6). This is consistent with data obtained previously (Fig 1A, lane 4).

3.2.2.2 *Polyclonal antiserum from rabbit B2 is able to immunoprecipitate transfected Ero1-Lβ*

Our next aim was to ascertain whether or not the polyclonal antiserum from the 3rd bleed of rabbit B2 was able to isolate Ero1-Lβ by immunoprecipitation. This would provide us with a useful tool since the current anti-Ero1-Lβ antibody will not recognise Ero1-Lβ in immunoprecipitations. Transfected, tissue and non-transfected lysates were generated as previously and were subjected to immunoprecipitation using the B2 pre-immune serum, the 3rd bleed serum and the anti-myc antibody. Lysates were incubated with protein A sepharose beads for 2 h at 4 °C before being washed. Proteins were then liberated and separated by SDS-PAGE. Proteins were transferred and subsequently immunoblotted with the anti-myc antibody in order to detect any immunoprecipitating myc-tagged Ero1-Lβ (Fig. 3).

Immunoblotting with the anti-myc antibody showed that the anti-myc control IP had been successful since Ero1-Lβ-myc could be detected (Fig. 3, lane 7). Analysis of the anti-myc immunoblot of lysates subjected to IP with the B2 pre-immune serum showed that no immunoprecipitation of myc-tagged Ero1-Lβ had taken place (Fig. 3, lane 1), thus, the pre-immune serum was unable to recognise Ero1-Lβ-myc in IP. This is consistent with previous work since B2 pre-immune serum was unable to recognise Ero1-Lβ-myc in Western blots (Fig. 2, lanes 1 and 4).
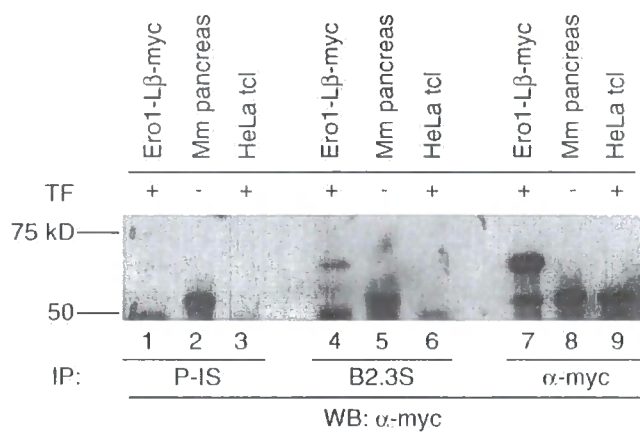
Figure 3. **B2 antiserum is able to immunoprecipitate transfected Ero1-Lβ**. Ero1-Lβ-myc transfected (TF), mouse (Mm) pancreas and HeLa total cell lysates (tcl) were generated for analysis. Lysates were subjected to immunoprecipitation (IP) using B2 pre-immune serum (P-IS) (lanes 1-3), 3rd bleed antiserum (B2.3S) (lanes 4-6) and the anti-myc antibody (lanes 7-9). After proteins were liberated from protein A sepharose beads they were separated by 8% SDS-PAGE and subsequently immunoblotted using the anti-myc antibody.

After immunoprecipitation with the B2 3rd bleed serum, immunoblotting with the anti-myc antibody revealed the presence of Ero1-Lβ-myc (Fig. 3, lane 4) indicating that the 3rd bleed polyclonal antiserum was able to recognise Ero1-Lβ-myc in immunoprecipitation. All mouse pancreas lysates and non-transfected HeLa total cell lysate controls were negative as expected.

3.2.2.3 Antisera from rabbit B2 do not cross-react with Ero1-Lα

We also tested the ability of the terminal bleed to recognise transfected Ero1-Lα as well as Ero1-Lβ. Since Ero1-Lα and Ero1-Lβ share structural characteristics, it was imperative that an investigation was carried out to see if the antisera would cross-react with Ero1-Lα. Since immunoblotting with the original anti-peptide Ero1-Lβ antibody was improved using 0.1% SDS (S. Dias-Gunasekara, and A. M. Benham, unpublished data), SDS was used in the incubation of some primary immunoblots to determine whether this would improve the B2 signal.

Both Ero1-Lα-myc and Ero1-Lβ-myc lysates were generated by transfection into HeLa cells. An untransfected HeLa cell lysate was used as a control. After separation of proteins by SDS-PAGE and subsequent transfer to nitrocellulose, membranes were immunoblotted using the anti-myc, anti-Ero1-Lβ, anti-PDI antibodies and the 3rd and terminal bleeds of the B2 rabbit (Fig. 4). The use of SDS in the primary immunoblot of anti-Ero1-Lβ and both B2 antisera cleaned up the background (Fig. 4, lanes 4-6 and 10-15). Both the 3rd and terminal bleed antisera recognised the Ero1-Lβ-myc transfected protein without cross-reacting with the Ero1-Lα-myc transfected protein (Fig. 4 compare lane 11 with lane 10 and lane 14 with lane 13). The terminal bleed antiserum however did not show improved recognition of Ero1-Lβ over the 3rd bleed antiserum (Fig. 4 compare lane 14 with lane 11). Taken together, these results show that although there is no increased recognition of Ero1-Lβ from the terminal bleed antiserum, antisera from the B2 rabbit does not cross-react with Ero1-Lα-myc.
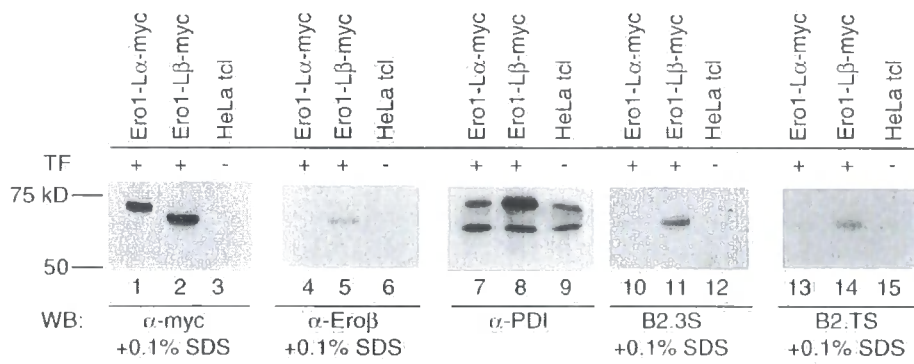
Figure 4. **B2 antisera do not cross-react with transfected Ero1-Lα-myc**. Both Ero1-Lα-myc and Ero1-Lβ-myc were transfected (TF) into HeLa cells. A HeLa total cell lysate (tcl) was also generated. Proteins were separated by SDS-PAGE and subsequently analysed by Western blotting (WB) using the anti-myc (lanes 1-3), anti-Ero1-Lβ (anti-Eroβ) (lanes 4-6), anti-PDI (lanes 7-9), B2 3rd bleed (B2.3S) (lanes 10-14) and B2 terminal bleed (B2.TS) (lanes 13-15).

3.2.3 Discussion

Here, we characterised a polyclonal antibody raised against the tissue-specific ER

oxidoreductase Ero1-Lβ. The intended use for this antibody was to recognise Ero1-Lβ or

complexes of Ero1-Lβ in both immunoblots and immunoprecipitations.

Initially, three rabbits were immunised but upon inspection of their bleeds, one antiserum

performed better – from rabbit B2 – when tested for immunoblotting on Ero1-Lβ-myc

transfected lysates (Fig. 1). However, the antiserum was unable to recognise endogenous

Ero1-Lβ from mouse pancreas. Polyclonal antisera consist of many antibodies raised

against the same antigen. This 3rd bleed antiserum should in theory be able to recognise

endogenous mouse pancreas Ero1-Lβ. One possible explanation is that the epitope(s) the

antiserum was raised against is not contained in murine Ero1-Lβ, perhaps because the

recombinant Ero1-Lβ used as antigen was not properly folded. The B2 antiserum was

also able to recognise Ero1-Lβ in immunoprecipitation reactions, something the current

anti-peptide anti-Ero1-Lβ antibody was unable to do (Fig. 2).

Checking for cross-reactivity of antisera is an important step. This is especially crucial

when studying a protein like Ero1-Lβ that may share epitopes with other proteins such as

Ero1-Lα. Thus, we showed that the 3rd bleed antiserum was unable to recognise Ero1-Lα

in immunoblots whilst recognising Ero1-Lβ (Fig. 4). Acquisition of the terminal bleed

from rabbit B2 allowed us to investigate whether or not recognition of Ero1-Lβ had

improved. Upon inspection, this was not the case. However, the addition of a small amount of the detergent SDS provided a cleaner Ero1-Lβ signal (Fig. 4).

Although B2 does not recognise Ero1-Lβ in pancreas, it may be worth testing other secretory tissues such as stomach and testis to determine whether all native Ero1-Lβ proteins fail to be recognised by this serum. It will also be interesting to test the new antiserum using immunohistochemistry to confirm these findings. The B2 serum could also prove useful in defining Ero1-Lβ complexes by IP in transfected cell lines.

3.3 Towards the characterisation of the interactions between the PDI homolog, PDIp and Ero1-Lα and Ero1-Lβ

3.3.1 Introduction

Numerous eukaryotic PDI homologs have been discovered with an extensive range of both domain organisation and active-site chemistries (Ferrari and Soling, 1999; Freedman *et al.*, 2002). A handful of human PDI homologs exhibit tissue-specific distribution. PDIp, endoPDI and PDILT are homologs of PDI restricted to the pancreas, endothelia and testis respectively (Desilva *et al.*, 1997; Sullivan *et al.*, 2003; van Lith *et al.*, 2005). The existence of tissue-specific PDI homologs may be due to the requirement for the folding of tissue-specific proteins. However, the identity of such tissue specific substrates is currently unknown.

PDIp was characterised in 1997 (Desilva *et al.*, 1997). PDIp shares the same **a b b' a'** domain organisation as PDI (but lacks the acidic C-terminal region), with around 45% identity and around 66% similarity to PDI (Volkmer *et al.*, 1997). Shortly after its identification, PDIp was shown to bind both peptides and misfolded proteins, something that has not been substantiated in other PDI homologs (Klappa *et al.*, 1998b). Interaction with native proteins however, was not detected, suggesting that, like PDI, PDIp is able to act as a molecular chaperone. This was further corroborated by the fact that some of the misfolded proteins PDIp was able to bind did not contain any Cys residues, suggesting

that in these cases, binding of PDIp to substrate proteins does not require any oxidase or isomerase activity. An experiment in the same study, however, did reveal that PDIp was able to reduce disulfide bonds in insulin, suggesting that, like PDI, PDIp is redox active (Klappa et al., 1998b).

More recently, peptides with tyrosine and tryptophan residues have be identified as recognition motifs for PDIp binding (Ruddock et al., 2000). Studies with non-peptide ligands have revealed that hydroxyaryl groups are the structural motifs for the binding of PDIp (Klappa et al., 2001). These key investigations were carried out using chemical cross-linkers and radio-labelled peptides to isolate substrate-enzyme interactions.

The **b'** domain of PDI is essential but not sufficient for peptide binding (Klappa et al., 1998a). The **b'** domain of PDIp shares around 39% identity with that of PDI. Further to this, translocation of presecretory proteins into dog pancreatic microsomes with subsequent cross-linking, shows that PDIp and PDI can interact with the same substrates (Klappa et al., 1995). More recent studies using domain fragments have substantiated that the peptide-binding properties of PDIp and PDI are similar (Klappa et al., 2001). Thus, it remains likely that members of the PDI family exhibit an overlap in substrate specificity despite the apparent elucidation of specific PDIp recognition motifs.

This is somewhat surprising when considering the tissue distribution of PDI and PDIp. Northern-blot analysis has revealed that PDIp mRNA is restricted to the pancreas

(Desilva *et al.*, 1996) and furthermore, this has been confirmed at the protein level (Dias-

Gunasekara et al., 2005; Klappa et al., 1998b). Specifically, PDIp is expressed in the

pancreatic exocrine system, in the acinar cells (Desilva *et al.*, 1997; Dias-Gunasekara *et*

al., 2005). Recent work has revealed that PDI is also expressed in the acinar cells,

alongside PDIp (Dias-Gunasekara *et al.*, 2005). The co-existence of PDI homologs in the

same intracellular compartment in the same cell type is not exclusive to PDIp or PDI.

However, it is conceivable that both PDI and PDIp are redox-active but do somehow

differ in their substrate specificity. Pancreatic zymogens were proposed as possible PDIp-

specific misfolded substrates although, studies have shown that sequences exposed in

unfolded forms of pancreatic zymogens can bind PDI as well as PDIp (Klappa et al.,

1998b).

The PDI homolog ERp57 is able to act specifically on glycoprotein substrates through

interaction with the ER chaperones calnexin and calreticulin via its **b'** domain (Oliver *et*

al., 1999; Russell *et al.*, 2004). It is possible that PDIp might exhibit substrate-specificity

in a similar manner, especially since both PDIp and ERp57 share roughly the same **b'**

domain sequence identity with PDI (Russell *et al.*, 2004). Conversely, PDIp substrate-

specificity might simply be the consequence of a small difference in protein sequence of

the **b'** domain and/or in other domains of PDIp, resulting in the binding of a set of

peptides inaccessible to PDI. Another theory proposed by Ruddock and colleagues is that

co-expressed members of the PDI family do not act on distinct proteins but rather

cooperate by interacting with different parts of the polypeptide (Ruddock *et al.*, 2000). As

of yet this has not been investigated. This could be confirmed by studying the ability of

PDIp and PDI to substitute for each other in a reconstituted system.

Despite the identification of numerous new human PDI family members in recent years,

the role of these proteins in the mechanics of the oxidative protein folding system

remains relatively unstudied. The identification and characterisation of the testis-specific

PDI homolog PDILT showed that it associated with the human Ero protein Ero1-Lα (van

Lith *et al.*, 2005). This was unusual since PDILT exhibits a non-classical S-X-X-C motif

and is unlikely to be redox-active as an oxidase.

The mechanism of oxidative protein folding in human pancreatic cells is of interest, given

that protein misfolding and UPR have been shown to contribute to type II diabetes

(Nakatani et al., 2005; Ozcan et al., 2004). In order to fully understand the redox activity

of PDI family members, it is of importance to not only characterise the interactions with

substrates, but also with the potential source of oxidising equivalents, the Eros. PDI

remains the only conventional human member of the PDI family that readily forms

trapped disulfides with Eros. Does PDIp bind Ero1-Lα or Ero1-Lβ? Ero1-Lβ is expressed

in acinar cells (Dias-Gunasekara *et al.*, 2005), however the expression pattern of Ero1-Lα

in pancreas is not known.

This chapter takes the first steps towards characterising the interactions of the pancreas-specific oxidoreductase PDIp with the human Eros, Ero1-Lα and Ero1-Lβ, comparing their interactions with the classical redox enzyme PDI.

3.3.2 Results

3.3.2.1 *The cell lines AR42J and Panc1 do not express detectable levels of endogenous PDIp*

The rationale for investigating the interactions of the human Eros with PDIp came from the observation that endogenous PDIp from mouse pancreas cells was able to interact with the human Ero, Ero1-Lβ (S. Dias-Gunasekara and A. M. Benham, unpublished data). Mouse pancreas tissue lysate was subjected to immunoprecipitation with the anti-PDIp antibody and then immunoblotted for Ero1-Lβ revealing an interaction.

We endeavoured to use pancreatic cell lines to further study the interaction of PDIp with the human Eros. Mammalian cell lines express Eros at very low levels (Dias-Gunasekara *et al.*, 2005). We therefore expected to have to transfect both Ero1-Lα and Ero1-Lβ into mammalian pancreatic cell lines in order to observe their interactions with other disulfide isomerases.

Initially, we tested the rat pancreatic cell line AR42J and the human pancreas epithelial cell line Panc1 for endogenous expression of PDIp. The mouse pancreas tissue lysate was used as a positive control and the human cervical carcinoma cell line HeLa was used as a negative control. Both cell lines and tissue were lysed in MNT lysis buffer, reduced and separated on a denaturing SDS-PAGE gel. Prior to this lysates were either incubated without (Fig. 1*A*) or with (Fig. 1*B*) ConA sepharose beads to isolate glycosylated, ER

resident proteins. Proteins were then transferred and subsequently immunoblotted using the polyclonal antibody anti-PDIp. The tissue lysate gave a strong PDIp signal (Fig. 1A, lane 1), consistent with the work of S. Dias-Gunasekara (data not shown). This signal was cleaned up and somewhat diminished by ConA sepharose isolation to pull down the glycosylated proteins in the lysate (Fig. 1B, lane 1). As expected, the lysate of the human cervical carcinoma cell line HeLa did not give a signal for PDIp (Fig. 1A, lane 4 and B, lane 4). Similarly, the human pancreatic cell line Panc1 showed no expression of PDIp (Fig. 1A, lane 3 and B, lane 3). Contrastingly, the rat pancreatic cell line AR42J showed expression of PDIp before ConA isolation (Fig. 1A, lane 2) and after ConA isolation (Fig. 1B, lane 2). The difference in expression level between the cell line AR42J and the mouse pancreas tissue lysate is most likely due to the volume/number of cells lysed. As a control, the same lysates were immunoblotted for the constitutively expressed PDI using the anti-PDI antibody (Fig. 1C). This confirmed that all samples had protein in.

Since the PDIp signal in the tissue lysate was so big, even after ConA sepharose clean up, the signal seen in the AR42J sample could possibly be from transfer of protein during loading or spill over from the lanes. In order to resolve this, ConA treated samples were rerun on an SDS-PAGE gel with a lane left in between the tissue lysate and the AR42J cell lysate (Fig. 1D). The AR42J sample showed expression of PDIp, suggesting that the original loaded sample was not the result of protein transfer from one lane to another. However this band ran at a lower molecular weight than that seen in figure 1A. The HeLa lysates also gave a signal in this region, despite not showing any signal in the previous

experiment. These data were not conclusive in distinguishing whether or not there was endogenous PDIp expression in the AR42J cell line.

We decided to further investigate which cell lines endogenously expressed the PDIp protein. We were careful this time to control loading by making sure the tissue lysate was the last sample to go on the gel. Again, lysates were immunoblotted for PDIp before and after being subjected to ConA sepharose treatment (Fig. 1*E*). PDIp expression was detected in the tissue lysate but not in either the HeLa or AR42J cell lysates (Fig. 1*E*, compare lanes 2 and 3 with lane 1). In order to confirm the presence of proteins in these samples, the same lysates were immunoblotted for PDI (Fig. 1*F*).

Interestingly, the size of the bands resulting form this anti-PDI immunoblot were slightly different between AR42J and HeLa suggesting that human and rat PDI have slightly different molecular weights. This was consistent with the data obtained in figure 1*C*.

Together these data provide evidence that PDIp is not endogenously expressed in the pancreatic cell lines AR42J and Panc1, despite being abundant in mouse pancreas tissue lysates. The initial detection of PDIp in these cell line lysates (Fig. 1*A* and *C*) was most likely a consequence of protein carry-over or due to a degree of cross-reactivity of the anti-PDIp antibody with rat and human PDI.
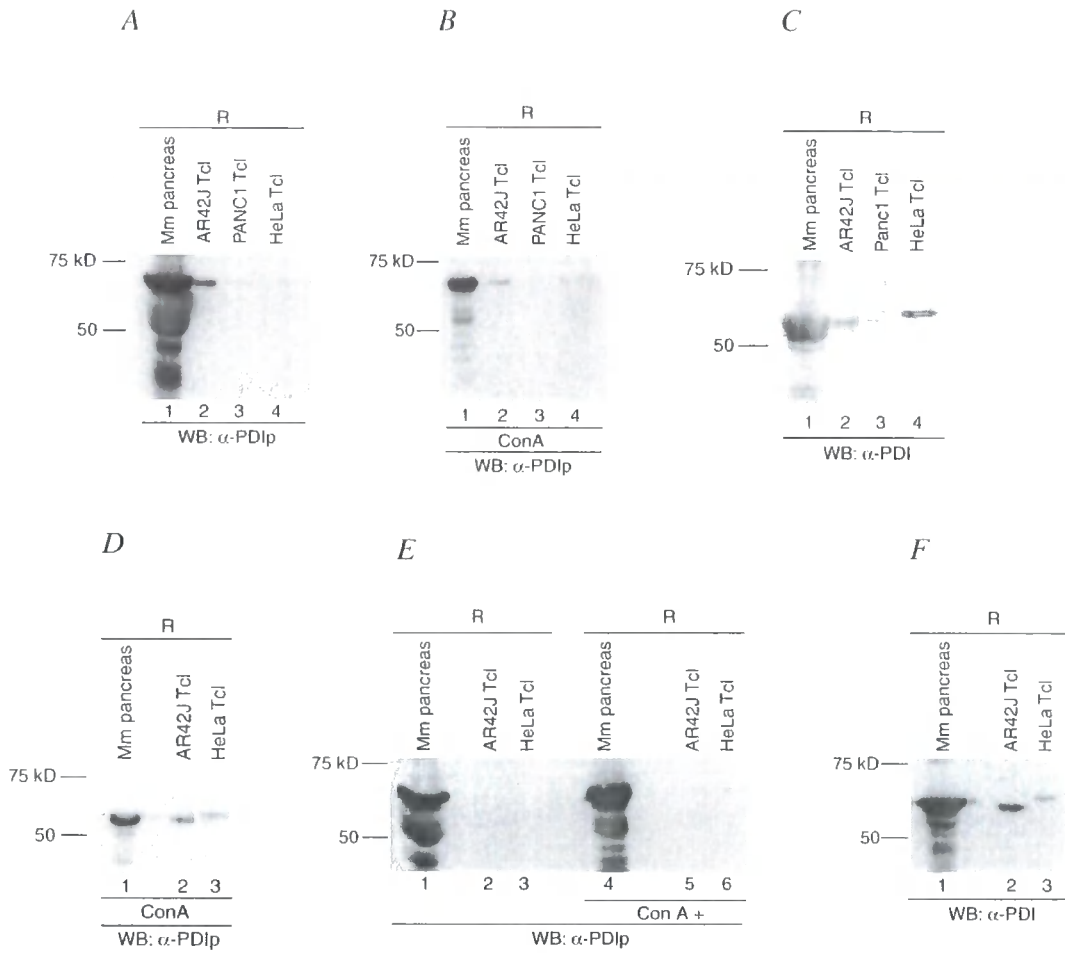
Figure 1. **The pancreatic cell lines AR42J and Panc1 do not express PDIp**. *A*, Post-nuclear total cell lysates (tcl) (lanes 2-4) or tissue lysates (lane 1) were run on a reducing (R) SDS-PAGE gel in order to resolve proteins. Proteins were then transferred to nitrocellulose and immunoblotted for PDIp. *B*, The same lysates from A, were subjected to ConA sepharose isolation at 4 °C for 2 h to separate out glycosylated proteins. Beads were spun down and washed before proteins were liberated. Proteins were then separated on gel and immunoblotted for PDIp. *C*, As in A, lysates were resolved on a reducing gel but immunoblotted for PDI. *D*, *E* and *F*, proteins were separated by SDS-PAGE as in A, B and C but a lane was left blank in between the tissue lysate (lane 1) and the cell line lysates (lanes 2 and 3).

3.3.2.2 *Establishing in vitro translation methods to study PDIp/Ero interactions*

Since endogenous expression of PDIp was not detected in the pancreatic cell lines we had, we explored *in vitro* translation methods in order to study the interactions of PDIp with the human Eros. We utilised the constructs available to us (Table 1). In order to translate proteins from the constructs available, plasmids were linearised using unique restriction sites. An example of pBS.PDIp linearisation with *XbaI* can be seen in figure 2.

Table 1 – Plasmid constructs for transcription and subsequent translation

Construct	Tag	Plasmid	Restriction Enzyme
Ero1-Lα	Myc (x 3)	pcDNA3.1	*EagI*
Ero1-Lβ	Myc (x 3)	pcDNA3.1	*EagI*
PDIp	-	pBluescript II SK	*XbaI*
PDILT	Myc (x 3)	pcDNA 3.1	*MluI*
PDI	-	pBluescript II SK	*XbaI*

Once subjected to restriction digest, linearised DNA was transcribed to obtain mRNA for use in *in vitro* translation experiments. Initially, we tested the RNAs individually to verify that they were translated. PDILT (control), PDIp, Ero1-Lα, Ero1-Lβ, and PDI mRNAs were translated using the rabbit reticulocyte lysate system from Promega (Fig. 3*A*, *B*, *C* and *D* respectively). As a negative control, the lysate mixture was loaded without any RNA so any antibody signal could be verified as the protein of interest and not due to cross-reactivity with lysate components.

As a positive control, transfected lysates were loaded. In figure 3, transfected proteins are labelled with a single asterix whilst translated proteins are labelled with a double asterix. PDILT-myc translated successfully (Fig. 3*A*, lane 1 (**)) but is smaller than the transfected protein (Fig. 3*A*, lane 2 (*)) due to the acquisition of *N*-linked glycans *in vivo*. Translation of PDIp was also successful (Fig. 3*B*, lane 1 (**)). In this case, the tissue lysate positive was also glycosylated and thus migrates higher up in the gel (Fig. 3*B*, lane 2 (*)). Some non-specific bands could be detected in the absence of RNA (Fig. 3*A* and *B*, lane 3). The translation reaction of Ero-Lα RNA produced low levels of protein (Fig. 3*C* lane 1 (**)) compared to the translation of Ero1-Lβ (Fig. 3*C*, lane 3 (**)). The positive Ero1-Lβ-myc migrates higher in the gel due to it being a glycoprotein (Fig. 3C, lane 4 (*)). PDI RNA was also translated successfully (Fig. 3D, lane 1 (**)) albeit at a lower level than PDILT (Fig. 3D, lane 2 (*)).

Since the transcripts were able to translate individually, we initially attempted to co-translate PDIp with both Ero1-Lα and Ero1-Lβ (Fig. 4). Proteins were co-translated together and individually as controls. Again, a negative control without RNA was used in order to detect any cross-reactivity with reticulocyte lysate components. PDIp translated in the presence of Ero1-Lα and Ero1-Lβ RNA as well as in the absence of other RNA and migrated as a ~45 kD protein (Fig. 4A, lanes 1-3). This was unexpected since PDIp previously migrated at ~60-65 kD in the absence of its glycans (Fig. 3B, lane 1). The tissue lysate PDIp positive was not detected by the anti-PDIp antibody (Fig. 4A, lane 4). The most likely explanation for this result is protein degradation of PDIp.

In order to detect any interaction between PDIp and Eros, the two proteins were co-immunoprecipitated from the co-translation reaction. The co-translation reaction mixture was made up to 100 μl for immunoprecipitation (IP). This mixture was subjected to IP using the anti-PDIp antibody. Immunoprecipitating and co-immunoprecipitating proteins were then isolated and separated by SDS-PAGE (Fig. 4B).
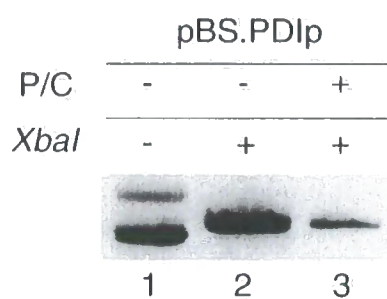
Figure 2. **Linearisation and extraction of the pBluescript.PDIp construct.** The pBluescript.PDIp construct (pBS.PDIp) was subjected to restriction digestion using the *XbaI* enzyme in order to linearise the plasmid for transcription (lane 2). After linearisation, the DNA was extracted from the reaction mixture using phenol/chloroform (P/C) techniques (lane 3). DNA was analysed on a 1% agarose gel.
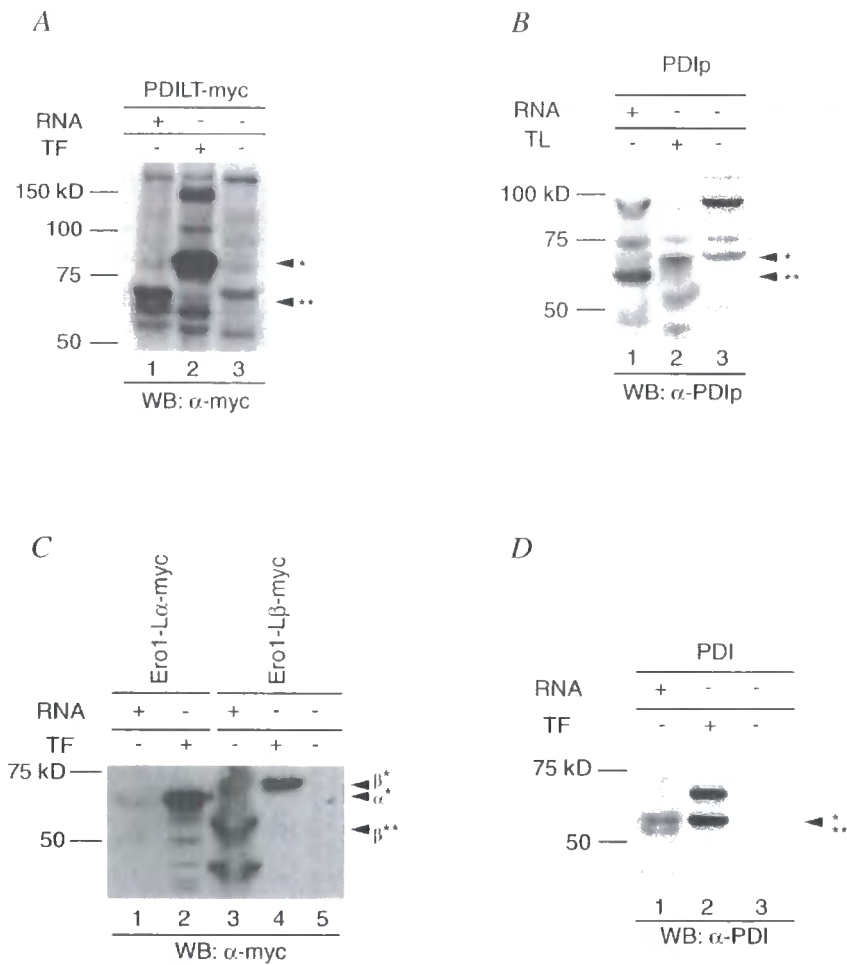
Figure 3. **Individual *in vitro* translation of disulfide oxidoreductase proteins**. Proteins were translated using the rabbit reticulocyte lysate method. RNA from PDILT (*A*, lane 1), PDIp (*B*, lane 1), Ero1-Lα (*C*, lane 1), Ero1-Lβ, (*C*, lane 3) and PDI (*D*, lane 1) was translated. Cell transfections (TF) or tissue lysates (TL) were run and used as positive controls (*). The reticulocyte lysate minus any RNA was run as a negative control. Translation products are denoted as **. All resolved proteins were transferred onto nitrocellulose membranes and subjected to immunoblotting using the anti-myc antibody (*A* and *C*) for myc-tagged proteins or the anti-PDIp (*B*) or anti-PDI (*D*) antibodies.
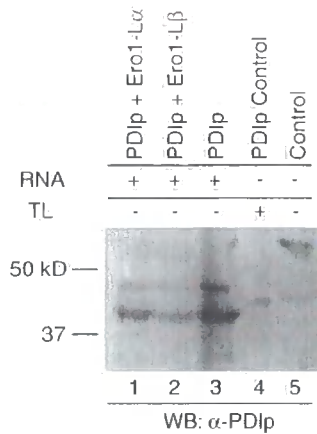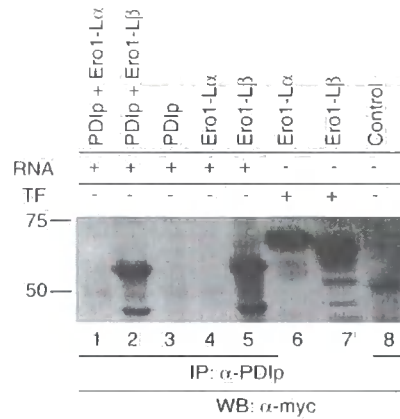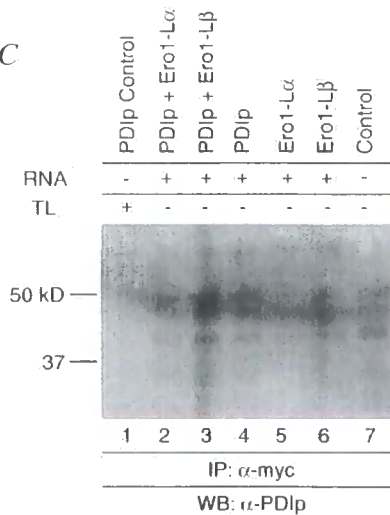
Figure 4. **Co-translation of PDIp with Eros *in vitro*.** Proteins were translated individually or co-translated using the rabbit reticulocyte lysate method. *A*, PDIp was translated individually (lane 3) or co-translated with either Ero1-Lα (lane 1) or Ero1-Lβ (lane 2). Mouse pancreas tissue lysate was used as a positive control for PDIp expression (lane 4). Control translations without RNA were also carried out (lane 5). Membranes were subsequently immunoblotted with the anti-PDIp antibody. *B*, PDIp and Eros were either co-translated (lanes 1 and 2), or individually translated (lane 3-5). Positive transfected lysates were used as Ero controls (lanes 6 and 7) and a control without RNA was also used (lane 8). Translated proteins were immunoprecipitated with the anti-PDIp antibody. Proteins were then subjected to western blot for myc-tagged proteins using the anti-myc antbody. *C*, PDIp and Eros were either co-translated (lanes 2 and 3) or individually translated (lanes 4-6). A mouse pancreas lysate was used as a positive control (lane 1) and a negative control lacking RNA was loaded (lane 7). Proteins were immunoprecipitated using the anti-myc antibody and subjected to immunoblotting using the anti-PDIp antibody.

Membranes were then immunoblotted with the anti-myc antibody in order to detect co-immunoprecipitating myc-tagged Ero proteins. Positive myc-tagged Ero transfected lysates were run as controls (Fig. 4*B*, lanes 6 and 7). Ero1-Lβ appeared to co-immunoprecipitate with PDIp (Fig. 4*B*, lane 2) however, Ero1-Lβ was also detected in the individually translated Ero1-Lβ sample (Fig. 4*B*, lane 5). Individually translated Ero1-Lβ should not have been detected by the anti-myc immunoblot after PDIp IP since PDIp was not present. Thus, the detection of Ero1-Lβ in the co-translation and the individual translation were most likely due to non-specific binding of reticulocyte lysate to the beads and inefficient washing of the Protein A sepharose beads after IP.

Co-immunoprecipitation was attempted the other way around, by immunoprecipitation using the anti-myc antibody and immunoblotting with the anti-PDIp antibody (Fig. 4*C*). No PDIp was detected in the individual and co-translations (Fig. 4*C*, lanes 2-6) or in the tissue lysate control from the mouse pancreas which was not subjected to anti-myc IP (Fig. 4*C*, lane 1). In this case the tissue lysate was the same as that in figure 4*A* and thus a lack of signal may be attributed to protein degradation. Alternatively, PDIp may not have been detected in this immunoblot as a consequence of a failed anti-myc IP. To test this, reprobing with the anti-myc antibody verified that antibodies were present (data not shown).

A
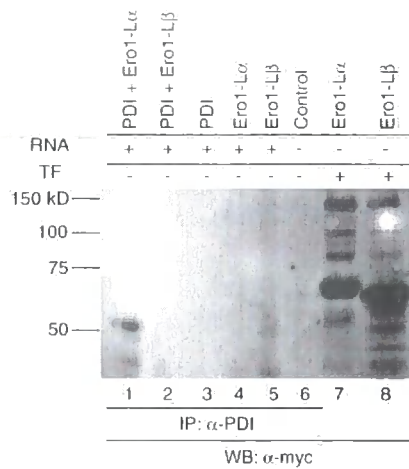
B
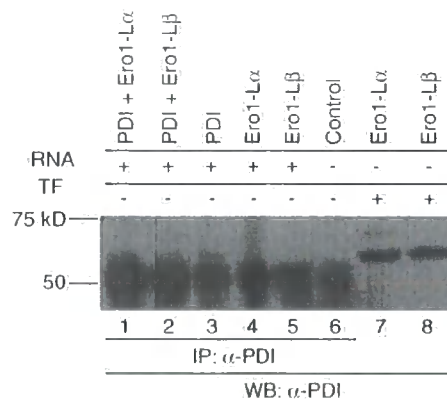
Figure 5. **Co-translation of PDI with Eros shows no interaction *in vitro*.** As in figure 4, proteins were translated individually or co-translated using the rabbit reticulocyte lysate method. *A*, PDI (lane 3), Ero1-Lα (lane 4) and Ero1-Lβ (lane 5) were translated individually or PDI was co-translated with either Ero1-Lα (lane 1) or Ero1-Lβ (lane 2). Transfected lysates (TF) were used as a positive control for Ero1-Lα or Ero1-Lβ expression (lane 7 and 8). The translation reactions were subjected to anti-PDI immunoprecipitation and subsequently immunoblotted with the anti-myc antibody. *B*, The same membrane used in A, was blotted back using the anti-PDI antibody to confirm that the immunoprecipitation had isolated PDI.

The interactions of the human Eros with PDI have been documented (Benham *et al.*, 2000; Dias-Gunasekara *et al.*, 2005). We attempted to use this *in vitro* translation system to verify that both Ero1-Lα and Ero1-Lβ are able to interact with PDI. The human myc-tagged Eros were individually translated or co-translated with PDI (Fig. 5). As previously described, the volume of the reaction was increased to 100 µl for immunoprecipitation with the anti-PDI antibody. Proteins were liberated from the beads and immunoblotted for the myc-tagged Eros using the anti-myc antibody (Fig. 5*A*). Both the positive transfected Eros were detected strongly (Fig. 5*A*, lanes 7 and 8). However, no myc-tagged Eros were detectable in any of the translation reactions (Fig. 5*A*, lanes 1-5). In order to verify that the anti-PDI immunoprecipitation was successful, IP samples were rerun and immunoblotted for PDI (Fig. 5*B*). Blotting back with PDI revealed that the immunoprecipitation had worked since PDI could be weakly detected in those samples in which it had either been individually translated or co-translated at a similar position to the positive controls (Fig. 5*B*, compare lanes 1-3 with lanes 7 and 8). Antibody heavy chains ran at 50 kD, showing that antibody had bound to the Protein A sepharose beads.

Taken together these data did not show any interaction between the human Eros and PDIp or indeed PDI. A failure to detect interactions with PDI using *in vitro* translations is contrary to published data, and thus may be a consequence of low translation efficiency. The IPs did not co-immunoprecipitate any complexed proteins. This could be due to the fact that only small amounts of protein were recovered in the anti-PDI and anti-myc IPs

(Fig. 5*B*, lanes 1-3 and data not shown) or that PDIp may indeed not interact with either

Ero protein *in vitro.*

3.3.2.3 *Cloning of PDIp for human cell line transfection*

Liposome-mediated transfection of plasmid constructs containing a gene of interest is a popular and successful method of studying protein interactions. This technique has been employed both in this project and published data (Dias-Gunasekara et al., 2006; van Lith et al., 2005). We have previously transfected both myc-tagged Ero1-Lα and Ero1-Lβ into human HeLa cells (Chapter 3.1). Since there is no endogenous expression of PDIp in HeLa cells, we would have to transfect in a plasmid containing the PDIp gene. Unfortunately, the construct we kindly received from M. Lan was in the pBluescript II vector. Since pBluescript II does not have a human cytomegalovirus (hCMV) promoter, the gene will not transcribe *in vivo*.

The human Ero pcDNA 3.1 constructs contain the vital hCMV promoter required for human cell expression. In order to express PDIp in HeLa cells, the PDIp construct would have to be removed from the pBluescript II vector and ligated into the pcDNA 3.1 vector. *EcoRI* and *XbaI* were identified on pBS-PDIp and the empty pcDNA 3.1 plasmid as compatible restriction sites (Appendix 1). These enzymes are able to digest the multiple cloning site of the empty vector and either side of the PDIp insert of the pBluescript II vector. Therefore, 5 μg of both DNA constructs were subjected to double-digestion with the *EcoRI* and *XbaI* restriction enzymes.

In order to isolate the liberated PDIp insert from the pBluescript II vector, the products of both double-digestions were run on an agarose gel (Fig. 6A). The PDIp insert and the

linearised pcDNA 3.1 vector were cut out of the gel and subsequently isolated by gel extraction methods. The amount of the insert and vector were verified by running the extracted products on an agarose gel together with DNA standards of known concentration (Fig. 6*B*). An approximation of both insert and vector concentration was determined by analysing pixel definition in the samples and comparing them with the DNA standards using the program TINA 2.0 (Table 2).

Table 2 – Vector and insert DNA concentrations

Band	Pixel Density Value	Ratio (in x 10^{-3} ng pixel^{-1})	Amount of DNA (ng)
100 ng Standard	97931	1.02	121
200 ng Standard	159008	1.26	197
500 ng Standard	349470	1.43	433
Average		**1.24**	
Purified Insert DNA	164590		**204**
Purified Vector DNA	160262		**199**
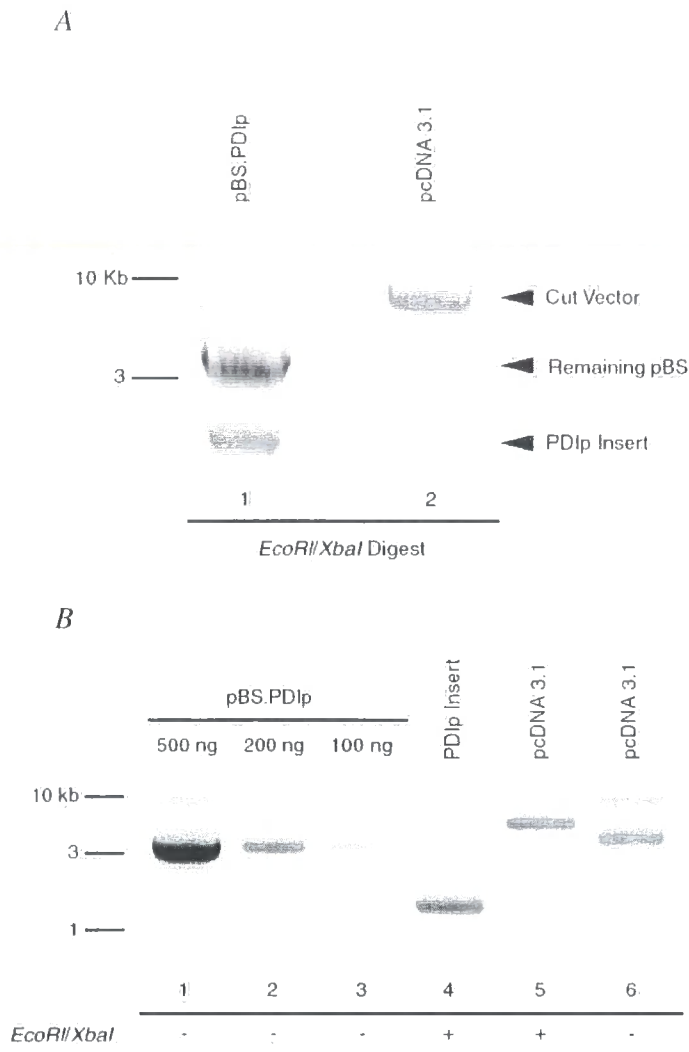
Figure 6. *EcoRI/XbaI* **digestion, purification and concentration determination of the PDIp gene insert and the pcDNA 3.1 vector.** A, Both the pBS.PDIp and pcDNA 3.1 vector were subjected to double digestion using the *EcoRI* and *XbaI* restriction enzymes. Restriction digests took place at 37 °C for 2 h. The PDIp insert and cut vector were separated by loading the digest reaction on a 1% agarose gel. The insert and pcDNA 3.1 vector were cut out of the gel and purified by gel extraction methods. B, In order to determine the concentration of the purified vector and insert, a small amount of DNA (lanes 4-6) was loaded on a 1% agarose gel together with DNA standards (lanes 1-3). A pcDNA 3.1 vector was loaded as a control (lane 6). Concentration was determined by pixel definition of these bands (See Table 2).

Purified PDIp insert and pcDNA 3.1 vector then required ligation. This was carried out using a vector:insert ratio of 1:20 at room temperature for 2 h using T4 ligase. Controls were also carried out using a) a ligation without an insert; this ruled out the possibility that colonies produced from the ligation were derived from vectors that had re-ligated due to single digestion or no digestion at all, b) a ligation without ligase; this ruled out the possibility that if colonies grew, they were due to undigested vector. This also served as a negative control for vector/insert ligation. A positive control for transformation was carried out by transforming the original pcDNA 3.1 empty vector.

After ligation, *E. coli* DH5α were subjected to aseptic transformation with 0.5 ng of DNA from the ligations. Small cultures of transformed *E. coli* were then plated on LB agar plates plus 100 μg ml^{-1} ampicillin and incubated overnight. The resulting agar plates harboured colonies in the positive control pcDNA 3.1 transformation. No colonies were present on any of the agar plates from the ligation samples (data not shown).

Ligation was repeated using the same purified vector and insert at different ratios. The original 1:20 ratio was kept, as well as including a 1:10 and 1:1 ratio. The ligations were performed at room temperature but were carried out overnight in this instance. The resulting transformed *E. coli* produced colonies on agar plates from the positive pcDNA 3.1 transformation but failed to produce colonies from any of the ligations (data not

shown). The ligation was attempted a third time, using only the 1:10 ratio. Temperature was kept constant in this instance by incubating the ligation reactions at 16 °C overnight. The resulting plates failed to produce any colonies yet again despite the control for transformation being successful (data not shown).

Subsequently, new restriction sites were chosen for digestion. However, due to limitations on available sites, a blunt-ended restriction site had to be created using the *SmaI* and *EcoRV* restriction enzymes. *HindIII* was used as the sticky-ended restriction enzyme. Although blunt ended digestion is not ideal, a blunt-ended and a sticky-ended restriction site should allow correct orientation so long as the original vectors fully digest.

Because of the incompatibility of restriction digestion temperatures, the digestions were completed sequentially. After double-digestion, fragments were run on a 1% agarose gel to isolate the vector and insert (Fig. 7A). Fragments were cut out and purified. As previously, DNA concentration was estimated from the pixel definition of the image obtained from transillumination (Fig. 7B). Ligation was carried out at a ratio of vector:insert of 1:20 using a brand new ligase and buffer as well as the old one in order to assess whether the buffer was a problem. Ligations were performed at room temperature for 2 h as per the original protocol.

DH5α was once again transformed with the ligated DNA. The resulting plates showed no growth of colonies besides the positive for transformation, indicating that the old ligase

was not solely responsible for defective ligation (data not shown). Due to time constraints

this investigation was not completed and ligation was not successful during the course of

study.
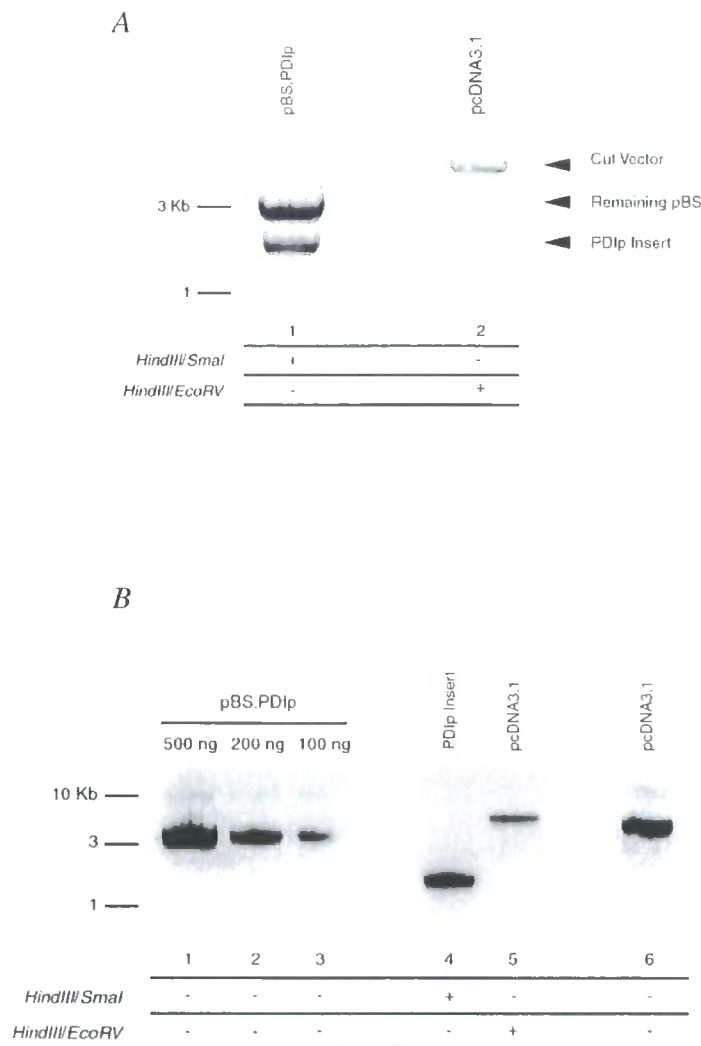
Figure 7. *HindIII/SmaI/EcoRV* **digestion, purification and concentration determination of the PDlp gene insert and the pcDNA 3,1 vector**. A, As in figure 6, however this time both pBS.PDlp and pcDNA 3.1 vector were subjected to different double digestions resulting in two different blunt ended restriction digests and a common 'sticky-ended' restriction digest. pBS.PDlp was digested using *HindIII* and *SmaI* restriction enzymes (lane 1), whilst the pcDNA 3.1 vector was digested using the *HindIII* and *EcoRV* restriction enzymes (lane 2). The PDlp insert and cut vector were separated by loading the digest reaction on a 1% agarose gel. *B*, In order to determine the concentration of the purified vector (lane 5) and insert (lane 4), a small amount was loaded on a 1% agarose gel together with DNA standards (lanes 1-3). An unrestricted pcDNA 3.1 vector was loaded as a control (lane 6). Concentration was determined by pixel definition of these bands.

3.3.3 Discussion

In order to fully understand the redox role of PDI and its homologs, we must not only study the interactions of oxidoreductases with their substrates, but also their source of oxidising equivalents, the Eros. Classical PDI has been shown to bind both Ero1-Lα and Ero1-Lβ (Benham *et al.*, 2000; Dias-Gunasekara *et al.*, 2005). Some human homologs of PDI, however, do not seem to bind some human Eros (Benham *et al.*, 2000). Since the recent identification of Ero1-Lβ, there has not been a systematic study of PDI homolog-Ero interactions.

Here, we attempted to characterise the binding of human Eros with the pancreas-specific PDI homolog PDIp. We initially attempted to use *in vivo* techniques using the endogenous expression of PDIp in the pancreatic cell lines available to us to study PDIp-Ero interactions. Despite the fact that the rat cell line AR42J is a pancreatic acinar cell type, no endogenous PDIp was reproducibly detected in this cell line (Fig. 1*E*). Thus, AR42J may not express PDIp, or the PDIp antibody may not recognise rat PDIp. This seems unlikely, since the antibody was raised against the whole protein rather than a peptide (Desilva *et al.*, 1996). An alignment of human, murine and rat PDIp shows that the three proteins have very high homology (Fig. 8).

Attempts were then made to study the interactions *in vitro* using a co-translation method where proteins that could potentially interact were translated together in a closed system.
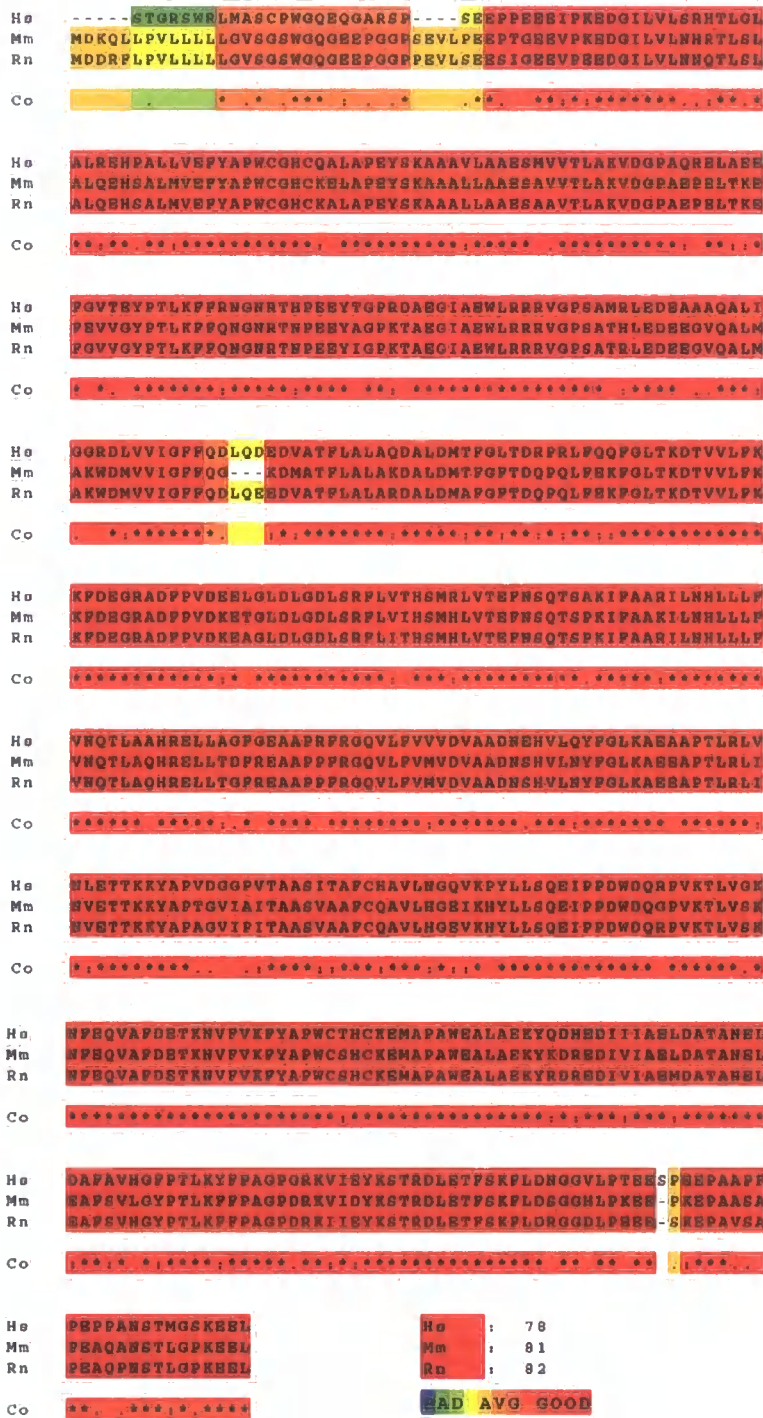
Figure 8. **A human, mouse and rat PDIp protein sequence alignment**. PDIp protein sequence from human (*Homo sapiens*) (Hs) (AAH75029), mouse (*Mus musculus*) (Mm) (AAI16672) and rat (*Rattus norvegicus*) (Rn) (XP_213263) were aligned using the T-coffee multiple alignment program.

Co-immunoprecipitation of complexes, however, proved difficult using the rabbit reticulocyte translation method due to protein expression levels and non-specific binding. The data obtained did not allow us to define whether PDIp is able to interact with either Ero1-Lα or Ero1-Lβ (Fig. 4B and C). Analysis of the IPs revealed that the technique was successful in isolating the myc-tagged proteins (data not shown), but no co-immunoprecipitating PDIp could be detected (Fig. 4C). Using the same technique, neither Ero1-Lα nor Ero1-Lβ were detected co-immunoprecipitating with PDI; an observation that is contrary to published data (Fig. 5A). It is more likely that *in vitro* translation was inefficient, giving too little protein to observe PDIp/Ero interactions. Given more time, improving reticulocyte translation efficiency by testing temperature, using different concentrations of Cap analog and different concentrations of Mg^{2+} and DTT could be attempted.

The cloning of the PDIp gene into a vector capable of being transfected into human cells was initially promising, with digestion and isolation of the PDIp gene proving successful (Fig. 6A and B). Despite perseverance, the ligation of the PDIp gene into the new vector was unsuccessful. Unfortunately, due to time restrictions, this study was not completed. Future work will concentrate on completing the optimisation of ligation to allow us to use transfection in order to study PDIp/Ero interactions. Transfection of PDIp and both Ero1-Lα and Ero1-Lβ will allow us to observe protein interactions both by co-immunoprecipitation techniques and by using alkylating agents to trap any potential disulfide-bonded complexes. Site-directed mutagenesis of active site residues of both

PDIp and the Eros would allow for analysis of the active-site chemistry of PDIp. Recent evidence also points to the requirement of PDI and ERp44 for ER retention of the Eros by covalent interactions (Otsu *et al.*, 2006). It would be interesting therefore to investigate if PDIp was also able to assist in the retention of the Eros in the ER.

Both the substrate-binding properties of PDIp and the role of PDIp as a chaperone have been studied (Klappa *et al.*, 1998a; Klappa *et al.*, 1998b; Ruddock *et al.*, 2000). Work now also needs to focus on substrate binding by studying the possible role of glycosylation and the **b'** domain in substrate selection and binding. This will help to elucidate the specific, specialised function of PDIp, a disulfide oxidoreductase that co-exists with the ubiquitously expressed classical oxidoreductase PDI.

3.4 ER stress response signalling in HLA-B27-expressing cells

3.4.1 Introduction

The major histocompatability complex is a set of cell surface molecules involved in the presentation of peptides for immune surveillance (Pamer and Cresswell, 1998). Possession of the human MHC class I molecule human leukocyte antigen B27 (HLA-B27) is highly associated with the development of a group of chronic inflammatory diseases known as the spondyloarthropathies (SpA). HLA-B27 is present in the overwhelming majority of individuals suffering from ankylosing spondylitis (AS) – around 90-95% (Brewerton et al., 1973) – and is also associated with other forms of SpA, such as reactive arthritis (ReA) and inflammatory bowel disease (IBD)-associated SpA. However, possession of the allele alone is not enough to cause onset of AS since 5% of HLA-B27-positive individuals can develop the disease in the absence of family history. AS is typically characterised by inflammation of the axial skeleton, which manifests itself as lower back pain due to sacroilitis and/or spondylitis.

The use of HLA-B27-expressing transgenic rodent models has proven vital in furthering our understanding of the development of the spondyloarthropathies as well as providing compelling evidence for a direct link between HLA-B27 expression and SpA pathogenesis. HLA-B27/hβ_2m transgenic (B27-Tg) rats develop a multi-system spontaneous inflammatory disease closely resembling that of human SpA (Hammer et al., 1990; Taurog et al., 1999; Taurog et al., 1993; Taurog et al., 1994; Tran et al., 2004).

Overexpression of HLA-B27 and $h\beta_2m$ initially results in colitis and localized inflammation, finally leading to inflammation of the gastrointestinal tract and joints (Hammer *et al.*, 1990). Despite showing many of the characteristics of human SpA, B27-Tg rats do not present the full phenotype of human AS, since these animals a) do not develop ankylosis of the axial skeleton and b) exhibit a more prominent inflammation of the bowel.

A link between the development of SpA-related phenotypes and environmental factors has been suggested, since the development of disease in the B27-Tg rats is dependent on being housed in probiotic conditions. In contrast, when B27-Tg rats are housed in germ-free conditions, these animals do not develop the disease or any associated phenotypes (Taurog *et al.*, 1994). Evidence from Rath and colleagues has shown that colonization of the gastrointestinal tract with normal gut flora, particularly *Bacteroides* ssp., is sufficient to trigger the development of characteristic gut inflammation (Rath *et al.*, 1996).

A large body of evidence points to an intimate link between intestinal inflammation and the pathogenesis of AS in patients. This evidence includes the prevalence of inflammatory bowel disease (IBD) in patients suffering from AS and family members of these patients (Dekker-Saeys *et al.*, 1978; Woodrow, 1985), antigenic and structural cross-reactivity between HLA-B27 and components of enteric bacteria (Scofield *et al.*, 1993; Williams and Raybourne, 1990) and diminished internalization of enteric bacteria by B27-expressing fibroblasts (Kapasi and Inman, 1992). In addition to this, several gastrointestinal and genito-urinary pathogens including *Campylobacter* ssp., *Chlamydia*

ssp., *Salmonella* ssp. and *Shigella* ssp. have been implicated as triggers of HLA-B27-associated reactive arthritis (Colmegna *et al.*, 2004).

Since the presence of pathogens seems to be correlated with disease development, pathogenesis of the disease has been linked with the physiological role of the class I molecule. MHC class I molecules present intracellularly derived peptides to CD8$^+$ cytotoxic T-lymphocytes (Pamer and Cresswell, 1998). Usually, these peptides are derived from self-proteins, however during infection by intracellular pathogens, foreign peptides are presented. It has been proposed that pathogenesis is a consequence of the presentation of a peptide or series of peptides specific to the B27 molecule (Benjamin and Parham, 1990). Residues in the peptide binding groove of HLA-B27 might allow the binding of joint-specific arthritogenic peptide(s), recognised by autoreactive T-lymphocytes which may elicit a novel cytotoxic T-cell response leading to chronic inflammation. This remains a popular theory of pathogenesis since only a small number of polymorphic HLA-B27 subtypes are associated with the disease (Colbert *et al.*, 1994; D'Amato *et al.*, 1995; Lopez-Larrea *et al.*, 1995).

The possibility that peptides responsible for potential AS-associated autoreactivity are derived from self-proteins is still being disputed. Although B27 molecules binding bacterially-derived or indeed self-derived peptides have been discovered in the synovium of both sufferers of ReA and AS, no self peptides that may be targeted by T-cells have been defined (Hermann *et al.*, 1993; Kuon *et al.*, 2001). Conversely, the search for

candidate bacterial arthritogenic peptides that may trigger inflammation in AS remains arduous (Smith *et al.*, 2006).

Recent work has revealed that depletion of CD8$\alpha\beta^+$ T-lymphocytes by adult thymectomy plus short-term anti-CD8α mAb treatment fails to suppress the development of arthritis and colitis in B27-Tg rats (May *et al.*, 2003). However, these data did implicate a CD8$^+$ monocyte population whose numbers expand in disease. Classical T cell recognition therefore does not appear to be required for pathogenesis. Interestingly, MHC class I molecules have been found to react with additional cell surface receptors including the killer immunoglobulin receptor (KIR), the leukocyte immunoglobulin receptor (LIR) and CD4$^+$ receptors found on a variety of immune cells including natural killer cells (Allen and Trowsdale, 2004; Boyle *et al.*, 2001; Lopez-Larrea *et al.*, 2006). Taken together these data highlight the potential complexity of receptor-mediated autoreactive responses.

The unusual cell biology of HLA-B27 has also been the subject of investigation in an attempt to elucidate the pathogenesis of AS. Allen and colleagues were the first to document that, in the absence of β_2m, HLA-B27 is able to form disulfide-linked homodimers *in vitro* via its highly reactive, unpaired cysteine residue at position 67 (Cys^{67}) of the B pocket in the peptide-binding groove (Allen *et al.*, 1999). Since then, homodimers have been discovered at the cell surface. It appears that cell-surface heterodimeric HLA-B27 disassociates, heavy chains dimerise in endosomes and are then recycled back to the cell surface (Bird *et al.*, 2003). These homodimeric HLA-B27 molecules are able to be interact with killer immunoglobulin receptors (KIR) and

immunoglobulin-like transcripts (ILT) on T and B lymphocytes, NK cells and monocytes (Kollnberger *et al.*, 2002). Recognition of aberrant forms of HLA-B27 may contribute to pathogenesis through a modulation of leukocyte function.

Additionally, a distinct population of homodimers exists in the ER. This aberrantly folded, or misfolded, population is not due to the dissociation of β_2m from a natively folded heterodimer, but rather the lack of/delayed association of β_2m due to the architecture of the B pocket region of the heavy chain (Antoniou *et al.*, 2004; Dangoria *et al.*, 2002; Mear *et al.*, 1999). When a transgenic murine model lacking β_2m was developed by Kingsbury and colleagues in 2000, it was shown that misfolding of endogenous class I molecules due to lack of β_2m was sufficient to cause spontaneous inflammatory disease (Kingsbury *et al.*, 2000). Recently, evidence has shown that the formation of misfolded heavy chain dimers is related to the rate of assembly of the HLA-B27 molecule in addition to residues flanking the reactive Cys^{67} residue (Antoniou *et al.*, 2004).

How this ER-restricted population of homodimers might be related to SpA pathogenesis is still unclear, however, recent studies have focused on ER stress responses as a consequence of HLA-B27-associated misfolding (Turner *et al.*, 2005). HLA-B27 heavy chains are thought to misfold as a consequence of the residues in the B pocket of the peptide-binding groove (Mear *et al.*, 1999). Because of the unique residues in the HLA-B27 B pocket, the peptide-binding groove is inefficient at loading antigenic peptide.

Prolonged retention of the class I molecule in the ER in its unfolded conformation may lead to aberrant disulfide formation thought to be promoted by Cys^{67} and possibly other Cys residues (Antoniou *et al.*, 2004). Misoxidation of proteins in the ER can result in the dislocation and subsequent degradation of these proteins by ER-associated degradation (ERAD) (Trombetta and Parodi, 2003). Shortly after synthesis, some HLA-B27 molecules have been shown to undergo cytosolic degradation (Mear *et al.*, 1999) which may be the consequence of inefficiently folded and/or misfolded HLA-B27 in the ER.

Newly synthesised proteins that fold slowly and/or unstably have been shown to preferentially bind the abundant ER chaperone immunoglobulin binding protein (BiP) (Hellman *et al.*, 1999). Appropriately, evidence has been provided for the prolonged association of HLA-B27 with BiP in the ER (Tran *et al.*, 2004). One job of the chaperone BiP is to retain misfolded proteins in the ER in order to prevent inefficiently folded proteins from exiting the ER into the secretory pathway. Thus, association of BiP with HLA-B27, although a quality control measure, may indeed serve to promote aberrant disulfide formation since misfolding is a consequence of prolonged retention in the ER.

Continued retention of misfolded proteins in the ER and inefficient degradation of these aberrant proteins may lead to an accumulation of BiP-bound proteins. The consequence of exceeding the folding capacity of the ER is the activation of the unfolded protein response (UPR). The UPR is a series of cellular signaling pathways which monitor the folding capacity of the ER and seeks to resolve any imbalance. In mammals three signaling branches of the UPR have evolved involving the transmembrane proteins;

ATF6, IRE1 and PERK (Shi *et al.*, 1998; Yoshida *et al.*, 1998; Yoshida *et al.*, 2001).

Upon detection of ER stress, these proteins regulate the folding capacity of the ER at the

translational and transcriptional levels in an attempt to restore homeostasis by

upregulating both genes involved in the ER-associated degradation of terminally

misfolded proteins and ER chaperones to facilitate the binding of newly synthesised

polypeptides.

Recently, Turner and colleagues provided evidence linking HLA-B27 misfolding in bone

marrow-derived cells from B27-Tg rats with activation of the UPR (Turner *et al.*, 2005).

In this key paper, they also drew attention to the presence of pro-inflammatory cytokines

in cells exhibiting UPR activation, proposing a possible role for IFN-γ in the process.

Another potential link between UPR activation and a pro-inflammatory effect is

suggested by the recent study providing evidence that NF-κB is activated by ER stress-

induced reduction in the synthesis of the NF-κB inhibitor IκBα (Deng *et al.*, 2004). The

effects of an ER overload therefore could potentially upregulate a number of cytokines

and chemokines dependent on NF-κB (Baeuerle and Henkel, 1994).

Whether or not HLA-B27 misfolding is pathogenic remains to be seen. However, it is

worth noting that accumulation of misfolded proteins has been shown to be pathogenic in

polyglutamine diseases and common neurodegenerative diseases such as Alzheimer's and

Parkinson's (Imaizumi *et al.*, 2001; Yoneda *et al.*, 2002). The consequence of UPR

signaling in HLA-B27-expressing cells will also require investigation. Work now needs to focus on linking UPR activation in human disease.

This chapter investigates the levels of UPR induction in typed lymphoblastoid cells – positive for HLA-B27 – and the effects of the pharmacological agents DTT and tunicamycin on UPR induction.

3.4.2 Results

3.4.2.1 *Differential effects of DTT and tunicamycin on XBP1 processing*

In order to study the effects of HLA-B27 expression on ER stress, we initially optimised the system for detection of activation of the UPR. We used the IRE1/XBP1 signalling pathway to initially determine UPR activation using pharmacological agents. IRE1 is a transmembrane ER protein, which is kept in an inactive, monomeric form by BiP, bound to its lumenal portion. During an accumulation of misfolded and/or unfolded proteins, BiP preferentially binds to these aberrantly folded proteins and is sequestered away from IRE1, activating the signaling pathway. IRE1 then dimerises and consequently autophosphorylates resulting in activation of its site-specific endo-RNase activity.

The target of IRE1 is the ubiquitously expressed *Xbp1* (X-box binding protein 1) message. The removal of a 26-nucleotide intron from *Xbp1* mRNA generates a translational frame shift producing a protein encoded by two different open reading frames (ORFs). The resulting XBP1 protein acts as a transcription factor, targeting unfolded protein response elements (UPRE) upstream of many UPR-inducible genes, upregulating or activating their transcription (Lee *et al.*, 2002; Shen *et al.*, 2001; Yoshida *et al.*, 2001).

In order to detect activation of the IRE1/XBP1 signalling pathway, we utilised the fact that the removal of the 26-nucleotide intron from *Xbp1* mRNA removes a unique *Pst1* site (Calfon *et al.*, 2002). Thus, activation can be monitored by a simple *Pst1* digest of

Xbp1 mRNA (Fig. 1). Initially the human acute monocyte cell line THP1 was studied for levels of UPR induction with pharmacological agents.

Dithiothreitol (DTT), a reductant able to stimulate misfolding by altering the oxidising environment of the ER and tunicamycin, an agent that prevents correct glycosylation, were used to promote ER stress and activate the UPR over a time course of either 0, 3, 6 or 24 hours (Fig. 2*A* and *B*). THP1 cells were treated with 10 mM DTT or 10 μg/ml tunicamycin for the indicated time course; cells were then lysed for RNA extraction. Total cell RNA was then subjected to reverse transcriptase PCR (RT-PCR) using primers for *Xbp1* and *β-actin* as a control. Amplified XBP1 cDNA was then digested with the *Pst1* restriction enzyme to detect activation of IRE1-mediated splicing. The resulting digest was then purified and run on a 2% agarose gel to separate the sensitive and resistant products. The products running higher in the gel are resistant to digestion and thus are the spliced form of XBP1 (XBP1 (S)). These products represent activation of the UPR. Products running lower in the gel are sensitive to the digestion by *Pst1* and thus remain unspliced (XBP1 (U)) (Fig. 1).

At time point 0 h, with no treatment, *Xbp1* mRNA existed at a low level of expression and as a doublet running at the height of the unspliced, inactive form of XBP1 (Fig 2*A* and *B*, lane 1). This doublet of 289 and 255 nucleotides is the product of *Pst1* digestion. Upon treatment of cells with DTT for 3 h, IRE1-mediated XBP1 processing was induced resulting in a single band representing the spliced version of XBP1 (Fig 2*A*, lane 2). Upon DTT treatment for longer periods of 6 and 24 h, XBP1 continued to be processed,

indicated by the persistence of the resistant band higher in the gel (Fig. 2A, lanes 3 and 4). Conversely, when cells were treated with tunicamycin, a doublet persisted representing the spliced version of XBP1 (Fig. 2B, lanes 2 and 3). The top band in the doublet ran at the same height to that of the DTT induced resistant band. The lower band therefore must represent a nucleic acid sequence of smaller length to the band running above it. The presence of this smaller product may be a consequence of a further splicing or processing event. Stimulation with tunicamycin for 24 h, however, resulted in a single resistant species (Fig. 2B, lane 4). THP1 cells partially recovered from tunicamycin stimulation, indicated by the reemergence of the sensitive, unspliced species after 24 h (Fig. 2B, lane 4). This is in contrast to DTT treatment, which kept XBP1 processing switched on after 24 h treatment (compare Fig. 2B, lane 4 with Fig. 2A, lane 4). This was surprising, as one would expect DTT to become oxidised after such an extended period of time in culture medium due to the fact that it is a labile reductant.

Size:

Pst1 site

544 nt   Unspliced –
inactive XBP1
RNA

518 nt   Spliced –
active XBP1
RNA

+ *Pst1* digestion

255 nt
and   +   Unspliced –
289 nt   digested XBP1
RNA

Spliced –
518 nt   undigested
XBP1 RNA
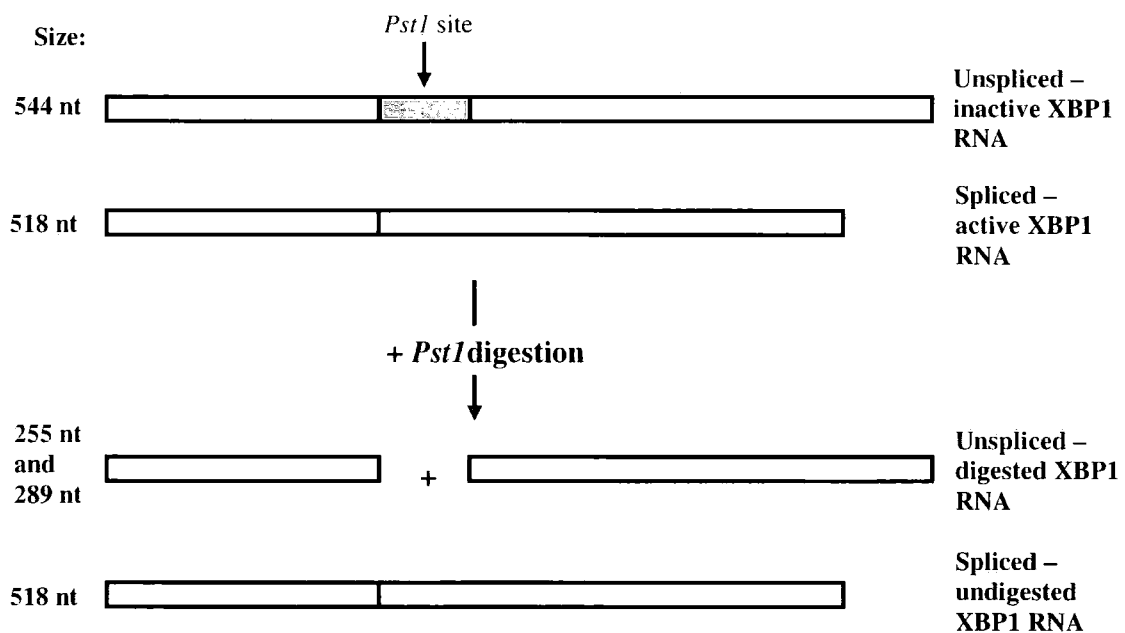
Figure 1. *Pst1* **digestion as a technique for analysing XBP1 processing.** When inactive XBP1 RNA is spliced, a 26 nucleotide intron is removed containing a unique *Pst1* site. Upon digestion of inactive XBP1 RNA, two fragments are generated of 255 and 289 nucelotides (nt) due to the presence of the *Pst1* site. Activated (spliced) RNA however is not digested by the restriction enzyme due to its removal by IRE1 and thus migrates as a single 518 nt fragment.

A

THP1

DTT   -   +   +   +

0 h   3 h   6 h   24 h

518 nt —   ▬▬ ▬▬ ▬▬   ◄ XBP1 (S)

289
255   ═   ◄ XBP1 (U)

775 nt — ▬▬ ▬▬ ▬▬ ▬▬   ◄ β-actin

1   2   3   4

B

THP1

Tm   -   +   +   +

0 h   3 h   6 h   24 h

518 nt —   ▬▬ ▬▬ ▬   ◄ XBP1 (S)

289
255   —   ▬   ◄ XBP1 (U)

775 nt —   ▬▬ ▬▬ ▬▬   ◄ β-actin

1   2   3   4
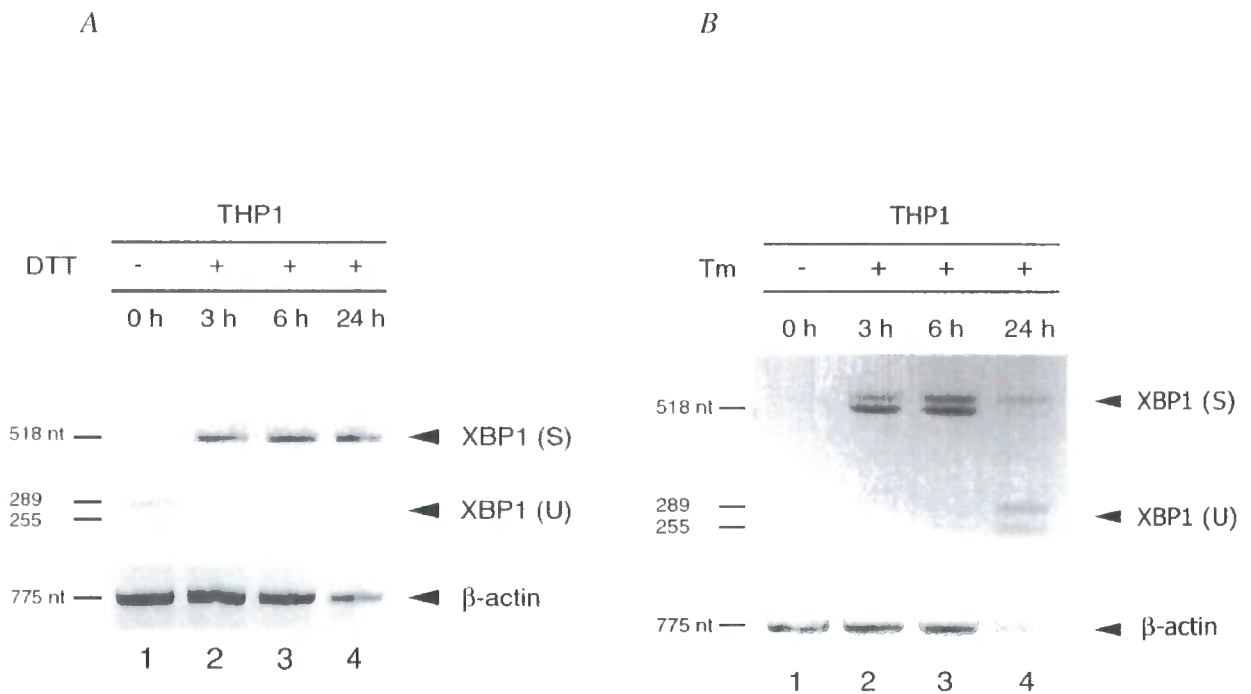
Figure 2. **DTT and tunicamycin induce different pathways of XBP1 processing.** *A*, THP1 cells were stimulated with (lanes 2-4) DTT or without (lane 1) for given time periods and lysed in TRIreagent. Total cell RNA was subjected to RT-PCR for XBP1 and β-actin. Total XBP1 PCR product was digested with *Pst1* enzyme, purified and run on 2% agarose gel to resolve the resistant, spliced product (XBP1 (S)) and the digested, unspliced produced (XBP1 (U)). *B*, Cells were stimulated with tunicamycin (Tm) (lanes 2-4) or without (lane 1) for given time periods and analysed as in *A*.

3.4.2.2 *XBP1 processing in HLA-B27-positive lymphoblastoid cell lines*

After characterising UPR induction in THP1 cells using DTT and Tm as stimulants, we investigated the level of XBP1 processing in immune cells expressing HLA-B27. We chose typed lymphoblastoid cell lines WEWAK1, positive for subtype HLA-B27*04 and HOM-2 and JESTHOM, both positive for subtype HLA-B27*05. Both HOM-2 and JESTHOM cell lines are known to have come from patients suffering from AS.

We examined the sensitivity of these cell lines to UPR induction upon treatment with both DTT and tunicamycin (Fig. 3). In addition, we used the THP1 cell line studied previously as a control. We treated THP1 cells with lipopolysaccharide (LPS) for 4 days to stimulate the differentiation of THP1 monocytes to adherent macrophages. This differentiation results in a reorganisation of the ER. Treatment with LPS however, was not sufficient to activate XBP1 processing, as expected (Fig. 3, compare lanes 11 and 10).

In the absence of ER stress-inducing stimuli, WEWAK1, HOM-2 and JESTHOM showed higher levels of XBP1 processing than that of the untreated monocytes (Fig. 3, compare lanes 1, 4 and 7 with lane10). All three of these cell lines showed similar levels of spliced and unspliced XBP1 RNA, the spliced version migrating as a singlet. Upon treatment with DTT however, full activation of XBP1 splicing was achieved, indicated by the loss of the unspliced XBP1 species and an increase in intensity of the resistant band (Fig. 3, compare lanes 2, 5 and 8 with lanes 1, 4 and 7). In contrast, treatment with tunicamycin resulted in a small increase in activation of XBP1 processing over the non-treated control (Fig. 3, compare lanes 3, 6 and 9 with lanes 1, 4 and 7). Tunicamycin-

induced, processed XBP1 migrated as a doublet in WEWAK1 cells but the lower band

was very faint in both HOM-2 and JESTHOM cell lines (Fig. 3, lanes 3, 6 and 9). It

appears evident that the HLA-B27-expressing lymphocytes studied, show background

levels of XBP1 processing above that of the non-HLA-B27-expressing THP1 cells.

XBP1 processing in lymphoblastoid cell lines shows a cell-line variation in response to

tunicamycin treatment (Compare Fig. 3 lanes 3 with lanes 6 and 9). Tunicamycin

treatment on WEWAK1 cells resulted in the generation of similar sized spliced products

as those generated from the 6 h tunicamycin treatment of monocytic THP1 cells

(compare Fig. 3, lane 3 with Fig. 2B, lane 3). Spliced products generated from

tunicamycin treatments of HOM-2 and JESTHOM cell lines are similar to those

generated by 24 h treatment of THP1 cells (compare Fig. 3, lanes 6 and 9 with Fig. 2B,

lane 4). Thus, we conclude that different cell lines may begin to restore homeostasis at

different rates when UPR is activated using the agent tunicamycin indicating a possible

cell line-specific response.

Consistent with figure 2, processing of XBP1 using different stimuli results in either a

doublet or smeared singlet with tunicamycin (compare Fig. 2B, lanes 2-4 with Fig. 3,

lanes 3, 6 and 9) or a sharp single band with DTT, running at the same height as the

lower band in the doublet seen with tunicamycin treatment (Fig. 2A, lanes 2-4 and Fig. 3

lanes 2, 5 and 8). The different products of IRE1-mediated splicing lead us to conclude
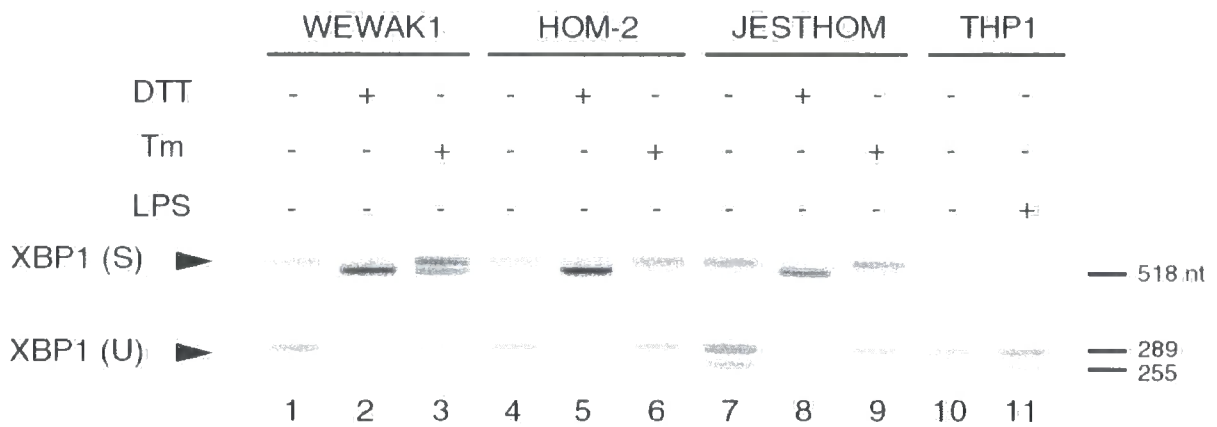
Figure 3. **HLA-B27-positive lymphoblastoid cell lines show background levels of UPR signalling.** WEWAK1 cells were stimulated with DTT (lane 2), tunicamycin (Tm) (lane 3) or mock treated (lane 1). Similarly, lymphocyte cell lines HOM-2 and JESTHOM were stimulated either with DTT (lanes 5 and 8) or with Tm (lanes 6 and 9) or mock treated (lanes 4 and 7). The monocytic cell line THP1 was stimulated with lipopolysaccharide (LPS) as a control (lane 11) or mock treated (lane 10). Cells were then lysed and subjected to techniques described in Fig. 2 in order to resolve both activated and inactivated forms of XBP1.

that DTT- and tunicamycin-induced XBP1 processing may occur via different pathways. Sequencing of these products is required to clarify this further.

Notably, the background levels of UPR activation seen in all three of the untreated HLA-B27-expressing lymphocytes are similar to those of the tunicamycin treatments of HOM-2 and JESTHOM cell lines. Thus, XBP1 processing in non-stimulated cells may occur via a tunicamycin-like pathway as opposed to a DTT-like pathway. The unstimulated cells show band architecture similar to that of the recovering 24 h tunicamycin-treated THP1 cells (compare Fig. 3, lanes 1, 4 and 7 with Fig. 2B, lane 4). If indeed, a tunicamycin-induced singlet represents a UPR intermediate on the way to recovery of homeostasis, then HLA-B27-expressing cells may exhibit intermediate activation of the UPR. Whether or not XBP1 processing and UPR induction is a consequence of HLA-B27 misfolding remains to be seen.

3.4.2.3 *Misoxidation of MHC class I heavy chains induces XBP1 processing in HeLa cells*

Since HLA-B27-positive lymphocytes induced activation of the UPR in the absence of pharmacological agents, we were now interested in whether or not misfolding of class I molecules would trigger XBP1 processing. In order to do this, we transfected the human cervical carcinoma cell line HeLa with the B27 subtype HLA-B27*05. Previous work has shown that overexpression of HLA-B27*05 in HeLa cells causes misoxidation of heavy chains and the formation of disulfide-dependent high-molecular weight complexes (Saleki *et al.*, 2006). Cells were lysed in the presence of an alkylating agent in order to trap any free disulfides thus, preserving any disulfide bonds present at lysis. Post-nuclear cell lysates were separated by SDS-PAGE under non-reducing (NR) and reducing (R) conditions and immunoblotted. Transfected cell lysates were analysed by Western blotting for misoxidation using the pan-MHC class I HC antibody HC10 (Fig. 4*A*). SDS-PAGE resolved the class I heavy chain in HLA-B27*05 transfected and mock transfected lysates indicating the presence of endogenous MHC class I (Fig. 4*A*, lanes 1-4). Under non-reducing conditions, high-molecular weight complexes were resolved in the B27*05 transfected lysates (Fig. 4*A*, lane 1). Upon reduction of this sample with DTT, the majority of high-molecular weight species were disrupted and observed instead as a single species (Fig. 4A, lane 3). No disulfide-dependent complexes were resolved in the mock transfected samples (Fig. 4A, lanes 2 and 4) indicating that misoxidation was due to the overexpression of HLA-B27*05 and not endogenous class I molecules. Lysates were also immunoblotted for the presence of PDI as a control (Fig. 4A, lanes 5 and 6).

In parallel, transfected cells were lysed with tri reagent for subsequent RT-PCR analysis. Total cell RNA was extracted and both XBP1 and β-actin cDNA was amplified using RT-PCR techniques. As previously described, amplified XBP1 cDNA was digested with *Pst1* restriction enzyme and run on a 2% agarose gel to resolve the two XBP1 species.

As controls, HeLa cells were treated with both DTT and tunicamycin for 6 h, lysed and analysed for XBP1 processing in the normal way. Consistent with results from both THP1 cells and the lymphoblastoid cell lines, induction of the UPR by tunicamycin resulted in the generation of a two resistant, spliced XBP1 products migrating as a doublet (Fig. 4*B*, lane 2). Similarly, UPR induction by DTT in HeLa cells resulted in a single resistant XBP1 band, also consistent with previous work (Fig. 4*B*, lane 6). When mock transfected cells were analysed for UPR induction, they showed very low levels, in line with the untreated HeLa cells (compare Fig 4*B*, lane 3 with lanes 1 and 5). In contrast, transfection of HeLa cells with HLA-B27*05 resulted in activation of XBP1 processing (Fig. 4*B*, lane 4). Furthermore, the spliced products migrated as a doublet, consistent with the lymphoblastoid results suggesting that possession of HLA-B27 activates XBP1 processing in a similar fashion to that of tunicamycin. Moreover, these data now link UPR activation not only with possession of HLA-B27 but with the misoxidation and aberrant formation of MHC class I heavy chains.
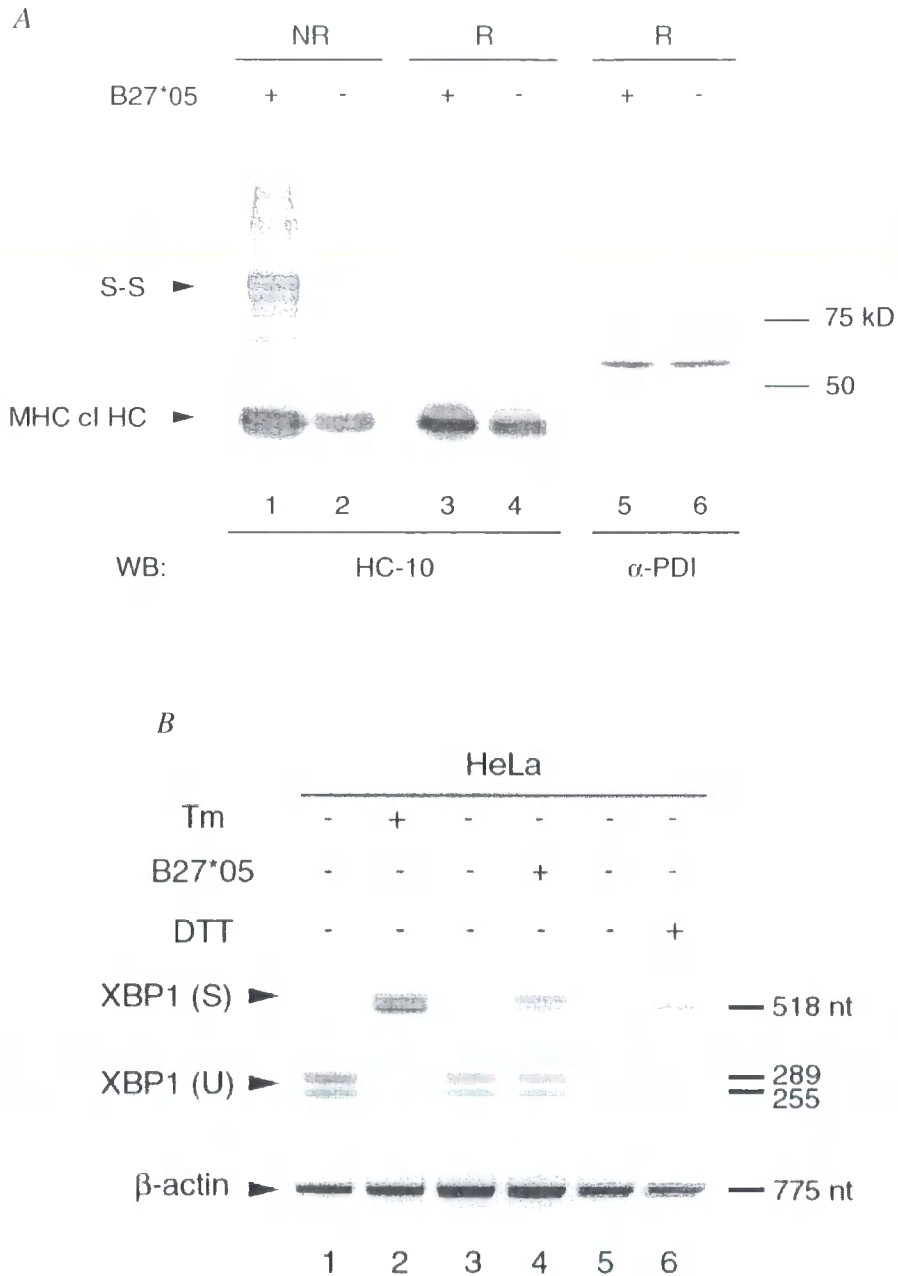
Figure 4. **UPR induction as a consequence of MHC class I HC misoxidation.** *A*, HeLa cells were transfected with the HLA-B27*05 construct (lanes 1, 3 and 5) or mock transfected (lanes 2, 4 and 6). Post-nuclear lysates were then analysed under reducing (R) (lanes 3-6) or non-reducing (lanes 1 and 2) conditions by 8% SDS-PAGE. Proteins were transferred and immunoblotted for the presence of MHC class I heavy chains using the monoclonal antibody HC-10 (lanes 1-4) or with anti-PDI (lane 5 and 6) as a control. *B*, HeLa cells were treated with DTT (lane 6) or tunicamycin (Tm) (lane 2) or mock treated (lanes 1 and 5) for 6 h. RNA was extracted and XBP1 RNA analysed as in Fig. 2. As in *A*, HeLa cells were transfected with HLA-B27*05 (lane 4) or mock transfected (lane 3) but this time analysed for XBP1 processing.

3.4.3 Discussion

3.4.3.1 *Differential effects of DTT and tunicamycin on XBP1 processing*

A recent paper by DuRose and colleagues highlighted the apparent complexity of the unfolded protein response to different forms of ER stress (DuRose *et al.*, 2006). Their studies suggested that different branches of the UPR were able to respond to specific inducers of ER stress with distinct sensitivity. Specific branches of the UPR differed in the rapidity of their response to specific ER stresses, allowing DuRose and colleagues to propose the existence of additional regulatory mechanisms or components in the UPR. Consistent with this, we provide evidence that IRE1-mediated XBP1 processing can discriminate between different stimuli (Fig. 2*A* and *B*). We demonstrate that induction of XBP1 processing by DTT and tunicamycin generates distinct XBP1 products. We propose that the ability of the UPR to discriminate between different stimuli is due to the existence of distinct pathways of XBP1 processing. These pathways may be uniquely sensitive to different modes of induction.

Regulation of UPR activity could potentially take place at both the IRE1 activation level and the XBP1 splicing level in the XBP1 processing pathway. The recent publication of the human IRE1α luminal domain structure has allowed identification of a conserved dimer interface and shown that this interface is required for autophosphorylation (Zhou *et al.*, 2006). If however, differential processing of XBP1 was regulated further downstream, IRE1 RNase activity or mammalian ligase activity may be involved in inducer-specific UPR induction.

The reproducibility of these data within and across different cell lines justifies further investigation. Differentially spliced products induced by DTT and tunicamycin would require purification and subsequent sequencing to aid the elucidation of their function. The ability of tunicamycin-induced XBP1 processing to progress from generating two spliced products upon both 3 h and 6 h treatment to a single spliced product upon treatment for 24 h is interesting (Fig. 1*B* compare lane 4 with lanes 2 and 3). This difference may be due to THP1 cells beginning to recover from tunicamycin-induced ER stress. Is this recovery a direct consequence of the UPR or is recovery a consequence of the effect of tunicamycin weakening after 24 h? Despite DTT readily becoming oxidised, XBP1 processing is 'switched-on' 24 h after DTT is provided to the cells. Analysis of DTT treatment in excess of 24 h may allow us to see if any recovery of XBP1 processing occurs. Moreover, can XBP1 processing be recovered by washing out DTT or by adding an oxidant? Comparisons of the effect of other reductants such as β-2 mercaptoethanol may help aid our understanding of XBP1 processing. Analysis of the direct effects of these agents – disruption of ER oxidation with DTT and disruption of glycosylation with tunicamycin – over the time course in parallel with the effects on XBP1 processing and other branches of the UPR might also aid our understanding of what is happening here.

3.4.3.2 *HLA-B27-positive cells show pre-activation of the UPR*

Here, we provide evidence that possession of the MHC class I allele HLA-B27 in lymphocytes results in a background level of XBP1 processing not seen in monocytic cells (Fig. 3). This pre-activation of HLA-B27-positive lymphocytes appears to be similar to that of tunicamycin-induced XBP1 processing since IRE1-mediated splicing of XBP1

RNA results in two products of the same size. This background UPR induction in lymphocytes may or may not be a consequence of chronic misfolding in the ER. Analysis of the oxidation status of proteins in the ER using the conformation-specific antibodies HC-10 and ME1 may further our understanding in this respect.

All three lymphoblastoid cell lines – WEWAK1, HOM-2 and JESTHOM – showed pre-activation of XBP1 splicing. Despite only differing by three residues, the B27 subtypes HLA-B27*04 – expressed in WEWAK1 cells – and HLA-B27*05 – expressed in both HOM-2 and JESTHOM cells – have been shown to differ in their disulfide-dependent conformations (Saleki et al., 2006). The subtype HLA-B27*04 is associated with AS; predominantly in the Asian population, and HLA-B27*05 – sometimes referred to as the 'parent' subtype since it is the most common – is also associated with the development of the SpAs (Reveille, 2006). Indeed, the immortalised cell lines HOM-2 and JESTHOM were believed to be from AS sufferers. It is unfortunate that the clinical details of the WEWAK1 cell line are unclear. Future work will concentrate on studying and comparing lymphocytes positive for HLA-B27 with cells from patients suffering from AS. To further confirm pre-activation of the UPR in these cell lines, studies will also be targeted towards the IRE1 and PERK branches of the UPR.

In order to show whether class I misfolding triggered the UPR, we used the human carcinoma cell HeLa, into which we overexpressed the subtype HLA-B27*05. We demonstrate that pre-activation of the UPR is caused by the formation of a high-molecular weight, disulfide-dependent, misoxidised ladder of class I heavy chains due to

overexpression (Fig. 4A). Consistent with the lymphoblastoid cell lines, HLA-B27-restricted XBP1 induction showed similarities to activation of XBP1 processing induced by tunicamycin. Thus, we conclude that tunicamycin is a better mimic of UPR induction by MHC class I heavy chain misoxidation.

Although this work further corroborates that of Turner and colleagues' (Turner et al., 2005), the link between MHC class I misfolding and AS pathogenesis remains unknown. Activation of the UPR or the ER overload response has been hypothesised as integral in the increased production of inflammatory cytokines in monocytes/macrophages (Baeuerle and Henkel, 1994; Colbert, 2000). The potential result of increased levels of NF-κB, TNF-α and interleukins could in fact be the stimulation of MHC class I heavy chain expression, further adding to the problem (Ikawa et al., 1998) as well as direct inflammation as a consequence of ER stress (Zhang et al., 2006).

The role of ER stress responses to both misoxidation and pharmacological agents appears to be a complex one. Recently, NF-κB activation has been shown to require phosphorylation of the alpha subunit of eukaryotic initiation factor 2 (eIF2) by the PERK branch of UPR (Deng et al., 2004; Jiang et al., 2003). How intimately linked the ER overload response and UPR are is currently unknown. How misfolding and associated UPR induction might function in individuals with the disease is also unknown. Thus, work on patient cells will serve to aid our understanding in this respect.

Chapter 4

Final Discussion

4. Final Discussion

4.1 *The importance of FAD and Ero-Ero dimerisation in oxidative protein folding*

In eukaryotes, disulfide bond formation is catalysed by the PDI-Ero system, a partnership that mirrors the prokaryotic DsbA-DsbB redox cycle in the periplasm. Unlike the prokaryotic system, disulfide bond formation is not linked to respiration, but instead utilises the flavin FAD (Tu *et al.*, 2000). The ability of FAD to couple its reoxidation to molecular oxygen (Tu and Weissman, 2002) allows for the reoxidation of Ero and the subsequent transfer of oxidising equivalents to PDI. The mechanisms by which oxidising equivalents are passed from molecular oxygen through to PDI is not fully understood.

Together with the work of Dias-Gunasekara and colleagues (Dias-Gunasekara *et al.*, 2005), we show that the human Ero1-Lβ protein is able to form homodimers *in vivo* (Chapter 3.1, figure 3). Previous work has shown that both Ero1-Lα and Ero1-Lβ associate with PDI in a redox-dependent manner (Benham *et al.*, 2000; Dias-Gunasekara *et al.*, 2005). Since the Ero1-Lα C-X-X-C-X-X-C mutant C391A can rescue the temperature-sensitive yeast *ero1-1* mutant despite exhibiting reduced affinity for PDI, these data suggest that Ero-PDI association and Ero dimerisation may be important in maintaining the oxidative folding pathway in the ER. Further work by Dias-Gunasekara and colleagues has revealed that dimerisation is partly controlled by the C-X-X-C-X-X-C motif (Dias-Gunasekara *et al.*, 2005). Homodimers detected in this study are most likely

a consequence of both covalent and non-covalent association. The functional significance of Ero1-Lβ homodimers is unknown. Future work will endeavour to elucidate the role of dimeric Ero1-Lβ in oxidative protein folding.

The mechanism by which FAD passes oxidising equivalents to Ero is still not fully understood. By utilising mutants of the human Ero1-Lβ protein, we were able to study the effect of G252S and H254Y mutations in the FAD-binding site on homodimerisation of Ero1-Lβ and interaction with PDI. Association of the Ero1-Lβ mutants with PDI was impaired (Chapter 3.1, figure 5). Thus, Ero1-Lβ may require bound-FAD in order to form efficient covalent associations with PDI. The presence of the co-factor may be essential for recognition and subsequent binding of PDI by Ero1-Lβ. However, recent evidence has suggested that yeast Ero1p is fairly non-specific in its recognition of thioredoxin domains (Kulp *et al.*, 2006). Non-covalent Ero-PDI interactions were largely unaffected, suggesting that interaction between Ero1-Lβ and PDI can occur in a disulfide and flavin-independent manner. Ero-Ero interactions, however, were not affected by mutations in the FAD-binding site, suggesting that the phenotypes observed in the yeast *ero1-1* and *ero1-2* mutants may not be accredited to the failure of Ero1p to form homodimers.

The recent publication of the Ero1p crystal structure has allowed us to generate a possible Ero homodimer model allowing us to further understand the role of FAD in both homodimer formation and Ero reoxidation (Chapter 3.1, figure 14). In this model, the likely site for PDI binding is away from the dimer interface, suggesting that the formation

of Ero-PDI and Ero-Ero complexes are not necessarily mutually exclusive. The two

bound-FAD molecules sit near the dimer interface. In light of this, it seems unusual that

mutations in the FAD-binding site were unable to affect homodimerisation.

This work highlights the complexity of oxidative protein folding in the mammalian

system. It was not previously known that Eros form homodimers *in vivo*, or if the absence

of bound FAD is able to prevent Ero-PDI association, thus this work significantly

enhances our knowledge on the molecular mechanisms that underlie disulfide bond

formation. Future work will focus on further elucidating the mechanism behind the

passing of oxidising equivalents from FAD to Ero, the effect of FAD binding on PDI

recognition and the role of FAD in Ero dimer stability. Site-directed mutagenesis

experiments can be planned that could determine whether, by targeting the dimer

interface, the process of disulfide bond formation could be manipulated.

4.2 *Interactions of the pancreatic PDIp with the Eros*

In order to understand the redox roles of PDI and its homologs, their interactions with the

Eros must be studied. We studied the pancreas-specific PDI homolog, PDIp. The

restricted tissue distribution of PDIp suggests a role in the oxidative folding of pancreas

specific proteins. However, PDI is also present in the same pancreatic acinar cells where

PDIp can be found (Dias-Gunasekara *et al.*, 2006). It has also been shown that PDI is

able to interact with some of the same substrates as PDIp (Klappa *et al.*, 1995),

suggesting a level of functional redundancy in the system.

Using *in vitro* translation techniques we studied the binding of PDIp with Ero1-Lα and Ero1-Lβ. No PDIp-Ero interactions could be detected (Chapter 3.3, figure 4). This was probably a consequence of low translation efficiency. Interactions between the Eros and PDI could also not be detected using this method (Chapter 3.3, figure 5) suggesting that *in vitro* translation was not fully optimised. Attempts were also made to transfect PDIp into mammalian cells. The cDNA was successfully liberated from pBS and purified (Chapter 3.3, figure 6 and 7). Future work will concentrate on optimising ligation for mammalian transfection. This will allow us to study the molecular detail of PDIp-Ero interaction and experiments can be planned to mutate the active-site cysteines of both redox proteins in order to elucidate their mechanism of interaction. It is possible that the mode of interaction between PDIp and the Eros – further to substrate specificity – is able to account for its specialisation in the pancreas, especially since distribution of Ero1-Lβ overlaps with that of PDIp.

4.3 *Characterisation of a polyclonal anti-Ero1-Lβ antibody*

Polyclonal antibodies are essential tools for studying protein interactions by co-immunoprecipitation and immunoblotting. Here, we characterised a new polyclonal antibody raised against Ero1-Lβ.

The B2 antibody was successful at recognising Ero1-Lβ in immunoblots (Chapter 3.2, figure 1) and was able to isolate Ero1-Lβ from transfected lysates by immunoprecipitation methods (Chater 3.2, figure 3). This will allow us to isolate Ero1-

Lβ and any proteins complexed either covalently or non-covalently with Ero1-Lβ. This has practical implications, since this antibody can now aid characterisation of the interactions of PDIp with Ero1-Lβ by co-immunoprecipitation. Importantly, the B2 antibody did not cross-react with human Ero1-Lα (Chapter 3.2, figure 4) despite potentially sharing a number of epitopes.

4.4 *Misoxidation of HLA-B27 and induction of the unfolded protein response*

Misoxidation of the MHC class I molecule HLA-B7 may have implications in the pathogenesis of ankylosing spondylitis (AS). Misfolding of HLA-B27 has recently been linked to induction of the unfolded protein response (UPR) using macrophages derived from bone marrow of HLA-B27 transgenic rats (Turner *et al.*, 2005).

Here we provide novel evidence linking the misoxidation of HLA-B27 in HeLa cells to activation of the UPR via IRE1-mediated XBP1 splicing. We show that pre-activation of the UPR is caused by the formation of a high-molecular weight ladder of class I heavy chains (Chapter 3.4, figure 4). Additionally, we demonstrate that possession of the HLA-B27 allele results in background levels of XBP1 processing in lymphoblastoid cell lines (Chapter 3.4, figure 3). This pre-activation appears to be similar to that of tunicamycin-induced XBP1 processing suggesting that HLA-B27 may induce UPR using a similar pathway to tunicamycin. As part of this study we also observed a distinct difference in the sensitivity of XBP1 splicing to tunicamycin and DTT (Chapter 3.2, figure 2). The

generation of distinct spliced XBP1 products may suggest that XBP1 processing is able to discriminate between different stimuli; a theory very recently proposed by DuRose and colleagues (DuRose *et al.*, 2006).

Future work will focus on testing other branches of the UPR such as IRE1 and PERK in order to distinguish whether or not they exhibit a similar ability to discriminate between stimuli. Studying the UPR response to other stimuli such as thapsigargin and calcium ionophores such as calcimycin (A23187) will further elucidate the sensitivity of the UPR machinery to different stimuli. The ability of HLA-B27 expression and misfolding to pre-activate XBP1 splicing must also be investigated further. Use of stably transfected HLA-B27 cell lines will allow us to determine whether UPR induced by misoxidation can be attenuated with time.

Taken together, this work adds to that of Turner and colleagues (Turner *et al.*, 2005) by coupling misoxidation of class I heavy chains to induction of the UPR. Given that induction of the UPR can be linked to inflammation (Zhang *et al.*, 2006) possibly through cytokines, chronic UPR signalling may be a component of diseases such as AS. However, since cells at the site of inflammation in AS sufferers (e.g. dendritic and endothelial cells) may behave differently to the immortilised lymphocytes observed here, the contribution of UPR induction to inflammation may best be studied in professional APCs.

4.5 *Concluding Remarks*

This thesis addresses some important questions underlying the mechanisms behind oxidative protein folding in the ER and the consequences of protein misfolding for the cell. We explore the importance of FAD in the binding of PDI by Ero1-Lβ and demonstrate the existence of Ero1-Lβ homodimers (together with Dias-Gunasekara and colleagues). The interactions of members of the oxidative protein folding machinery define the process of disulfide bond formation since these bonds are passed up a chain – through a series of electron transfers – to the substrate. Thus, understanding the associations of members of this system adds to our molecular knowledge of oxidative folding.

The consequence of non-native folding of proteins is not restricted to the ER, but has global physiological consequences. We show that responses to ER stress may be specific to different stimuli and that misoxidation of MHC class I heavy chains induces a cellular splicing event. This, in the context of the work by Turner and colleagues (Turner *et al.*, 2005), demonstrates a link between misoxidation of MHC class I heavy chains and induction of the UPR. The full role of UPR induction in AS pathogenesis remains to be addressed by future experimental work.

Chapter 5

References

5. References

Akiyama, Y., Kamitani, S., Kusukawa, N., and Ito, K. (1992). In vitro catalysis of oxidative folding of disulfide-bonded proteins by the Escherichia coli dsbA (ppfA) gene product. J Biol Chem *267*, 22440-22445.

Alanen, H. I., Salo, K. E., Pekkala, M., Siekkinen, H. M., Pirneskoski, A., and Ruddock, L. W. (2003). Defining the domain boundaries of the human protein disulfide isomerases. Antioxid Redox Signal *5*, 367-374.

Allen, R. L., and Trowsdale, J. (2004). Recognition of classical and heavy chain forms of HLA-B27 by leukocyte receptors. Curr Mol Med *4*, 59-65.

Allen, R. L., O'Callaghan, C. A., McMichael, A. J., and Bowness, P. (1999). Cutting edge: HLA-B27 can form a novel beta 2-microglobulin-free heavy chain homodimer structure. J Immunol *162*, 5045-5048.

Andersen, C. L., Matthey-Dupraz, A., Missiakas, D., and Raina, S. (1997). A new Escherichia coli gene, dsbG, encodes a periplasmic protein involved in disulphide bond formation, required for recycling DsbA/DsbB and DsbC redox proteins. Mol Microbiol *26*, 121-132.

Anelli, T., Alessio, M., Mezghrani, A., Simmen, T., Talamo, F., Bachi, A., and Sitia, R. (2002). ERp44, a novel endoplasmic reticulum folding assistant of the thioredoxin family. Embo J *21*, 835-844.

Anfinsen, C. B., and Haber, E. (1961). Studies on the reduction and re-formation of protein disulfide bonds. J Biol Chem *236*, 1361-1363.

Anfinsen, C. B., Haber, E., Sela, M., and White, F. H., Jr. (1961). The kinetics of formation of native ribonuclease during oxidation of the reduced polypeptide chain. Proc Natl Acad Sci U S A *47*, 1309-1314.

Antoniou, A. N., Ford, S., Alphey, M., Osborne, A., Elliott, T., and Powis, S. J. (2002). The oxidoreductase ERp57 efficiently reduces partially folded in preference to fully folded MHC class I molecules. Embo J *21*, 2655-2663.

Antoniou, A. N., Ford, S., Taurog, J. D., Butcher, G. W., and Powis, S. J. (2004). Formation of HLA-B27 homodimers and their relationship to assembly kinetics. J Biol Chem *279*, 8895-8902.

Aslund, F., Ehn, B., Miranda-Vizuete, A., Pueyo, C., and Holmgren, A. (1994). Two additional glutaredoxins exist in Escherichia coli: glutaredoxin 3 is a hydrogen donor for ribonucleotide reductase in a thioredoxin/glutaredoxin 1 double mutant. Proc Natl Acad Sci U S A *91*, 9813-9817.

Bader, M. W., Xie, T., Yu, C. A., and Bardwell, J. C. (2000). Disulfide bonds are generated by quinone reduction. J Biol Chem 275, 26082-26088.

Bader, M., Muse, W., Ballou, D. P., Gassner, C., and Bardwell, J. C. (1999). Oxidative protein folding is driven by the electron transport system. Cell 98, 217-227.

Baeuerle, P. A., and Henkel, T. (1994). Function and activation of NF-kappa B in the immune system. Annu Rev Immunol 12, 141-179.

Bardwell, J. C., Lee, J. O., Jander, G., Martin, N., Belin, D., and Beckwith, J. (1993). A pathway for disulfide bond formation in vivo. Proc Natl Acad Sci U S A 90, 1038-1042.

Bardwell, J.C., McGovern, K., and Beckwith, J. (1991). Identification of a protein required for disulfide bond formation in vivo. Cell 67, 581-589.

Benham, A. M., and Braakman, I. (2000). Glycoprotein folding in the endoplasmic reticulum. Crit Rev Biochem Mol Biol 35, 433-473.

Benham, A.M., Cabibbo, A., Fassio, A., Bulleid, N., Sitia, R., and Braakman, I. (2000). The CXXCXXC motif determines the folding, structure and stability of human Erol-Lalpha. Embo J 19, 4493-4502.

Benjamin, R., and Parham, P. (1990). Guilt by association: HLA-B27 and ankylosing spondylitis. Immunol Today *11*, 137-142.

Berg, R. A., and Prockop, D. J. (1973). Affinity column purification of protocollagen proline hydroxylase from chick embryos and further characterization of the enzyme. J Biol Chem *248*, 1175-1182.

Bertoli, G., Simmen, T., Anelli, T., Molteni, S. N., Fesce, R., and Sitia, R. (2004). Two conserved cysteine triads in human Ero1alpha cooperate for efficient disulfide bond formation in the endoplasmic reticulum. J Biol Chem *279*, 30047-30052.

Bird, L. A., Peh, C. A., Kollnberger, S., Elliott, T., McMichael, A. J., and Bowness, P. (2003). Lymphoblastoid cells express HLA-B27 homodimers both intracellularly and at the cell surface following endosomal recycling. Eur J Immunol *33*, 748-759.

Bonifacino, J. S., and Weissman, A. M. (1998). Ubiquitin and the control of protein fate in the secretory and endocytic pathways. Annu Rev Cell Dev Biol *14*, 19-57.

Bourdi, M., Demady, D., Martin, J. L., Jabbour, S. K., Martin, B. M., George, J. W., and Pohl, L. R. (1995). cDNA cloning and baculovirus expression of the human liver endoplasmic reticulum P58: characterization as a protein disulfide isomerase isoform, but not as a protease or a carnitine acyltransferase. Arch Biochem Biophys *323*, 397-403.

Boyle, L. H., Goodall, J. C., Opat, S. S., and Gaston, J. S. (2001). The recognition of HLA-B27 by human CD4(+) T lymphocytes. J Immunol *167*, 2619-2624.

Brodsky, J. L., and McCracken, A. A. (1999). ER protein quality control and proteasome-mediated protein degradation. Semin Cell Dev Biol *10*, 507-513.

Cabibbo, A., Pagani, M., Fabbri, M., Rocchi, M., Farmery, M. R., Bulleid, N. J., and Sitia, R. (2000). ERO1-L, a human protein that favors disulfide bond formation in the endoplasmic reticulum. J Biol Chem *275*, 4827-4833.

Calfon, M., Zeng, H., Urano, F., Till, J. H., Hubbard, S. R., Harding, H. P., Clark, S. G., and Ron, D. (2002). IRE1 couples endoplasmic reticulum load to secretory capacity by processing the XBP-1 mRNA. Nature *415*, 92-96.

Carlson, E. J., Pitonzo, D., and Skach, W. R. (2006). p97 functions as an auxiliary factor to facilitate TM domain extraction during CFTR ER-associated degradation. Embo J *25*, 4557-4566.

Carvalho, A. P., Fernandes, P. A., and Ramos, M. J. (2006). Similarities and differences in the thioredoxin superfamily. Prog Biophys Mol Biol *91*, 229-248.

Chakravarthi, S., and Bulleid, N. J. (2004). Glutathione is required to regulate the formation of native disulfide bonds within proteins entering the secretory pathway. J Biol Chem 279, 39872-39879.

Chen, J., Song, J. L., Zhang, S., Wang, Y., Cui, D. F., and Wang, C. C. (1999). Chaperone activity of DsbC. J Biol Chem 274, 19601-19605.

Chivers, P. T., Laboissiere, M. C., and Raines, R. T. (1996). The CXXC motif: imperatives for the formation of native disulfide bonds in the cell. Embo J 15, 2659-2667.

Chivers, P. T., Prehoda, K. E., Volkman, B. F., Kim, B. M., Markley, J. L., and Raines, R. T. (1997). Microscopic pKa values of Escherichia coli thioredoxin. Biochemistry 36, 14985-14991.

Chung, J., Chen, T., and Missiakas, D. (2000). Transfer of electrons across the cytoplasmic membrane by DsbD, a membrane protein involved in thiol-disulphide exchange and protein folding in the bacterial periplasm. Mol Microbiol 35, 1099-1109.

Colbert, R. A. (2000). HLA-B27 misfolding: a solution to the spondyloarthropathy conundrum? Mol Med Today 6, 224-230.

Colbert, R. A., Rowland-Jones, S. L., McMichael, A. J., and Frelinger, J. A. (1994). Differences in peptide presentation between B27 subtypes: the importance of the P1 side chain in maintaining high affinity peptide binding to B*2703. Immunity *1*, 121-130.

Colmegna, I., Cuchacovich, R., and Espinoza, L. R. (2004). HLA-B27-associated reactive arthritis: pathogenetic and clinical considerations. Clin Microbiol Rev *17*, 348-369.

Cuozzo, J. W., and Kaiser, C. A. (1999). Competition between glutathione and protein thiols for disulphide-bond formation. Nat Cell Biol *1*, 130-135.

D'Amato, M., Fiorillo, M. T., Carcassi, C., Mathieu, A., Zuccarelli, A., Bitti, P. P., Tosi, R., and Sorrentino, R. (1995). Relevance of residue 116 of HLA-B27 in determining susceptibility to ankylosing spondylitis. Eur J Immunol *25*, 3199-3201.

Dangoria, N. S., DeLay, M. L., Kingsbury, D. J., Mear, J. P., Uchanska-Ziegler, B., Ziegler, A., and Colbert, R. A. (2002). HLA-B27 misfolding is associated with aberrant intermolecular disulfide bond formation (dimerization) in the endoplasmic reticulum. J Biol Chem *277*, 23459-23468.

Darby, N. J., and Creighton, T. E. (1995a). Catalytic mechanism of DsbA and its comparison with that of protein disulfide isomerase. Biochemistry *34*, 3576-3587.

Darby, N. J., and Creighton, T. E. (1995b). Characterization of the active site cysteine

residues of the thioredoxin-like domains of protein disulfide isomerase. Biochemistry *34*,

16770-16780.

Darby, N. J., and Creighton, T. E. (1995c). Functional properties of the individual

thioredoxin-like domains of protein disulfide isomerase. Biochemistry *34*, 11725-11735.

Darby, N. J., Penka, E., and Vincentelli, R. (1998). The multi-domain structure of protein

disulfide isomerase is essential for high catalytic efficiency. J Mol Biol *276*, 239-247.

de Vet, E. C., and van den Bosch, H. (2000). Alkyl-dihydroxyacetonephosphate synthase.

Cell Biochem Biophys *32 Spring*, 117-121.

Degen, E., and Williams, D. B. (1991). Participation of a novel 88-kD protein in the

biogenesis of murine class I histocompatibility molecules. J Cell Biol *112*, 1099-1115.

Dekker-Saeys, B. J., Meuwissen, S. G., Van Den Berg-Loonen, E. M., De Haas, W. H.,

Agenant, D., and Tytgat, G. N. (1978). Ankylosing spondylitis and inflammatory bowel

disease. II. Prevalence of peripheral arthritis, sacroiliitis, and ankylosing spondylitis in

patients suffering from inflammatory bowel disease. Ann Rheum Dis *37*, 33-35.

Deng, J., Lu, P. D., Zhang, Y., Scheuner, D., Kaufman, R. J., Sonenberg, N., Harding, H.

P., and Ron, D. (2004). Translational repression mediates activation of nuclear factor

kappa B by phosphorylated translation initiation factor 2. Mol Cell Biol *24*, 10161-10168.

Desilva, M. G., Lu, J., Donadel, G., Modi, W. S., Xie, H., Notkins, A. L., and Lan, M. S. (1996). Characterization and chromosomal localization of a new protein disulfide isomerase, PDIp, highly expressed in human pancreas. DNA Cell Biol *15*, 9-16.

Desilva, M. G., Notkins, A. L., and Lan, M. S. (1997). Molecular characterization of a pancreas-specific protein disulfide isomerase, PDIp. DNA Cell Biol *16*, 269-274.

Dias-Gunasekara, S., Gubbens, J., van Lith, M., Dunne, C., Williams, J. A., Kataky, R., Scoones, D., Lapthorn, A., Bulleid, N. J., and Benham, A. M. (2005). Tissue-specific expression and dimerization of the endoplasmic reticulum oxidoreductase Ero1beta. J Biol Chem *280*, 33066-33075.

Dias-Gunasekara, S., van Lith, M., Williams, J. A., Kataky, R., and Benham, A. M. (2006). Mutations in the FAD binding domain cause stress-induced misoxidation of the endoplasmic reticulum oxidoreductase ERO1beta. J Biol Chem.

Dick, T. P., Bangia, N., Peaper, D. R., and Cresswell, P. (2002). Disulfide bond isomerization and the assembly of MHC class I-peptide complexes. Immunity *16*, 87-98.

Dillet, V., Dyson, H. J., and Bashford, D. (1998). Calculations of electrostatic interactions and pKas in the active site of Escherichia coli thioredoxin. Biochemistry *37*, 10298-10306.

DuRose, J. B., Tam, A. B., and Niwa, M. (2006). Intrinsic capacities of molecular sensors of the unfolded protein response to sense alternate forms of endoplasmic reticulum stress. Mol Biol Cell *17*, 3095-3107.

Dyson, H. J., Tennant, L. L., and Holmgren, A. (1991). Proton-transfer effects in the active-site region of Escherichia coli thioredoxin using two-dimensional 1H NMR. Biochemistry *30*, 4262-4268.

Edman, J. C., Ellis, L., Blacher, R. W., Roth, R. A., and Rutter, W. J. (1985). Sequence of protein disulphide isomerase and implications of its relationship to thioredoxin. Nature *317*, 267-270.

Ellgaard, L., Molinari, M., and Helenius, A. (1999). Setting the standards: quality control in the secretory pathway. Science *286*, 1882-1888.

Ellgaard, L., Riek, R., Herrmann, T., Guntert, P., Braun, D., Helenius, A., and Wuthrich, K. (2001). NMR structure of the calreticulin P-domain. Proc Natl Acad Sci U S A *98*, 3133-3138.

Ellis, R. J., and Hemmingsen, S. M. (1989). Molecular chaperones: proteins essential for the biogenesis of some macromolecular structures. Trends Biochem Sci *14*, 339-342.

Farquhar, R., Honey, N., Murant, S. J., Bossier, P., Schultz, L., Montgomery, D., Ellis, R. W., Freedman, R. B., and Tuite, M. F. (1991). Protein disulfide isomerase is essential for viability in Saccharomyces cerevisiae. Gene *108*, 81-89.

Fernandes, A. P., and Holmgren, A. (2004). Glutaredoxins: glutathione-dependent redox enzymes with functions far beyond a simple thioredoxin backup system. Antioxid Redox Signal *6*, 63-74.

Ferrari, D. M., and Soling, H. D. (1999). The protein disulphide-isomerase family: unravelling a string of folds. Biochem J *339 (Pt 1)*, 1-10.

Ferrari, D. M., Nguyen Van, P., Kratzin, H. D., and Soling, H. D. (1998). ERp28, a human endoplasmic-reticulum-lumenal protein, is a member of the protein disulfide isomerase family but lacks a CXXC thioredoxin-box motif. Eur J Biochem *255*, 570-579.

Ferrari, D.M., and Soling, H.D. (1999). The protein disulphide-isomerase family: unravelling a string of folds. Biochem J *339 (Pt 1)*, 1-10.

Forman-Kay, J. D., Clore, G. M., and Gronenborn, A. M. (1992). Relationship between electrostatics and redox function in human thioredoxin: characterization of pH titration

shifts using two-dimensional homo- and heteronuclear NMR. Biochemistry *31*, 3442-3452.

Forster, M. L., Sivick, K., Park, Y. N., Arvan, P., Lencer, W. I., and Tsai, B. (2006). Protein disulfide isomerase-like proteins play opposing roles during retrotranslocation. J Cell Biol *173*, 853-859.

Frand, A. R., and Kaiser, C. A. (1998). The ERO1 gene of yeast is required for oxidation of protein dithiols in the endoplasmic reticulum. Mol Cell *1*, 161-170.

Frand, A. R., and Kaiser, C. A. (1999). Ero1p oxidizes protein disulfide isomerase in a pathway for disulfide bond formation in the endoplasmic reticulum. Mol Cell *4*, 469-477.

Frand, A. R., and Kaiser, C. A. (2000). Two pairs of conserved cysteines are required for the oxidative activity of Ero1p in protein disulfide bond formation in the endoplasmic reticulum. Mol Biol Cell *11*, 2833-2843.

Frand, A. R., Cuozzo, J. W., and Kaiser, C. A. (2000). Pathways for protein disulphide bond formation. Trends Cell Biol *10*, 203-210.

Freedman, R. B., Hawkins, H. C., and McLaughlin, S. H. (1995). Protein disulfide-isomerase. Methods Enzymol *251*, 397-406.

Freedman, R. B., Hawkins, H. C., Murant, S. J., and Reid, L. (1988). Protein disulphide-isomerase: a homologue of thioredoxin implicated in the biosynthesis of secretory proteins. Biochem Soc Trans *16*, 96-99.

Freedman, R. B., Hirst, T. R., and Tuite, M. F. (1994). Protein disulphide isomerase: building bridges in protein folding. Trends Biochem Sci *19*, 331-336.

Freedman, R. B., Klappa, P., and Ruddock, L. W. (2002). Protein disulfide isomerases exploit synergy between catalytic and specific binding domains. EMBO Rep *3*, 136-140.

Fuchs, S., De Lorenzo, F., and Anfinsen, C. B. (1967). Studies on the mechanism of the enzymic catalysis of disulfide interchange in proteins. J Biol Chem *242*, 398-402.

Fullekrug, J., Sonnichsen, B., Wunsch, U., Arseven, K., Nguyen Van, P., Soling, H. D., and Mieskes, G. (1994). CaBP1, a calcium binding protein of the thioredoxin family, is a resident KDEL protein of the ER and not of the intermediate compartment. J Cell Sci *107* (*Pt 10*), 2719-2727.

Gan, Z. R., and Wells, W. W. (1988). Immunological characterization of thioltransferase from pig liver. J Biol Chem *263*, 9050-9054.

Gething, M. J., and Sambrook, J. (1990). Transport and assembly processes in the endoplasmic reticulum. Semin Cell Biol *1*, 65-72.

Gilbert, H. F. (1998). Protein disulfide isomerase. Methods Enzymol *290*, 26-50.

Goldberger, R. F., Epstein, C. J., and Anfinsen, C. B. (1963). Acceleration of reactivation of reduced bovine pancreatic ribonuclease by a microsomal system from rat liver. J Biol Chem *238*, 628-635.

Grauschopf, U., Winther, J. R., Korber, P., Zander, T., Dallinger, P., and Bardwell, J. C. (1995). Why is DsbA such an oxidizing disulfide catalyst? Cell *83*, 947-955.

Gross, E., Kastner, D. B., Kaiser, C. A., and Fass, D. (2004). Structure of Ero1p, source of disulfide bonds for oxidative protein folding in the cell. Cell *117*, 601-610.

Guddat, L. W., Bardwell, J. C., Glockshuber, R., Huber-Wunderlich, M., Zander, T., and Martin, J. L. (1997). Structural analysis of three His32 mutants of DsbA: support for an electrostatic role of His32 in DsbA stability. Protein Sci *6*, 1893-1900.

Hammer, R. E., Maika, S. D., Richardson, J. A., Tang, J. P., and Taurog, J. D. (1990). Spontaneous inflammatory disease in transgenic rats expressing HLA-B27 and human beta 2m: an animal model of HLA-B27-associated human disorders. Cell *63*, 1099-1112.

Hayano, T., and Kikuchi, M. (1995). Molecular cloning of the cDNA encoding a novel protein disulfide isomerase-related protein (PDIR). FEBS Lett *372*, 210-214.

Helaakoski, T., Annunen, P., Vuori, K., MacNeil, I. A., Pihlajaniemi, T., and Kivirikko, K. I. (1995). Cloning, baculovirus expression, and characterization of a second mouse prolyl 4-hydroxylase alpha-subunit isoform: formation of an alpha 2 beta 2 tetramer with the protein disulfide-isomerase/beta subunit. Proc Natl Acad Sci U S A 92, 4427-4431.

Hellman, R., Vanhove, M., Lejeune, A., Stevens, F. J., and Hendershot, L. M. (1999). The in vivo association of BiP with newly synthesized proteins is dependent on the rate and stability of folding and not simply on the presence of sequences that can bind to BiP. J Cell Biol 144, 21-30.

Hermann, E., Yu, D. T., Meyer zum Buschenfelde, K. H., and Fleischer, B. (1993). HLA-B27-restricted CD8 T cells derived from synovial fluids of patients with reactive arthritis and ankylosing spondylitis. Lancet 342, 646-650.

Hirano, N., Shibasaki, F., Sakai, R., Tanaka, T., Nishida, J., Yazaki, Y., Takenawa, T., and Hirai, H. (1995). Molecular cloning of the human glucose-regulated protein ERp57/GRP58, a thiol-dependent reductase. Identification of its secretory form and inducible expression by the oncogenic transformation. Eur J Biochem 234, 336-342.

Holmgren, A. (1979). Thioredoxin catalyzes the reduction of insulin disulfides by dithiothreitol and dihydrolipoamide. J Biol Chem 254, 9627-9632.

Holmgren, A. (1985). Thioredoxin. Annu Rev Biochem 54, 237-271.

Holmgren, A. (1988). Thioredoxin and glutaredoxin: small multi-functional redox proteins with active-site disulphide bonds. Biochem Soc Trans *16*, 95-96.

Holmgren, A. (1989). Thioredoxin and glutaredoxin systems. J Biol Chem *264*, 13963-13966.

Holmgren, A. (1995). Thioredoxin structure and mechanism: conformational changes on oxidation of the active-site sulfhydryls to a disulfide. Structure *3*, 239-243.

Holmgren, A., and Aslund, F. (1995). Glutaredoxin. Methods Enzymol *252*, 283-292.

Hoog, J. O., Jornvall, H., Holmgren, A., Carlquist, M., and Persson, M. (1983). The primary structure of Escherichia coli glutaredoxin. Distant homology with thioredoxins in a superfamily of small proteins with a redox-active cystine disulfide/cysteine dithiol. Eur J Biochem *136*, 223-232.

Hsu, T. A., Watson, S., Eiden, J. J., and Betenbaugh, M. J. (1996). Rescue of immunoglobulins from insolubility is facilitated by PDI in the baculovirus expression system. Protein Expr Purif *7*, 281-288.

Huber-Wunderlich, M., and Glockshuber, R. (1998). A single dipeptide sequence modulates the redox properties of a whole enzyme family. Fold Des *3*, 161-171.

Hughes, E. A., and Cresswell, P. (1998). The thiol oxidoreductase ERp57 is a component of the MHC class I peptide-loading complex. Curr Biol *8*, 709-712.

Hurtley, S. M., Bole, D. G., Hoover-Litty, H., Helenius, A., and Copeland, C. S. (1989). Interactions of misfolded influenza virus hemagglutinin with binding protein (BiP). J Cell Biol *108*, 2117-2126.

Hwang, C., Sinskey, A. J., and Lodish, H. F. (1992). Oxidized redox state of glutathione in the endoplasmic reticulum. Science *257*, 1496-1502.

Ikawa, T., Ikeda, M., Yamaguchi, A., Tsai, W. C., Tamura, N., Seta, N., Trucksess, M., Raybourne, R. B., and Yu, D. T. (1998). Expression of arthritis-causing HLA-B27 on Hela cells promotes induction of c-fos in response to in vitro invasion by Salmonella typhimurium. J Clin Invest *101*, 263-272.

Imaizumi, K., Miyoshi, K., Katayama, T., Yoneda, T., Taniguchi, M., Kudo, T., and Tohyama, M. (2001). The unfolded protein response and Alzheimer's disease. Biochim Biophys Acta *1536*, 85-96.

Jeng, M. F., Holmgren, A., and Dyson, H. J. (1995). Proton sharing between cysteine thiols in Escherichia coli thioredoxin: implications for the mechanism of protein disulfide reduction. Biochemistry *34*, 10101-10105.

Jeng, M. F., Reymond, M. T., Tennant, L. L., Holmgren, A., and Dyson, H. J. (1998). NMR characterization of a single-cysteine mutant of Escherichia coli thioredoxin and a covalent thioredoxin-peptide complex. Eur J Biochem 257, 299-308.

Jessop, C. E., Chakravarthi, S., Watkins, R. H., and Bulleid, N. J. (2004). Oxidative protein folding in the mammalian endoplasmic reticulum. Biochem Soc Trans 32, 655-658.

Jiang, H. Y., Wek, S. A., McGrath, B. C., Scheuner, D., Kaufman, R. J., Cavener, D. R., and Wek, R. C. (2003). Phosphorylation of the alpha subunit of eukaryotic initiation factor 2 is required for activation of NF-kappaB in response to diverse cellular stresses. Mol Cell Biol 23, 5651-5663.

Joly, J. C., and Swartz, J. R. (1997). In vitro and in vivo redox states of the Escherichia coli periplasmic oxidoreductases DsbA and DsbC. Biochemistry 36, 10067-10072.

Kamitani, S., Akiyama, Y., and Ito, K. (1992). Identification and characterization of an Escherichia coli gene required for the formation of correctly folded alkaline phosphatase, a periplasmic enzyme. Embo J 11, 57-62.

Kapasi, K., and Inman, R. D. (1992). HLA-B27 expression modulates gram-negative bacterial invasion into transfected L cells. J Immunol 148, 3554-3559.

Katayama, T., Imaizumi, K., Manabe, T., Hitomi, J., Kudo, T., and Tohyama, M. (2004).
Induction of neuronal death by ER stress in Alzheimer's disease. J Chem Neuroanat 28,
67-78.

Katti, S. K., LeMaster, D. M., and Eklund, H. (1990). Crystal structure of thioredoxin
from Escherichia coli at 1.68 A resolution. J Mol Biol 212, 167-184.

Kemmink, J., Darby, N. J., Dijkstra, K., Nilges, M., and Creighton, T. E. (1996).
Structure determination of the N-terminal thioredoxin-like domain of protein disulfide
isomerase using multidimensional heteronuclear 13C/15N NMR spectroscopy.
Biochemistry 35, 7684-7691.

Kemmink, J., Darby, N. J., Dijkstra, K., Nilges, M., and Creighton, T. E. (1997). The
folding catalyst protein disulfide isomerase is constructed of active and inactive
thioredoxin modules. Curr Biol 7, 239-245.

Kemmink, J., Dijkstra, K., Mariani, M., Scheek, R. M., Penka, E., Nilges, M., and Darby,
N. J. (1999). The structure in solution of the b domain of protein disulfide isomerase. J
Biomol NMR 13, 357-368.

Kingsbury, D. J., Mear, J. P., Witte, D. P., Taurog, J. D., Roopenian, D. C., and Colbert,
R. A. (2000). Development of spontaneous arthritis in beta2-microglobulin-deficient

mice without expression of HLA-B27: association with deficiency of endogenous major histocompatibility complex class I expression. Arthritis Rheum *43*, 2290-2296.

Kivirikko, K. I., and Myllyla, R. (1982). Posttranslational enzymes in the biosynthesis of collagen: intracellular enzymes. Methods Enzymol *82 Pt A*, 245-304.

Klappa, P., Freedman, R. B., and Zimmermann, R. (1995). Protein disulphide isomerase and a lumenal cyclophilin-type peptidyl prolyl cis-trans isomerase are in transient contact with secretory proteins during late stages of translocation. Eur J Biochem *232*, 755-764.

Klappa, P., Freedman, R.B., Langenbuch, M., Lan, M.S., Robinson, G.K., and Ruddock, L.W. (2001). The pancreas-specific protein disulphide-isomerase PDIp interacts with a hydroxyaryl group in ligands. Biochem J *354*, 553-559.

Klappa, P., Ruddock, L. W., Darby, N. J., and Freedman, R. B. (1998a). The b' domain provides the principal peptide-binding site of protein disulfide isomerase but all domains contribute to binding of misfolded proteins. Embo J *17*, 927-935.

Klappa, P., Stromer, T., Zimmermann, R., Ruddock, L. W., and Freedman, R. B. (1998b). A pancreas-specific glycosylated protein disulphide-isomerase binds to misfolded proteins and peptides with an interaction inhibited by oestrogens. Eur J Biochem *254*, 63-69.

Kobayashi, T., and Ito, K. (1999). Respiratory chain strongly oxidizes the CXXC motif of DsbB in the Escherichia coli disulfide bond formation pathway. Embo J *18*, 1192-1198.

Kobayashi, T., Kishigami, S., Sone, M., Inokuchi, H., Mogi, T., and Ito, K. (1997). Respiratory chain is required to maintain oxidized states of the DsbA-DsbB disulfide bond formation system in aerobically growing Escherichia coli cells. Proc Natl Acad Sci U S A *94*, 11857-11862.

Koivu, J., Myllyla, R., Helaakoski, T., Pihlajaniemi, T., Tasanen, K., and Kivirikko, K. I. (1987). A single polypeptide acts both as the beta subunit of prolyl 4-hydroxylase and as a protein disulfide-isomerase. J Biol Chem *262*, 6447-6449.

Koivunen, P., Helaakoski, T., Annunen, P., Veijola, J., Raisanen, S., Pihlajaniemi, T., and Kivirikko, K. I. (1996). ERp60 does not substitute for protein disulphide isomerase as the beta-subunit of prolyl 4-hydroxylase. Biochem J *316 (Pt 2)*, 599-605.

Kollnberger, S., Bird, L., Sun, M. Y., Retiere, C., Braud, V. M., McMichael, A., and Bowness, P. (2002). Cell-surface expression and immune receptor recognition of HLA-B27 homodimers. Arthritis Rheum *46*, 2972-2982.

Kortemme, T., and Creighton, T. E. (1995). Ionisation of cysteine residues at the termini of model alpha-helical peptides. Relevance to unusual thiol pKa values in proteins of the thioredoxin family. J Mol Biol 253, 799-812.

Krause, G., Lundstrom, J., Barea, J. L., Pueyo de la Cuesta, C., and Holmgren, A. (1991). Mimicking the active site of protein disulfide-isomerase by substitution of proline 34 in Escherichia coli thioredoxin. J Biol Chem 266, 9494-9500.

Kulp, M. S., Frickel, E. M., Ellgaard, L., and Weissman, J. S. (2006). Domain architecture of protein-disulfide isomerase facilitates its dual role as an oxidase and an isomerase in Ero1p-mediated disulfide formation. J Biol Chem 281, 876-884.

Kuon, W., Holzhutter, H. G., Appel, H., Grolms, M., Kollnberger, S., Traeder, A., Henklein, P., Weiss, E., Thiel, A., Lauster, R., et al. (2001). Identification of HLA-B27-restricted peptides from the Chlamydia trachomatis proteome with possible relevance to HLA-B27-associated diseases. J Immunol 167, 4738-4746.

LaMantia, M. L., and Lennarz, W. J. (1993). The essential function of yeast protein disulfide isomerase does not reside in its isomerase activity. Cell 74, 899-908.

Lamberg, A., Jauhiainen, M., Metso, J., Ehnholm, C., Shoulders, C., Scott, J., Pihlajaniemi, T., and Kivirikko, K. I. (1996). The role of protein disulphide isomerase in

the microsomal triacylglycerol transfer protein does not reside in its isomerase activity. Biochem J *315 (Pt 2)*, 533-536.

Langsetmo, K., Fuchs, J. A., Woodward, C., and Sharp, K. A. (1991). Linkage of thioredoxin stability to titration of ionizable groups with perturbed pKa. Biochemistry *30*, 7609-7614.

Lee, K., Tirasophon, W., Shen, X., Michalak, M., Prywes, R., Okada, T., Yoshida, H., Mori, K., and Kaufman, R. J. (2002). IRE1-mediated unconventional mRNA splicing and S2P-mediated ATF6 cleavage merge to regulate XBP1 in signaling the unfolded protein response. Genes Dev *16*, 452-466.

Leenaars, M., and Hendriksen, C.F. (2005). Critical steps in the production of polyclonal and monoclonal antibodies: evaluation and recommendations. Ilar J *46*, 269-279.

Liepinsh, E., Baryshev, M., Sharipo, A., Ingelman-Sundberg, M., Otting, G., and Mkrtchian, S. (2001). Thioredoxin fold as homodimerization module in the putative chaperone ERp29: NMR structures of the domains and experimental model of the 51 kDa dimer. Structure *9*, 457-471.

Lindquist, J. A., Hammerling, G. J., and Trowsdale, J. (2001). ER60/ERp57 forms disulfide-bonded intermediates with MHC class I heavy chain. Faseb J *15*, 1448-1450.

Lindquist, J. A., Jensen, O. N., Mann, M., and Hammerling, G. J. (1998). ER-60, a chaperone with thiol-dependent reductase activity involved in MHC class I assembly. Embo J *17*, 2186-2195.

Lipman, N.S., Jackson, L.R., Trudel, L.J., and Weis-Garcia, F. (2005). Monoclonal versus polyclonal antibodies: distinguishing characteristics, applications, and information resources. Ilar J *46*, 258-268.

Lopez-Larrea, C., Blanco-Gelaz, M. A., Torre-Alonso, J. C., Armas, J. B., Suarez-Alvarez, B., Pruneda, L., Couto, A. R., Gonzalez, S., Lopez-Vazquez, A., and Martinez-Borra, J. (2006). Contribution of KIR3DL1/3DS1 to ankylosing spondylitis in human leukocyte antigen-B27 Caucasian populations. Arthritis Res Ther *8*, R101.

Lopez-Larrea, C., Sujirachato, K., Mehra, N. K., Chiewsilp, P., Isarangkura, D., Kanga, U., Dominguez, O., Coto, E., Pena, M., Setien, F., and et al. (1995). HLA-B27 subtypes in Asian patients with ankylosing spondylitis. Evidence for new associations. Tissue Antigens *45*, 169-176.

Lundstrom, J., and Holmgren, A. (1990). Protein disulfide-isomerase is a substrate for thioredoxin reductase and has thioredoxin-like activity. J Biol Chem *265*, 9114-9120.

Lundstrom, J., Krause, G., and Holmgren, A. (1992). A Pro to His mutation in active site of thioredoxin increases its disulfide-isomerase activity 10-fold. New refolding systems for reduced or randomly oxidized ribonuclease. J Biol Chem 267, 9047-9052.

Lundstrom-Ljung, J., Birnbach, U., Rupp, K., Soling, H. D., and Holmgren, A. (1995). Two resident ER-proteins, CaBP1 and CaBP2, with thioredoxin domains, are substrates for thioredoxin reductase: comparison with protein disulfide isomerase. FEBS Lett 357, 305-308.

Luthman, M., and Holmgren, A. (1982). Rat liver thioredoxin and thioredoxin reductase: purification and characterization. Biochemistry 21, 6628-6633.

Lyles, M. M., and Gilbert, H. F. (1991). Catalysis of the oxidative folding of ribonuclease A by protein disulfide isomerase: pre-steady-state kinetics and the utilization of the oxidizing equivalents of the isomerase. Biochemistry 30, 619-625.

Lyles, M. M., and Gilbert, H. F. (1994). Mutations in the thioredoxin sites of protein disulfide isomerase reveal functional nonequivalence of the N- and C-terminal domains. J Biol Chem 269, 30946-30952.

May, E., Dorris, M. L., Satumtira, N., Iqbal, I., Rehman, M. I., Lightfoot, E., and Taurog, J. D. (2003). CD8 alpha beta T cells are not essential to the pathogenesis of arthritis or colitis in HLA-B27 transgenic rats. J Immunol 170, 1099-1105.

Mazzarella, R. A., Srinivasan, M., Haugejorden, S. M., and Green, M. (1990). ERp72, an abundant luminal endoplasmic reticulum protein, contains three copies of the active site sequences of protein disulfide isomerase. J Biol Chem 265, 1094-1101.

Mear, J. P., Schreiber, K. L., Munz, C., Zhu, X., Stevanovic, S., Rammensee, H. G., Rowland-Jones, S. L., and Colbert, R. A. (1999). Misfolding of HLA-B27 as a result of its B pocket suggests a novel mechanism for its role in susceptibility to spondyloarthropathies. J Immunol 163, 6665-6670.

Mezghrani, A., Fassio, A., Benham, A., Simmen, T., Braakman, I., and Sitia, R. (2001). Manipulation of oxidative protein folding and PDI redox state in mammalian cells. Embo J 20, 6288-6296.

Miranda-Vizuete, A., Damdimopoulos, A. E., Gustafsson, J., and Spyrou, G. (1997). Cloning, expression, and characterization of a novel Escherichia coli thioredoxin. J Biol Chem 272, 30841-30847.

Missiakas, D., Georgopoulos, C., and Raina, S. (1993). Identification and characterization of the Escherichia coli gene dsbB, whose product is involved in the formation of disulfide bonds in vivo. Proc Natl Acad Sci U S A 90, 7084-7088.

Missiakas, D., Georgopoulos, C., and Raina, S. (1994). The Escherichia coli dsbC (xprA) gene encodes a periplasmic protein involved in disulfide bond formation. Embo J *13*, 2013-2020.

Missiakas, D., Schwager, F., and Raina, S. (1995). Identification and characterization of a new disulfide isomerase-like protein (DsbD) in Escherichia coli. Embo J *14*, 3415-3424.

Molinari, M., and Helenius, A. (1999). Glycoproteins form mixed disulphides with oxidoreductases during folding in living cells. Nature *402*, 90-93.

Molteni, S. N., Fassio, A., Ciriolo, M. R., Filomeni, G., Pasqualetto, E., Fagioli, C., and Sitia, R. (2004). Glutathione limits Ero1-dependent oxidation in the endoplasmic reticulum. J Biol Chem *279*, 32667-32673.

Mossner, E., Huber-Wunderlich, M., and Glockshuber, R. (1998). Characterization of Escherichia coli thioredoxin variants mimicking the active-sites of other thiol/disulfide oxidoreductases. Protein Sci *7*, 1233-1244.

Myllyharju, J. (2003). Prolyl 4-hydroxylases, the key enzymes of collagen biosynthesis. Matrix Biol *22*, 15-24.

Nakatani, Y., Kaneto, H., Kawamori, D., Yoshiuchi, K., Hatazaki, M., Matsuoka, T.A., Ozawa, K., Ogawa, S., Hori, M., Yamasaki, Y., *et al.* (2005). Involvement of

endoplasmic reticulum stress in insulin resistance and diabetes. The Journal of biological chemistry *280*, 847-851.

Nelson, J. W., and Creighton, T. E. (1994). Reactivity and ionization of the active site cysteine residues of DsbA, a protein required for disulfide bond formation in vivo. Biochemistry *33*, 5974-5983.

Nigam, S. K., Goldberg, A. L., Ho, S., Rohde, M. F., Bush, K. T., and Sherman, M. (1994). A set of endoplasmic reticulum proteins possessing properties of molecular chaperones includes Ca(2+)-binding proteins and members of the thioredoxin superfamily. J Biol Chem *269*, 1744-1749.

Oliver, J. D., van der Wal, F. J., Bulleid, N. J., and High, S. (1997). Interaction of the thiol-dependent reductase ERp57 with nascent glycoproteins. Science *275*, 86-88.

Oliver, J.D., Roderick, H.L., Llewellyn, D.H., and High, S. (1999). ERp57 functions as a subunit of specific complexes formed with the ER lectins calreticulin and calnexin. Mol Biol Cell *10*, 2573-2582.

Ostermeier, M., De Sutter, K., and Georgiou, G. (1996). Eukaryotic protein disulfide isomerase complements Escherichia coli dsbA mutants and increases the yield of a heterologous secreted protein with disulfide bonds. J Biol Chem *271*, 10616-10622.

Otsu, M., Bertoli, G., Fagioli, C., Guerini-Rocco, E., Nerini-Molteni, S., Ruffato, E., and Sitia, R. (2006). Dynamic retention of Ero1alpha and Ero1beta in the endoplasmic reticulum by interactions with PDI and ERp44. Antioxid Redox Signal *8*, 274-282.

Ozcan, U., Cao, Q., Yilmaz, E., Lee, A.H., Iwakoshi, N.N., Ozdelen, E., Tuncman, G., Gorgun, C., Glimcher, L.H., and Hotamisligil, G.S. (2004). Endoplasmic reticulum stress links obesity, insulin action, and type 2 diabetes. Science *306*, 457-461.

Pagani, M., Fabbri, M., Benedetti, C., Fassio, A., Pilati, S., Bulleid, N. J., Cabibbo, A., and Sitia, R. (2000). Endoplasmic reticulum oxidoreductin 1-lbeta (ERO1-Lbeta), a human gene induced in the course of the unfolded protein response. J Biol Chem *275*, 23685-23692.

Pamer, E., and Cresswell, P. (1998). Mechanisms of MHC class I--restricted antigen processing. Annu Rev Immunol *16*, 323-358.

Pankalainen, M., Aro, H., Simons, K., and Kivirikko, K. I. (1970). Protocollagen proline hydroxylase: molecular weight, subunits and isoelectric point. Biochim Biophys Acta *221*, 559-565.

Papp, E., Nardai, G., Mandl, J., Banhegyi, G., and Csermely, P. (2005). FAD oxidizes the ERO1-PDI electron transfer chain: the role of membrane integrity. Biochem Biophys Res Commun *338*, 938-945.

Pazur, J. H., and Kleppe, K. (1964). The Oxidation of Glucose and Related Compounds by Glucose Oxidase from Aspergillus Niger. Biochemistry *3*, 578-583.

Pihlajaniemi, T., Helaakoski, T., Tasanen, K., Myllyla, R., Huhtala, M. L., Koivu, J., and Kivirikko, K. I. (1987). Molecular cloning of the beta-subunit of human prolyl 4-hydroxylase. This subunit and protein disulphide isomerase are products of the same gene. Embo J *6*, 643-649.

Plemper, R. K., and Wolf, D. H. (1999). Endoplasmic reticulum degradation. Reverse protein transport and its end in the proteasome. Mol Biol Rep *26*, 125-130.

Pollard, M. G., Travers, K. J., and Weissman, J. S. (1998). Ero1p: a novel and ubiquitous protein with an essential role in oxidative protein folding in the endoplasmic reticulum. Mol Cell *1*, 171-182.

Primm, T. P., Walker, K. W., and Gilbert, H. F. (1996). Facilitated protein aggregation. Effects of calcium on the chaperone and anti-chaperone activity of protein disulfide-isomerase. J Biol Chem *271*, 33664-33669.

Puig, A., and Gilbert, H. F. (1994). Protein disulfide isomerase exhibits chaperone and anti-chaperone activity in the oxidative refolding of lysozyme. J Biol Chem *269*, 7764-7771.

Puig, A., Lyles, M. M., Noiva, R., and Gilbert, H. F. (1994). The role of the thiol/disulfide centers and peptide binding site in the chaperone and anti-chaperone activities of protein disulfide isomerase. J Biol Chem 269, 19128-19135.

Raina, S., and Missiakas, D. (1997). Making and breaking disulfide bonds. Annu Rev Microbiol 51, 179-202.

Rand, T., Qvist, K. B., Walter, C. P., and Poulsen, C. H. (2006). Characterization of the flavin association in hexose oxidase from Chondrus crispus. Febs J 273, 2693-2703.

Rath, H. C., Herfarth, H. H., Ikeda, J. S., Grenther, W. B., Hamm, T. E., Jr., Balish, E., Taurog, J. D., Hammer, R. E., Wilson, K. H., and Sartor, R. B. (1996). Normal luminal bacteria, especially Bacteroides species, mediate chronic colitis, gastritis, and arthritis in HLA-B27/human beta2 microglobulin transgenic rats. J Clin Invest 98, 945-953.

Reveille, J. D. (2006). Major histocompatibility genes and ankylosing spondylitis. Best Pract Res Clin Rheumatol 20, 601-609.

Rietsch, A., Belin, D., Martin, N., and Beckwith, J. (1996). An in vivo pathway for disulfide bond isomerization in Escherichia coli. Proc Natl Acad Sci U S A 93, 13048-13053.

Rodan, A. R., Simons, J. F., Trombetta, E. S., and Helenius, A. (1996). N-linked oligosaccharides are necessary and sufficient for association of glycosylated forms of bovine RNase with calnexin and calreticulin. Embo J *15*, 6921-6930.

Rodighiero, C., Tsai, B., Rapoport, T. A., and Lencer, W. I. (2002). Role of ubiquitination in retro-translocation of cholera toxin and escape of cytosolic degradation. EMBO Rep *3*, 1222-1227.

Ruddock, L.W., Freedman, R.B., and Klappa, P. (2000). Specificity in substrate binding by protein folding catalysts: tyrosine and tryptophan residues are the recognition motifs for the binding of peptides to the pancreas-specific protein disulfide isomerase PDIp. Protein Sci *9*, 758-764.

Russell, S.J., Ruddock, L.W., Salo, K.E., Oliver, J.D., Roebuck, Q.P., Llewellyn, D.H., Roderick, H.L., Koivunen, P., Myllyharju, J., and High, S. (2004). The primary substrate binding site in the b' domain of ERp57 is adapted for endoplasmic reticulum lectin association. J Biol Chem *279*, 18861-18869.

Rybin, V., Zapun, A., Torronen, A., Raina, S., Missiakas, D., Creighton, T. E., and Metcalf, P. (1996). Crystallization of DsbC, the disulfide bond isomerase of Escherichia coli. Acta Crystallogr D Biol Crystallogr *52*, 1219-1221.

Saleki, K., Hartigan, N., Lith, M., Bulleid, N., and Benham, A. M. (2006). Differential oxidation of HLA-B2704 and HLA-B2705 in lymphoblastoid and transfected adherent cells. Antioxid Redox Signal 8, 292-299.

Scherens, B., Dubois, E., and Messenguy, F. (1991). Determination of the sequence of the yeast YCL313 gene localized on chromosome III. Homology with the protein disulfide isomerase (PDI gene product) of other organisms. Yeast 7, 185-193.

Schrag, J. D., Bergeron, J. J., Li, Y., Borisova, S., Hahn, M., Thomas, D. Y., and Cygler, M. (2001). The Structure of calnexin, an ER chaperone involved in quality control of protein folding. Mol Cell 8, 633-644.

Schwaller, M., Wilkinson, B., and Gilbert, H. F. (2003). Reduction-reoxidation cycles contribute to catalysis of disulfide isomerization by protein-disulfide isomerase. J Biol Chem 278, 7154-7159.

Scofield, R. H., Warren, W. L., Koelsch, G., and Harley, J. B. (1993). A hypothesis for the HLA-B27 immune dysregulation in spondyloarthropathy: contributions from enteric organisms, B27 structure, peptides bound by B27, and convergent evolution. Proc Natl Acad Sci U S A 90, 9330-9334.

Shen, X., Ellis, R. E., Lee, K., Liu, C. Y., Yang, K., Solomon, A., Yoshida, H., Morimoto, R., Kurnit, D. M., Mori, K., and Kaufman, R. J. (2001). Complementary

signaling pathways regulate the unfolded protein response and are required for C. elegans development. Cell *107*, 893-903.

Shevchik, V. E., Condemine, G., and Robert-Baudouy, J. (1994). Characterization of DsbC, a periplasmic protein of Erwinia chrysanthemi and Escherichia coli with disulfide isomerase activity. Embo J *13*, 2007-2012.

Shi, Y., Vattem, K. M., Sood, R., An, J., Liang, J., Stramm, L., and Wek, R. C. (1998). Identification and characterization of pancreatic eukaryotic initiation factor 2 alpha-subunit kinase, PEK, involved in translational control. Mol Cell Biol *18*, 7499-7509.

Shiroishi, T., Evans, G. A., Appella, E., and Ozato, K. (1984). Role of a disulfide bridge in the immune function of major histocompatibility class I antigen as studied by in vitro mutagenesis. Proc Natl Acad Sci U S A *81*, 7544-7548.

Smith, J. A., Marker-Hermann, E., and Colbert, R. A. (2006). Pathogenesis of ankylosing spondylitis: Current concepts. Best Pract Res Clin Rheumatol *20*, 571-591.

Sone, M., Akiyama, Y., and Ito, K. (1997). Differential in vivo roles played by DsbA and DsbC in the formation of protein disulfide bonds. J Biol Chem *272*, 10349-10352.

Srivastava, S. P., Fuchs, J. A., and Holtzman, J. L. (1993). The reported cDNA sequence for phospholipase C alpha encodes protein disulfide isomerase, isozyme Q-2 and not phospholipase-C. Biochem Biophys Res Commun *193*, 971-978.

Sullivan, D.C., Huminiecki, L., Moore, J.W., Boyle, J.J., Poulsom, R., Creamer, D., Barker, J., and Bicknell, R. (2003). EndoPDI, a novel protein-disulfide isomerase-like protein that is preferentially expressed in endothelial cells acts as a stress survival factor. J Biol Chem *278*, 47079-47088.

Sun, F., Zhang, R., Gong, X., Geng, X., Drain, P. F., and Frizzell, R. A. (2006). Derlin-1 promotes the efficient degradation of CFTR and CFTR folding mutants. J Biol Chem.

Tachibana, C., and Stevens, T. H. (1992). The yeast EUG1 gene encodes an endoplasmic reticulum protein that is functionally related to protein disulfide isomerase. Mol Cell Biol *12*, 4601-4611.

Tachikawa, H., Funahashi, W., Takeuchi, Y., Nakanishi, H., Nishihara, R., Katoh, S., Gao, X. D., Mizunaga, T., and Fujimoto, D. (1997). Overproduction of Mpd2p suppresses the lethality of protein disulfide isomerase depletion in a CXXC sequence dependent manner. Biochem Biophys Res Commun *239*, 710-714.

Tachikawa, H., Takeuchi, Y., Funahashi, W., Miura, T., Gao, X. D., Fujimoto, D., Mizunaga, T., and Onodera, K. (1995). Isolation and characterization of a yeast gene,

MPD1, the overexpression of which suppresses inviability caused by protein disulfide isomerase depletion. FEBS Lett *369*, 212-216.

Tagaya, Y., Maeda, Y., Mitsui, A., Kondo, N., Matsui, H., Hamuro, J., Brown, N., Arai, K., Yokota, T., Wakasugi, H., and et al. (1989). ATL-derived factor (ADF), an IL-2 receptor/Tac inducer homologous to thioredoxin; possible involvement of dithiol-reduction in the IL-2 receptor induction. Embo J *8*, 757-764.

Taurog, J. D., Maika, S. D., Satumtira, N., Dorris, M. L., McLean, I. L., Yanagisawa, H., Sayad, A., Stagg, A. J., Fox, G. M., Le O'Brien, A., *et al.* (1999). Inflammatory disease in HLA-B27 transgenic rats. Immunol Rev *169*, 209-223.

Taurog, J. D., Maika, S. D., Simmons, W. A., Breban, M., and Hammer, R. E. (1993). Susceptibility to inflammatory disease in HLA-B27 transgenic rat lines correlates with the level of B27 expression. J Immunol *150*, 4168-4178.

Taurog, J. D., Richardson, J. A., Croft, J. T., Simmons, W. A., Zhou, M., Fernandez-Sueiro, J. L., Balish, E., and Hammer, R. E. (1994). The germfree state prevents development of gut and joint inflammatory disease in HLA-B27 transgenic rats. J Exp Med *180*, 2359-2364.

Tran, T. M., Satumtira, N., Dorris, M. L., May, E., Wang, A., Furuta, E., and Taurog, J. D. (2004). HLA-B27 in transgenic rats forms disulfide-linked heavy chain oligomers and multimers that bind to the chaperone BiP. J Immunol *172*, 5110-5119.

Travers, K. J., Patil, C. K., Wodicka, L., Lockhart, D. J., Weissman, J. S., and Walter, P. (2000). Functional and genomic analyses reveal an essential coordination between the unfolded protein response and ER-associated degradation. Cell *101*, 249-258.

Trombetta, E. S., and Parodi, A. J. (2003). Quality control and protein folding in the secretory pathway. Annu Rev Cell Dev Biol *19*, 649-676.

Tsai, B., and Rapoport, T. A. (2002). Unfolded cholera toxin is transferred to the ER membrane and released from protein disulfide isomerase upon oxidation by Ero1. J Cell Biol *159*, 207-216.

Tsai, B., Rodighiero, C., Lencer, W. I., and Rapoport, T. A. (2001). Protein disulfide isomerase acts as a redox-dependent chaperone to unfold cholera toxin. Cell *104*, 937-948.

Tsai, B., Ye, Y., and Rapoport, T. A. (2002). Retro-translocation of proteins from the endoplasmic reticulum into the cytosol. Nat Rev Mol Cell Biol *3*, 246-255.

Tu, B. P., and Weissman, J. S. (2002). The FAD- and O(2)-dependent reaction cycle of Ero1-mediated oxidative protein folding in the endoplasmic reticulum. Mol Cell 10, 983-994.

Tu, B. P., and Weissman, J. S. (2004). Oxidative protein folding in eukaryotes: mechanisms and consequences. J Cell Biol 164, 341-346.

Tu, B. P., Ho-Schleyer, S. C., Travers, K. J., and Weissman, J. S. (2000). Biochemical basis of oxidative protein folding in the endoplasmic reticulum. Science 290, 1571-1574.

Tuderman, L., Kuutti, E. R., and Kivirikko, K. I. (1975). An affinity-column procedure using poly(L-proline) for the purification of prolyl hydroxylase. Purification of the enzyme from chick embryos. Eur J Biochem 52, 9-16.

Turner, M. J., Sowders, D. P., DeLay, M. L., Mohapatra, R., Bai, S., Smith, J. A., Brandewie, J. R., Taurog, J. D., and Colbert, R. A. (2005). HLA-B27 misfolding in transgenic rats is associated with activation of the unfolded protein response. J Immunol 175, 2438-2448.

van Lith, M., Hartigan, N., Hatch, J., and Benham, A. M. (2005). PDILT, a divergent testis-specific protein disulfide isomerase with a non-classical SXXC motif that engages in disulfide-dependent interactions in the endoplasmic reticulum. J Biol Chem 280, 1376-1383.

Veijola, J., Koivunen, P., Annunen, P., Pihlajaniemi, T., and Kivirikko, K. I. (1994).

Cloning, baculovirus expression, and characterization of the alpha subunit of prolyl 4-

hydroxylase from the nematode Caenorhabditis elegans. This alpha subunit forms an

active alpha beta dimer with the human protein disulfide isomerase/beta subunit. J Biol

Chem *269*, 26746-26753.

Vlamis-Gardikas, A., and Holmgren, A. (2002). Thioredoxin and glutaredoxin isoforms.

Methods Enzymol *347*, 286-296.

Volkmer, J., Guth, S., Nastainczyk, W., Knippel, P., Klappa, P., Gnau, V., and

Zimmermann, R. (1997). Pancreas specific protein disulfide isomerase, PDIp, is in

transient contact with secretory proteins during late stages of translocation. FEBS Lett

406, 291-295.

Vuori, K., Pihlajaniemi, T., Myllyla, R., and Kivirikko, K. I. (1992). Site-directed

mutagenesis of human protein disulphide isomerase: effect on the assembly, activity and

endoplasmic reticulum retention of human prolyl 4-hydroxylase in Spodoptera frugiperda

insect cells. Embo J *11*, 4213-4217.

Walker, K. W., and Gilbert, H. F. (1997). Scanning and escape during protein-disulfide

isomerase-assisted protein folding. J Biol Chem *272*, 8845-8848.

Walker, K. W., Lyles, M. M., and Gilbert, H. F. (1996). Catalysis of oxidative protein folding by mutants of protein disulfide isomerase with a single active-site cysteine. Biochemistry 35, 1972-1980.

Wang, Q., and Chang, A. (1999). Eps1, a novel PDI-related protein involved in ER quality control in yeast. Embo J 18, 5972-5982.

Wetterau, J. R., Combs, K. A., McLean, L. R., Spinner, S. N., and Aggerbeck, L. P. (1991). Protein disulfide isomerase appears necessary to maintain the catalytically active structure of the microsomal triglyceride transfer protein. Biochemistry 30, 9728-9735.

Wetterau, J. R., Combs, K. A., Spinner, S. N., and Joiner, B. J. (1990). Protein disulfide isomerase is a component of the microsomal triglyceride transfer protein complex. J Biol Chem 265, 9801-9807.

Williams, K. M., and Raybourne, R. B. (1990). Demonstration of cross-reactivity between bacterial antigens and class I human leukocyte antigens by using monoclonal antibodies to Shigella flexneri. Infect Immun 58, 1774-1781.

Wilson, N. A., Barbar, E., Fuchs, J. A., and Woodward, C. (1995). Aspartic acid 26 in reduced Escherichia coli thioredoxin has a pKa > 9. Biochemistry 34, 8931-8939.

Woodrow, J. C. (1985). Genetic aspects of the spondyloarthropathies. Clin Rheum Dis *11*, 1-24.

Wunderlich, M., and Glockshuber, R. (1993). Redox properties of protein disulfide isomerase (DsbA) from Escherichia coli. Protein Sci *2*, 717-726.

Wunderlich, M., Jaenicke, R., and Glockshuber, R. (1993). The redox properties of protein disulfide isomerase (DsbA) of Escherichia coli result from a tense conformation of its oxidized form. J Mol Biol *233*, 559-566.

Xiao, R., Lundstrom-Ljung, J., Holmgren, A., and Gilbert, H. F. (2005). Catalysis of thiol/disulfide exchange. Glutaredoxin 1 and protein-disulfide isomerase use different mechanisms to enhance oxidase and reductase activities. J Biol Chem *280*, 21099-21106.

Xiao, R., Solovyov, A., Gilbert, H. F., Holmgren, A., and Lundstrom-Ljung, J. (2001). Combinations of protein-disulfide isomerase domains show that there is little correlation between isomerase activity and wild-type growth. J Biol Chem *276*, 27975-27980.

Yang, Y. F., and Wells, W. W. (1991). Catalytic mechanism of thioltransferase. J Biol Chem *266*, 12766-12771.

Yoneda, T., Urano, F., and Ron, D. (2002). Transmission of proteotoxicity across cellular compartments. Genes Dev *16*, 1307-1313.

Yoshida, H., Haze, K., Yanagi, H., Yura, T., and Mori, K. (1998). Identification of the cis-acting endoplasmic reticulum stress response element responsible for transcriptional induction of mammalian glucose-regulated proteins. Involvement of basic leucine zipper transcription factors. J Biol Chem *273*, 33741-33749.

Yoshida, H., Matsui, T., Yamamoto, A., Okada, T., and Mori, K. (2001). XBP1 mRNA is induced by ATF6 and spliced by IRE1 in response to ER stress to produce a highly active transcription factor. Cell *107*, 881-891.

Zapun, A., and Creighton, T. E. (1994). Effects of DsbA on the disulfide folding of bovine pancreatic trypsin inhibitor and alpha-lactalbumin. Biochemistry *33*, 5202-5211.

Zapun, A., Bardwell, J. C., and Creighton, T. E. (1993). The reactive and destabilizing disulfide bond of DsbA, a protein required for protein disulfide bond formation in vivo. Biochemistry *32*, 5083-5092.

Zapun, A., Darby, N. J., Tessier, D. C., Michalak, M., Bergeron, J. J., and Thomas, D. Y. (1998). Enhanced catalysis of ribonuclease B folding by the interaction of calnexin or calreticulin with ERp57. J Biol Chem *273*, 6009-6012.

Zapun, A., Missiakas, D., Raina, S., and Creighton, T. E. (1995). Structural and

functional characterization of DsbC, a protein involved in disulfide bond formation in

Escherichia coli. Biochemistry *34*, 5075-5089.

Zhang, K., Shen, X., Wu, J., Sakaki, K., Saunders, T., Rutkowski, D. T., Back, S. H., and

Kaufman, R. J. (2006). Endoplasmic reticulum stress activates cleavage of CREBH to

induce a systemic inflammatory response. Cell *124*, 587-599.

Zhou, J., Liu, C. Y., Back, S. H., Clark, R. L., Peisach, D., Xu, Z., and Kaufman, R. J.

(2006). The crystal structure of human IRE1 luminal domain reveals a conserved

dimerization interface required for activation of the unfolded protein response. Proc Natl

Acad Sci U S A *103*, 14343-14348.